MODELLING OF REINFORCED CONCRETE SLAB DEFLECTIONS AT SERVICE LOADING

by

A. J. BOTING

B.Sc (Eng) in Civil Engineering

University of Cape Town

A thesis submitted to the University of Cape Town in partial fulfilment of the requirements for the degree of Master of Science in Engineering

Department of Civil Engineering
University of Cape Town
November 1994

ACKNOWLEDGEMENTS

I would like to express my appreciation to my supervisor, Associate Professor M.O. de Kock, for his patience, guidance and help.

Many thanks to Associate Professor R.D. Kratz for keeping an eye on my progress and for his assistance with the development of the two computational models.

Finally, I would like to thank my family for their support and encouragement during the difficult times. Without their motivation the timeous completion of this thesis would not have been possible.

SYNOPSIS

Deflection under service loading is an important aspect of reinforced concrete slab design. Under-design can cause large deflections which can be expensive to repair, if at all possible. Over-design can lead to material wastage and unnecessary dead load.

Deflection is inversely proportional to the effective moment of inertia of the section under consideration. Cracks, which may or may not be present at the serviceability limit state, have a profound effect on the moment of inertia. Many Codes of practice approach the calculation of deflection in a conservative manner by using the cracked moment of inertia in deflection calculations and ignoring the effect of the concrete in tension. Two of the Codes reviewed make an attempt at including the stiffening effect of the concrete in tension.

The theory in the CEB/FIP Model Code is used as a basis for the method that is developed to predict maximum deflections. This method proposes that the total maximum deflection is composed of two components: an elastic deflection and a deflection due to cracking. The elastic deflection for a beam is determined from elastic formulae that are developed from first principles for standard beam cases. The deflection due to cracking involves the cracking moment capacity of the beam, what portion of the beam is cracked, the formation of a hinge and the rotation of this hinge.

One-way spanning slabs can be treated as broad, shallow-beams. Two-way spanning slabs are more complicated and to determine the load dispersion of a uniformly distributed load on such a slab, it is divided into five sets of orthogonal strips. The two outer strips do not carry any load. The three inner strips intersect at nine points or nodes. The deflection of each pair of orthogonal strips at each of the nine nodes must be equal. Deflection equations are set up in terms of an unknown portion of the load at each node. Since the full load at each node is known, the sum of the loads in the orthogonal directions must be equal to this full load. A matrix is set up and solved and the

load dispersion at each node is determined. The equivalent load on a strip spanning through the region of maximum deflection is thus found. For the two orthogonal strips spanning through the region of maximum deflection, the average deflection is then taken.

A computer program is written which incorporates the above approach. The program is then run for slab configurations that were tested in the laboratory and the results are compared.

The results show that the proposed computational models over-predict slab deflections. As soon as the slab is clamped on more than one edge or if the aspect ratio increases above 1 then the results in the orthogonal directions differ by a large amount. The recommended improvements to these computational models are:

- Increase the number of orthogonal strips and introduce torsion. This will also improve the continuity between strips spanning in the same direction.

- The tension stiffening factor has to be redefined. This will reduce the contribution of deflection due to cracking.

TABLE OF CONTENTS

CONTENTS

LIST OF ILLUSTRATIONS

LIST OF FIGURES

FIGURE **PAGE**

LIST OF TABLES

TABLE **PAGE**

LIST OF SYMBOLS

a - deflection
a_1, a_2 - deflection in state I and state II_0 respectively
a_c - deflection of concrete section
a_{cs1} - shrinkage deflection in state I
a_{cs2} - shrinkage deflection in state II_0
a_{cs} - shrinkage deflection
A - short span of a slab
A_s - area of tension reinforcement
A_s' - area of compression reinforcement
b - width of section
b_{ef} - effective width of compression face of a beam
B - long span of a slab
c - factor accounting for creep
d - effective depth of the tension reinforcement
d' - effective depth of the compression reinforcement
D - flexural rigidity
E - elastic modulus
E_c - appropriate modulus of elasticity of concrete.
E_{eff} - age adjusted modulus of elasticity of concrete
E_s - modulus of elasticity of reinforcement
EI_c - flexural rigidity of the uncracked concrete section alone
f_c - specified compressive strength of the concrete
f_r - modulus of rupture of the concrete
f_s, f_y - design service stress in the reinforcement
h - depth of the slab
I - second moment of area of the transformed all-concrete uncracked section
I_{cr} - moment of inertia of transformed all-concrete cracked section in sagging
I_{cr}' - moment of inertia of transformed all-concrete cracked section in hogging

I_e - effective moment of inertia
I_{em} - effective moment of inertia at midspan
$I_{e1\&2}$ - effective moment of inertia at continuous ends 1 & 2
I_{eff} - effective moment of inertia
I_g - moment of inertia of gross concrete section, neglecting reinforcing steel
I_{uncr} - uncracked, transformed all-concrete moment of inertia
k - fraction of load
K - factor dependent on shape of bending moment diagram
L - effective span of member
L_x, L_y - effective span in x- and y-directions respectively
M - moment at the section under consideration
M_a - moment at the beam section under consideration
M_{cr} - cracking moment capacity of the section in sagging
M_{cr}' - cracking moment capacity of the section in hogging
M_d - maximum total service moment
M_m - geometric mean of the maximum moment in sagging and the cracking moment
M_{pl} - plastic moment capacity
M_r - cracking moment capacity of the section is sagging
M_{rd} - cracking moment capacity at the centre of the beam
$\bar{M}$ - moment due to virtual load
n - modular ratio
q - loading per unit area
$1/r_b$ - short-term curvature
$1/r_c$ - curvature of the concrete
$1/r_{cs}$ - shrinkage curvature
$1/r_m$ - average curvature
$1/r_x$ - curvature at point x
$1/r_1$ - total curvature in state I
$1/r_2$ - total curvature in state II_0
$1/r_{1cs}$ - curvature in state I due to shrinkage
$1/r_{2cs}$ - curvature in state II_0 due to shrinkage
$1/r_{10}$ - instantaneous curvature in state I
$1/r_{20}$ - instantaneous curvature in state II_0
$1/r_{1\phi}$ - curvature in state I due to creep
$1/r_{2\phi}$ - curvature in state II_0 due to creep
S_s - first moment of area of the reinforcement about the centroid of the cracked or uncracked (gross) section
w - transverse deflection of a slab
w_a - service load
w_s - long-term sustained load
w_v - service load
x - depth to the neutral axis

x_1, x_2 - co-ordinates of the cracking zone
y_t - distance from centroidal axis of gross section to extreme tension fibre

α, α_e - modular ratio
α_i - fraction of load at node i
β_1 - coefficient characterising the bond strength of the reinforcing bars
β_2 - coefficient representing the influence of the duration of application, or of repetition, of loading
δ - deflection due to cracking
ϵ - time dependent factor for sustained loads
ϵ_c - strain in the concrete
ϵ_{cs} - free shrinkage strain
ϵ_s - strain in the reinforcement
ζ - coefficient accounting for the stiffening effect of the tensile concrete
ζ_b - coefficient accounting for the stiffening effect of the tensile concrete assuming a bilinear moment-deflection relationship
η - correction coefficient allowing for the effect of compression reinforcement
θ - rotation of the cracking hinge
κ_{cs} - global correction coefficient for uniform shrinkage
$\kappa_{cs1}, \kappa_{cs2}$ - correction coefficients for the effect of shrinkage
κ_{s1}, κ_{s2} - correction coefficients for the effect of reinforcement
κ_t - correction coefficient for long-term loading
κ_0 - correction coefficient for instantaneous deflection
$\kappa_{\phi 1}, \kappa_{\phi 2}$ - correction coefficients for the effect of creep
λ - long-term multiplication factor
λ_1 - factor accounting for edge conditions of a unit width beam spanning in the short direction
λ_2 - factor accounting for the geometry of a beam section
λ_3 - factor dependent on aspect ratio
ν - Poisson's ratio
ρ - reinforcement ratio for nonprestressed tension reinforcment
ρ' - reinforcement ratio for nonprestressed compression reinforcment
ϕ - creep coefficient

CHAPTER 1

INTRODUCTION

The purpose of this thesis is to investigate the calculation of the maximum deflection of reinforced concrete suspended slabs, both one- and two-way spanning, under uniformly distributed service loading. To this end a method is to be developed for predicting the probable maximum deflection of a slab for different arrangements and circumstances.

Slabs are normally designed for ultimate loads against flexural and shear failure. These ultimate loads are determined by assuming what type of everyday imposed loads will be acting on the slab and then factoring them up. The dead loads are also factored up and added to these imposed loads. However, in reality the slab will normally never reach its ultimate limit state and spends all of its life at or below the serviceability limit state. This aspect of slab design has largely been neglected, yet is clearly very important. A slab may be adequate for its ultimate limit state, but can fail the serviceability limit state conditions. The two most important aspects of serviceability limit conditions are usually deflection and cracking and this thesis will concentrate on deflections. Excessive deflection can be unsightly, finishes can dislodge, doors and windows can jam, vibrations can be transmitted and sensitive floor-mounted equipment can be affected. The consequences of excessive deflection are far-reaching and repairs can be very expensive. Initial deflections are compounded by long-term effects. On the other hand, over-design of slabs can be a costly business. The amount of material used in the construction of slabs constitutes a large percentage of all the materials used in the construction of a typical multistorey building. The need for an accurate method for design of slabs under serviceability limit state conditions has therefore been established.

Most Concrete Codes deal with the problem of slab design for serviceability limit state conditions by introducing limiting span/depth or span/effective depth ratios. If these ratios are adhered to, then it is assumed that deflections will not be

unsightly and non-structural elements will not be damaged by any movement. However, such factors as amount of reinforcement, strength, elasticity, shrinkage and creep of concrete, nature and duration of loading, environmental conditions, the occurrence of cracking, etc. are largely ignored.

Two-way spanning slabs present a further problem. The portion of load acting in each direction of the span is generally not accurately known if a simple deflection analysis is to be done. A model is then needed to determine the dispersion of a uniformly distributed load at various points on the slab. The effect of cracking (if present at the serviceability limit state) on this load dispersion is then also needed.

This dissertation begins with a literature review of three Codes of Practice. The methods of dealing with deflections in beams are reviewed and compared, as are the methods of apportioning load in two-way spanning systems. Two models are then proposed, one for determining the load distribution and one for determining the probable maximum deflection under maximum service loading conditions (i.e. at the serviceability limit state). If cracking is present at this level of load, then it is incorporated into both models by introducing an effective moment of inertia, I_{eff}. This effective value is a combination of the uncracked moment of inertia and the cracked moment of inertia (which ignores concrete in tension) and it includes the stiffening effect of the cracked concrete in the tension zone.

A computer program is developed which incorporates the above two proposed models. Only short-term deflections are predicted and the results are then analyzed and compared with experimental results. These experimental results are obtained from a number of undergraduate theses in which small slabs were loaded and deflections measured in the laboratory. If the proposed models produce realistic short-term results then the program will be expanded to produce long-term results.

Finally, conclusions are drawn on the validity of the proposed method and recommendations are made for improving the two models.

CHAPTER 2

LITERATURE REVIEW

Predicting the deflection of a reinforced concrete member is complicated by the non-homogeneous nature of the material, the effect of the cracking and the time-dependent effects of creep and shrinkage. Various methods have been devised to assist the design engineer in determining the deflections under service load conditions of various structural elements. These are available for beams and one-way spanning slabs. The problem is much more complicated for two-way spanning slabs, due to the three-dimensional nature of plate behaviour. This aspect will be investigated in section 2.4.

The total deflection of a reinforced concrete structural element consists of two components. Firstly there is the instantaneous deflection and then secondly there are the time-dependent deflections due to creep and shrinkage. Instantaneous deflections are dependent upon the nature of the load, boundary conditions, flexural rigidity which is affected by the occurrence of cracks. Long-term deflections are influenced by the sustained load, flexural rigidity and environmental factors affecting the concrete.

Design codes generally treat the problem of slab deflection by specifying limiting span to depth ratios. These ratios may be overridden provided that the computed deflection does not exceed certain limiting values.

Three design codes will be investigated to see how they deal with the problem of computing deflections. These design codes are the British Code (BS 8110[1]), the American Code (ACI 318M - 83[2]) and the CEB-FIP Model Code[3]. The different methods for calculating deflections will briefly be summarised and compared in the sections that follow. Finally, the problem of two-way slabs is dealt with. It must be noted that prestressing is not included in this thesis and that the investigation is limited to slabs fully supported along their sides. Flat slabs, ribbed and coffer slabs were not investigated.

2.1 BRITISH CONCRETE CODE - BS 8110 [1]

"Structural Use of Concrete"

Chapters 3.5, 3.6 & 3.7 of Part 1 of the Code deal with slabs. Chapter 3.5 is concerned solely with solid slabs supported by beams or walls. Tables 3.14 and 3.15 on pages 3/17 and 3/18 respectively give bending moment coefficients for slabs spanning in two directions. These coefficients depend on the aspect ratio (l_y/l_x) of the slab, as well as the edge constraints. No consideration, however, is given to the effect of cracking on the dispersion of the load on two-way slabs.

Deflection of slabs is specifically considered in section 3.5.7. Use is made of limiting span/effective depth ratios. These ratios are given in table 3.10 for beams and modified for tension and compression reinforcement in tables 3.11 & 3.12 respectively. The Code states that the span/depth ratio for a two-way spanning slab should be based on the shorter span and its amount of reinforcement in that direction.

Chapter 3.6 deals with ribbed slabs and chapter 3.7 with flat slabs. These chapters are therefore not relevant to this thesis.

The Code does make provision, however, for a more detailed analysis of deflections. This procedure is described in Chapter 3 of Part 2 of the Code. According to section 3.6, the curvature of a structural element can be calculated by using a) a fully cracked section, or b) an uncracked section. Whichever method then yields the larger value, should be used.

For methods (a) & (b), the following formula is suggested:

$$curvature = \frac{1}{r_b} = \frac{f_c}{x\,E_c} = \frac{f_s}{(d - x)\,E_s}$$

where

$1/r_b$ is the curvature at mid-span (at support section

for cantilevers)

f_c is the design service stress in the concrete

E_c is the appropriate modulus of elasticity of the concrete (short-term or long-term)

f_s is the estimated design service stress in tension reinforcement

d is the effective depth of the section

x is the depth to the neutral axis

E_s is the modulus of elasticity of the reinforcement

For method (b), the following alternative formula can be used:

$$curvature = \frac{1}{r_b} = \frac{M}{E_c I}$$

where

M is the moment at the section under consideration

I is the second moment of area of the transformed all-concrete uncracked section

The Code furthermore recommends the use of method (b) and the second formula. The first method and the first formula is a trial-and-error approach and requires the use of a computer, whereas the second method is a straight-forward explicit approach.

The curvature due to shrinkage is calculated as follows:

$$\frac{1}{r_{cs}} = \frac{\epsilon_{cs}\, \alpha_e\, S_s}{I}$$

where

$1/r_{cs}$ is the shrinkage curvature

α_e is the modular ratio = E_s/E_{eff}

$E_{eff} = E_c/(1+\phi)$

ϕ = creep coefficient

ϵ_{cs} is the free shrinkage strain

I is the cracked or uncracked second moment of area, depending on whether method (a) or (b) is

being used

S_s is the first moment of area of the reinforcement about the centroid of the cracked or uncracked (gross) section, whichever is appropriate

The shrinkage curvature is added to the instantaneous and creep curvatures calculated in accordance with methods (a) or (b).

Section 3.7 describes the method of calculating deflections from curvatures. This is given as:

$$\frac{1}{r_x} = \frac{d^2a}{dx^2}$$

where

$1/r_x$ is the curvature at x

a is the deflection at x

Deflections may be calculated directly from this equation by calculating the curvatures at successive sections along the member and using a numerical integration technique, i.e. $a = \int\int d^2x/r_x$

Alternatively, the following simplified approach is given:

$$a = K L^2 \frac{1}{r_b}$$

where

L is the effective span of the member

$1/r_b$ is the curvature at midspan (support section for cantilevers)

K is given in table 3.1 of Part 2 of the Code and is dependent on the shape of the bending moment diagram

Section seven of Part 2 of the code gives values for creep coefficients and free shrinkage strain. These values are then

used in the deflection calculation formulae described above.

The procedures described in the Code are over-simplifications of what happens in reality. While it is appreciated that there can be no accurate prediction of deflections due to the vast number of variables, the Code has made little attempt to include the tension stiffening effect of the tensile concrete in cracked sections. The dispersion of loads in two-way slab systems is calculated on an elastic basis and the effect of cracking on this dispersion has also been ignored.

2.2 AMERICAN BUILDING CODE - ACI 318M - 83 [2]

"Building Code Requirements for Reinforced Concrete"

The Code deals with deflections in section 9.5. Structural elements are divided into:

i) One-way construction (nonprestressed) - this includes one-way spanning reinforced concrete slabs.
ii) Two-way construction (nonprestressed) - this caters for two-way spanning reinforced concrete slabs.
iii) Prestressed concrete construction.
iv) Composite construction.

One-way Spanning Slabs

Minimum thicknesses (h) of one-way spanning slabs with different edge constraints are given in table 9.5(a) on page 318M-34. Table 9.5(b) on page 318M-35 gives minimum permissable computed deflections for different types of member.

Section 9.5.2.2 on page 318M-33 states that where deflections are to be computed, deflections that occur immediately on application of load shall be computed by usual methods or formulae for elastic deflections, considering effects of cracking and reinforcement on member stiffnesses.

A formula is given for the "effective moment of inertia". This moment of inertia includes the effect of cracking and the tension stiffening effect of the concrete between cracks. It provides a transition between the uncracked and cracked moments of inertia. This formula, eqn (9-7) on page 318M-34, is as follows:

$$I_e = \left(\frac{M_{cr}}{M_a}\right)^3 I_g + \left[1 - \left(\frac{M_{cr}}{M_a}\right)^3\right] I_{cr} \quad \ldots \quad eqn(9\text{-}7)$$

where

I_g = moment of inertia of gross concrete section, neglecting reinforcing steel

I_{cr} = moment of inertia of transformed all-concrete cracked section

M_a = moment at the beam section under consideration

M_{cr} = cracking moment of the concrete section

$$M_{cr} = \frac{f_r \times I_g}{y_t} \quad \ldots \quad eqn(9\text{-}8)$$

y_t = distance from centroidal axis of gross section, neglecting reinforcement, to extreme tension fibre

f_r = modulus of rupture of the concrete and for normal density concrete

$$f_r = 0.7 \times \sqrt{f_c} \quad \ldots \quad eqn(9\text{-}9)$$

f_c = specified compressive strength of the concrete

The formula for I_e was developed by Branson[4] in his research on the effective stiffness of flexural concrete members. This moment of inertia is taken to be constant and acting over the whole length of a simply-supported, non-continuous member. The ACI publication on commentary on the Code[5] regards the formula for I_e as being sufficiently accurate for control of deflections.

For continuous members, the Code suggests that the effective moment of inertia be taken as the average of values obtained for the critical positive and negative moment regions. The

publication on commentary on the Code[5] gives the following two formulae for the averaging procedure:

Both ends continuous

$$\text{Ave } I_e = 0.70\ I_{em} + 0.15\ (I_{e1} + I_{e2})$$

Only one end continuous

$$\text{Ave } I_e = 0.85\ I_{em} + 0.15\ I_{e\ \text{contin. end}}$$

where I_{em} = effective moment of inertia at midspan

$I_{e1\&2}$ = effective moments of inertia at the continuous ends 1 and 2

The reason for the midspan moment of inertia being weighted higher is primarily because the midspan rigidity has the dominant effect on deflections.

Two-way spanning slabs

The Building Code gives formulae for recommended slab thicknesses (h) as well as minimum and maximum limits, under section 9.5.3. These formulae are based on the length of the longer span. The effective moment of inertia is computed in the same manner as for one-way spanning slabs i.e. use eqn (9-7).

Long-term deflections resulting from creep and shrinkage are determined by multiplying the instantaneous deflection caused by the sustained load by the following factor:

$$\lambda = \frac{\epsilon}{1 + 50\rho'} \quad \ldots \quad eqn(9\text{-}10)$$

where

ρ' = reinforcement ratio for nonprestressed compression reinforcement

$= A'_s/bd$

and ϵ = time-dependent factor for sustained load

values are given on page 318M-34

The ACI commentary on the Code[5] states that although eqn (9-10) is a simplification of all the factors that affect long-term deflections, it is considered to be satisfactory. The multiplier λ is presented as a quotient of two factors: a material property (ϵ) and a section property (ρ').

Chapter 13 of the Code deals solely with the design of two-way slab systems. Two methods are proposed for the determination of moments along the length and lines of support of the slab. These two methods are the Direct Design Method and the Equivalent Frame Method.

A number of researchers have adopted the Branson equation and have used the ACI Code as the basis for their own refined formulation of deflection formulae, for example Rangan[6]. However, even though the equation developed by Branson for the effective moment of inertia (eqn 9-7) for computing deflections has been found to correlate well with experimentally determined deflections, it appears to be an over-simplification. Two papers by Gilbert[7],[8] question the validity of the equation and state that most reinforced concrete slabs fall completely outside the limits of Branson's study.

2.3 MANUAL ON CEB/FIP MODEL CODE [3]

"Cracking and Deformation"

The Manual deals with two limiting situations when determining properties of a reinforced concrete section. These are:

- State I - Uncracked sections - behaviour is calculated assuming that all the concrete and the reinforcement are active both in tension and in compression.

- State II_0 - Cracked sections - behaviour is calculated assuming the reinforcement to be effective both in tension and compression, but that

the concrete is only effective in compression.

Average values are obtained from these two states by using coefficients which define the relative contributions of State I and State II_0. The stiffness of a cracked member varies from a minimum value at the location of the crack to a maximum value midway between the cracks. Therefore, the average value of the flexibility of the structural element should be used.

In chapter 3 of the Manual a model is developed for determining the curvature of a structural element. This model will be summarised over the next few pages.

At each point on a linear structure, the curvature is given by the following relationship.

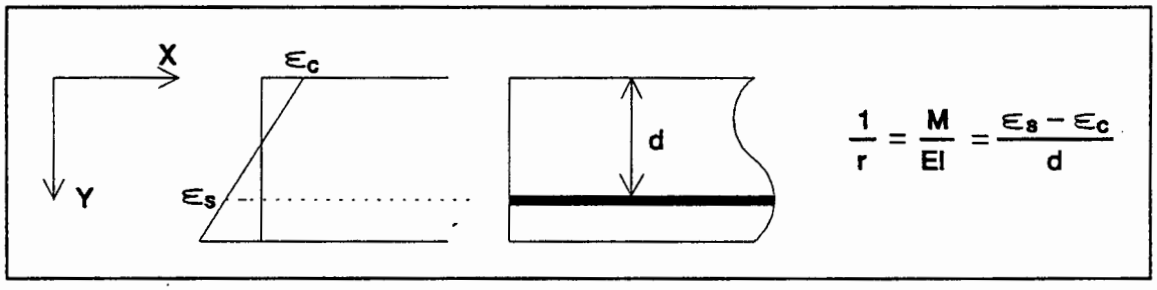

Fig 2.1 - Curvature relationship after Manual on CEB Model Code[3]

The curvatures in state I and state II_0 can be calculated from the basic curvature given by:

$$\frac{1}{r_c} = \frac{M}{E I_c}$$

where

M is the moment being applied

EI_c is the flexual rigidity of the uncracked concrete section alone

This can be modified by means of correction coefficients, κ, to take account of:

i) the effect of reinforcement (coefficients κ_{s1} and κ_{s2} for states I and II_o respectively),
ii) the effect of creep (coefficients $\kappa_{\phi 1}$ and $\kappa_{\phi 2}$),
iii) the effect of shrinkage (coefficients κ_{cs1} and κ_{cs2}).

Formulae and graphs of these correction coefficients are given in the Manual.

The total curvature in state I is defined by the expression

$$\frac{1}{r_1} = \frac{1}{r_{10}} + \frac{1}{r_{1\phi}} + \frac{1}{r_{1cs}}$$

where

$1/r_{10}$ is the instantaneous curvature in state I
$1/r_{1\phi}$ is the curvature in state I due to creep
$1/r_{1cs}$ is the curvature in state I due to shrinkage

The curvature $1/r_1$ constitutes, in the case of pure flexure, the <u>minimum</u> possible value of the average curvature, $1/r_m$.

Taking the correction coefficients into account, we get

$1/r_{10} = \kappa_{s1}/r_c$ - instantaneous curvature
$1/r_{1\phi} = (\kappa_{s1}\ \kappa_{\phi 1}\ \phi)/r_c$ - curvature due to creep
$1/r_{1cs} = \kappa_{cs1}\ |\epsilon_{cs}|/d$ - curvature due to shrinkage

thus,

$$\frac{1}{r_1} = \kappa_{s1}(1 + \kappa_{\phi 1}\phi)\frac{1}{r_c} + \kappa_{cs1}\frac{|\epsilon_{cs}|}{d}$$

Similarly, in state II_0,

$$\frac{1}{r_2} = \kappa_{s2}(1 + \kappa_{\phi 2}\phi)\frac{1}{r_c} + \kappa_{cs2}\frac{|\epsilon_{cs}|}{d}$$

The average curvature $1/r_2$ constitutes, in the case of pure flexure, the maximum possible value of the average curvature $1/r_m$.

The average curvature $1/r_m$ is defined by the following relationship:

$$\frac{1}{r_m} = (1 - \zeta)\frac{1}{r_1} + \zeta\frac{1}{r_2}$$

Experimentally, the coefficient ζ has been defined as:

$$\zeta = 1 - \beta_1 \beta_2 (M_r/M)^2$$
$$= 0 \text{ for } M < M_r$$

where

$\beta_1 = 1/(2.5\ \kappa_1)$ - a coefficient characterising the bond strength of the reinforcing bars

$\kappa_1 = 0.4$ for high bond bars

$\kappa_2 = 0.8$ for smooth bars

β_2 = a coefficient representing the influence of the duration of application, or of repetition of loading

$\beta_2 = 1.0$ for first loading

$\beta_2 = 0.5$ for long-term loads, or for a large number of cycles of load

M = Moment at the section under consideration

M_r = Cracking Moment

The above relationships are demonstrated in the following set of diagrams.

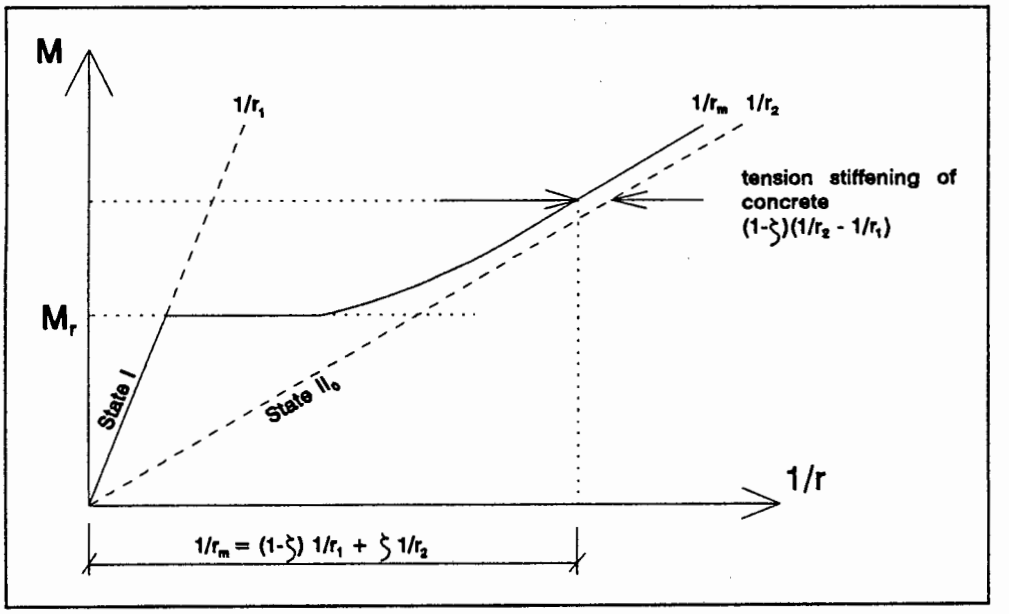

Fig 2.2 - Instantaneous moment - curvature relationship after Manual on CEB Model Code[3]

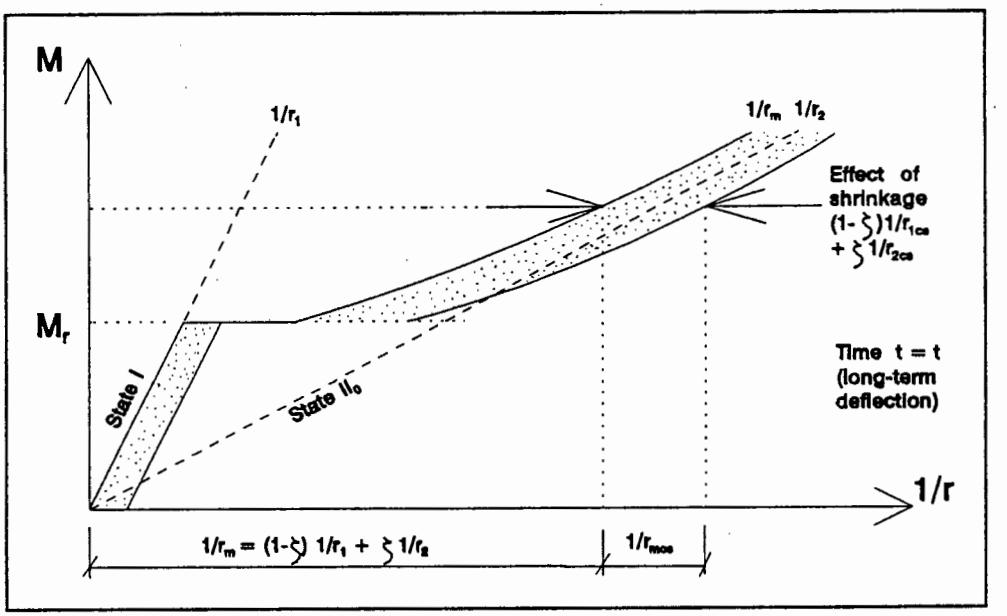

Fig 2.3 - Long-term moment - curvature relationship after Manual on CEB Model Code[3]

The Manual provides three methods for the calculation of deflections. These are:

i) Integration and theorem of virtual work.
ii) Bilinear Method.
iii) Method of Global Coefficients.

i) Integration and theorem of virtual work

The deformation a of a linear element can be obtained by integration of the average curvatures and applying the theorem of virtual work.

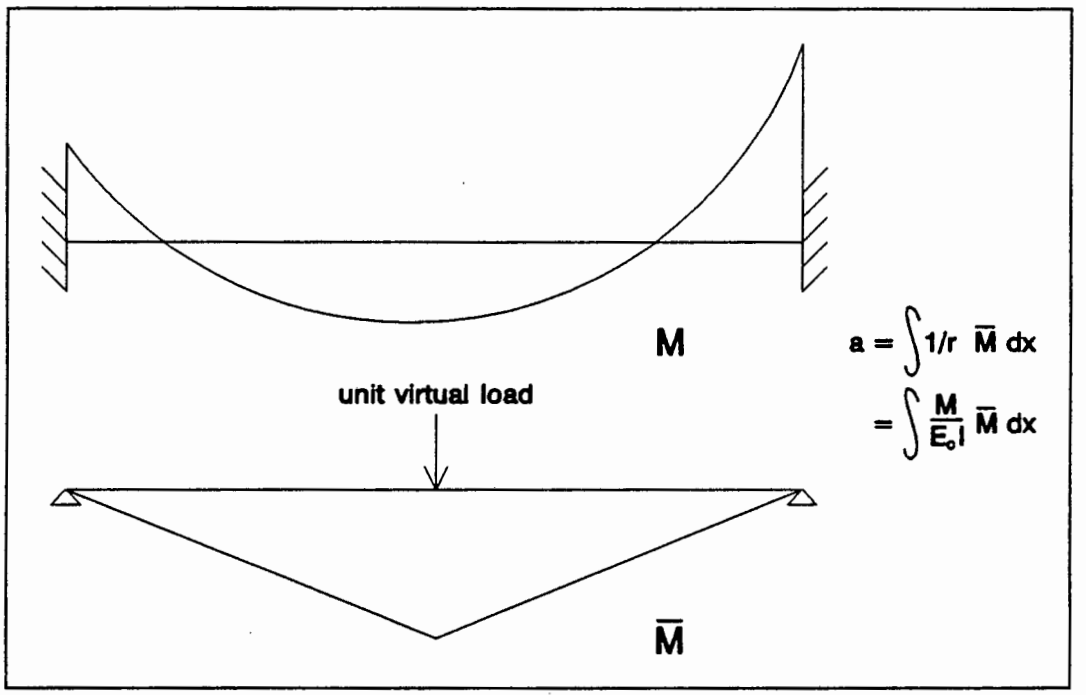

Fig 2.4 - Principle of virtual work after Manual on CEB Model Code[3]

At each section of the element the basic curvature $1/r_c = M/EI_c$ is calculated. From this curvature the two curvatures $1/r_1$ & $1/r_2$, corresponding to states I and II_0 respectively, are calculated. The average curvature $1/r_m$ is then calculated from

$$1/r_m = (1-\zeta)\ 1/r_1 + \zeta\ 1/r_2.$$

ii) Bilinear Method

This method is based on the observation that, for the serviceability limit state, the moment-deflection relationship may be approximated by a bilinear relation which represents in some way the overall effect of the moment-curvature relationships described previously. This is shown in the following set of

diagrams.

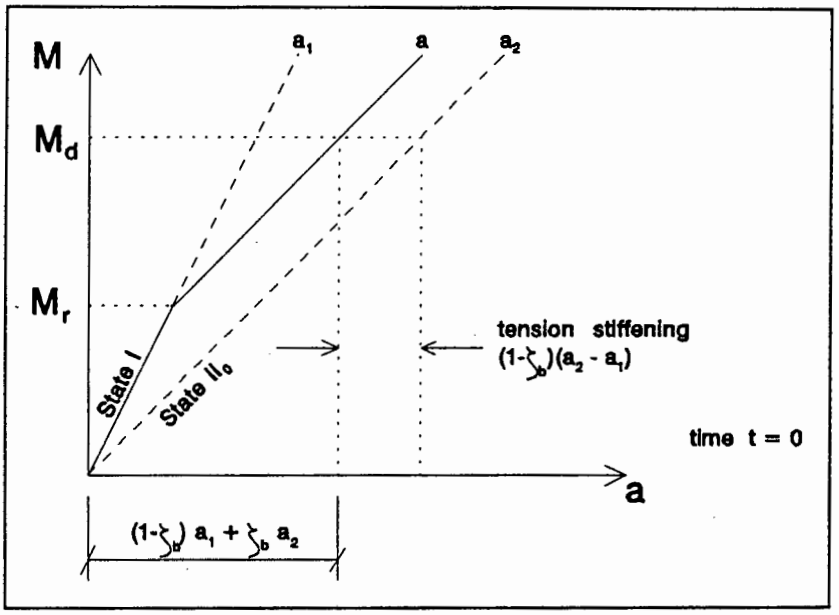

Fig 2.5 - Instantaneous moment - deflection relationship after Manual on CEB Model Code[3]

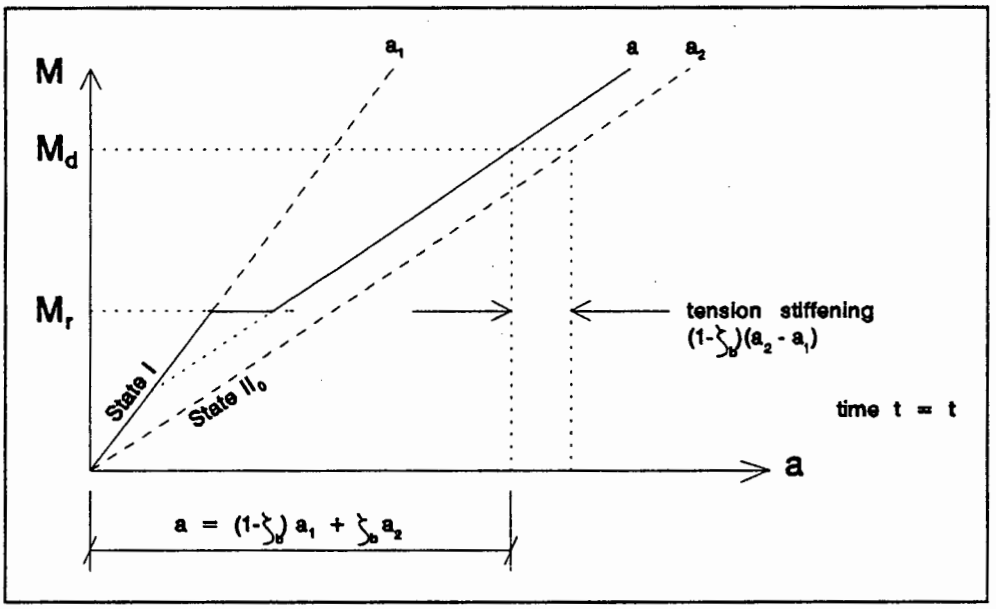

Fig 2.6 - Long-term moment - deflection relationship after Manual on CEB Model Code[3]

The following simplifications are made:

a) There is no redistribution of moments after an elastic calculation for a statically indeterminate

structure.

b) The coefficient ζ, which in reality varies along the element, is replaced by a constant value ζ_b calculated for the critical section (defined below).

c) The limiting deflections a_1 and a_2 are calculated on the basis of the characteristics of the critical section alone.

The probable deflection of a linear structure may be determined using the theorem of virtual work, similar to the previous method. The zone where the real positive moments due to the loading and the virtual moments are simultaneously close to their maximum values is called the critical zone. The critical section is defined as the mid-span section for simply supported or continuous beams and as the support section for cantilevers.

Further simplifications are:

d) The cracking moment M_r is assumed to be constant over the whole length of the structural element considered and equal to the cracking moment of the critical section.

$$M_r = M_{rd}$$

e) The bending moment M is defined as the geometric mean of the cracking moment M_{rd} and the maximum total service moment M_d due to loading at the critical section.

$$M = \sqrt{M_{rd}\, M_d}$$

The distribution coefficient thus becomes

$$\zeta_b = 1 - \beta_1\, \beta_2\, M_{rd}/M_d$$
$$= 0 \text{ for } M_d < M_{rd}$$

Therefore the probable deflection can be obtained as

$$a = (1 - \zeta_b) \int \frac{1}{r_1} \overline{M}\, dx + \zeta_b \int \frac{1}{r_2} \overline{M}\, dx$$

where $\overline{M}$ is the moment due to the virtual load.

iii) Method of Global Coefficients

This method is based on the bilinear method. The probable deflection a is estimated from the basic deflection a_c by means of global correction coefficients, κ. These global correction coefficients take into account the effects of reinforcement, cracking, creep and shrinkage and are obtained from graphs given in the Manual.

From the basic equation

$$a = (1-\zeta_b)a_1 + \zeta_b a_2$$
$$= a_2 - (1-\zeta_b)(a_2-a_1)$$

Initially ignoring the effects of shrinkage

$$a_1 = a_c\ (\kappa_{s1} + \kappa_{s1}\kappa_{\phi 1}\phi)$$
$$a_2 = a_c\ (\kappa_{s2} + \kappa_{s2}\kappa_{\phi 2}\phi)$$

Substituting these equations into the one above

$$a = a_c\ \{\kappa_{s2} - (1-\zeta_b)(\kappa_{s2}-\kappa_{s1}) + \phi[\kappa_{s2}\kappa_{\phi 2} - (1-\zeta_b)(\kappa_{s2}\kappa_{\phi 2} - \kappa_{s1}\kappa_{\phi 1})]\}$$

For instantaneous deflections, where $\phi = 0$

$$a = a_c\ \{\kappa_{s2} - (1-\zeta_b)(\kappa_{s2}-\kappa_{s1})\}$$
$$= a_c\ \kappa_o$$

κ_o is a global correction coefficient for instantaneous deflection, dependent on the level of loading and amount of tension steel. The influence of compression reinforcement is slight.

For long-term deflections

$$a_o = a_c\ \{...\}$$
$$= a_c\ \kappa_t\ \eta$$

κ_t is a global correction coefficient for long-term loading, taking into account the level of loading, the amount of tension reinforcement and the effect of creep

η is a correction coefficient which allows for the effect of compression reinforcement

Values for the global coefficients κ_o, κ_t and η have been calculated and are presented graphically in the Manual. The same simplifications that were made for the bilinear method were made.

Shrinkage is now included for the long-term deflections

$$a_{cs} = (1-\zeta_b)\, a_{cs1} + \zeta_b a_{cs2}$$

where

$$a_{cs1} = \int \frac{1}{r_{1cs}} \bar{M}\, dx$$

$$\approx \kappa_{cs1}\, |\epsilon_{cs}|\, \delta\, L^2/8d$$

and

$$a_{cs2} = \int \frac{1}{r_{2cs}} \bar{M}\, dx$$

$$\approx \kappa_{cs2}\, |\epsilon_{cs}|\, \delta\, L^2/8d$$

$$\delta = \frac{8}{L^2} \int |\bar{M}|\, dx$$

δ = 1 for a simple beam
= 0.5 for a fully encastre beam
= 4 for a cantilever
L = span of beam
d = effective depth of the slab

The deflection due to shrinkage can then be defined as

$$a_{cs}/L = \alpha_{cs}\, \kappa_{cs}$$

with $\alpha_{cs} = |\epsilon_{cs}|\, h/d\, \lambda/8$

$\lambda = \delta\, L/h$

κ_{cs} is the global correction coefficient for uniform shrinkage defined by:

$$\kappa_{cs} = (1-\zeta_b)\, \kappa_{cs1} + \zeta_b \kappa_{cs2}$$

The Manual then further simplifies the expression for a_{cs} by linearising the formula for κ_{cs}. These simplifications lead to the following expressions for a_{cs}:

In state I: $a_{cs}/L \approx \alpha_{cs}\ 7\alpha\rho\ (1-\rho'/\rho)$

In state II_0: $a_{cs}/L \approx \alpha_{cs}\ [0.75 + 7\alpha\rho(0.25-\rho'/\rho)]$

The bilinear method and, even more definitely, the method of global coefficients are based on many simplifications. The basic assumptions of the bilinear method that the section properties do not change along the length of the structural element, that the entire member is cracked and the use of the geometric mean moment are unrealistic. However, the procedure set out in the first method, namely the integration and theorem of virtual work, is sound and this will form the basis for the model developed in Chapter 3.

Of the three Codes examined, the principles of the CEB/FIP model appear to be the most sound. The British Code is the most simplistic and over-estimates deflections. The American Code falls between these two.

Scholz[9] made a comparison between measured short-term deflections in partially prestressed slabs and various models for predicting these deflections. Generally the ACI code method, based on Branson's formula for the effective moment of inertia (section 2.2), compares more favourably than the bilinear model of the CEB/FIP model (method (ii) of section 2.3). This view is supported by Bakoss et al[10]. Instantaneous and long-term deflections of simply-supported and continuous beams were measured and compared to theoretical results based on various Codes and on finite element analyses based on the ACI and CEB/FIP Codes. The ACI code predicted deflections more accurately, especially for shrinkage in simply-supported beams and for all long-term effects in continuous beams. The theory lying behind the CEB/FIP model is sound, however, and is the method favoured by a number of authors. Ghali and Favre[11], for example, have examined a number of methods for determining deflections but favour the bilinear model developed in the CEB Manual. Consequently, this theory will be used as a basis for the model

that is developed in the next chapter.

2.4 TWO - WAY SPANNING SLABS

For one-way slabs, the problem of predicting deflections is relatively simple. The slab is treated as a shallow, broad beam, However, for two-way slabs the problem is more complicated. The two-way nature of the load dispersion and the presence of plate action presents problems.

In addition to the factors[8] which affect beam and one-way slab deflections, the deflection of a two-way, edge-supported, rectangular slab panel depends on the boundary conditions at the supports and on the aspect ratio. The load on the slab is resisted not only by orthogonal bending moments, but also by twisting moments.

Bruinette[12] argues that small deflection theory is more relevant to slab deformation than large deflection theory. Small deflection theory makes use of the following Lagrange equation:

$$D\left[\frac{\partial^4 w}{\partial x^4} + 2\frac{\partial^4 w}{\partial x^2 \partial y^2} + \frac{\partial^4 w}{\partial y^4}\right] = q(x;y)$$

where:

$D = Eh^3/12(1-\nu^2)$
= flexural rigidity of the plate
E = Elastic modulus of the material
h = plate thickness
ν = Poisson's ratio for the material
q(x;y) is the loading per unit area
w = transverse deflection of the slab
x & y are two orthogonal axes

According to Bruinette[12] various solutions have been proposed for solving the fourth order differential equation. However, these solutions are complicated and cumbersome to use. A number of

approximate methods have been adopted. These are:

i) The Finite Element Method - the standard finite element method is used and is very effective if a linear elastic analysis is used and the material is treated as uncracked throughout. It becomes very complicated, however, when cracking is included in the analysis and the effects of creep and shrinkage are taken into account.

ii) Crossing Beam Analogies - two unit-width beams span across the slab in the directions of the principal axes. These two beams intersect at midspan. If the deflection of both beams is equal, then the fraction of the uniform load carried by the short beam is

$$k = B^4/(A^4+B^4)$$

where B is the long span
A is the short span

The long beam will carry 1-k of the load. This method neglects twisting moments and consequently overestimates deflections.

iii) Analogous Grid Method - this is an improvement of the crossing beam analogy and recognizes torsional moments directly. The slab is divided into strips in orthogonal directions and these are replaced by equivalent beams. The beams are connected to each other at crossing points. At every crossing point distribution factors for flexure and torsion are calculated. Each joint is given in succession a vertical displacement. The fixed end moments produced are distributed and carried over to adjacent joints. The procedure is a two-dimensional adaptation of the conventional moment-distribution analysis of a plane frame with sway. A set of simultaneous equations results, in terms of arbitrary joint displacements. Solving this set produces the displacements. The method is tedious however and the number of simultaneous equations is too large for manual

solution.

iv) Wide Beam Method - the slab is considered to act as a broad shallow beam. The beam spans alternatively in the x- and y-directions, carrying full load in each case and assuming a fixed line of support. The slab is then further sub-divided into a middle strip (of half width) and the deflection of each strip determined. The total mid-panel deflection is obtained for bending in each direction. The method is approximate, but produces satisfactory results.

v) Equivalent Frame Method - the slab panel is analyzed as a continuous frame. The frame is composed of column strips and a middle strip. The load is apportioned to the column and middle strip according to various factors. This apportioning is obtained from Codes of practice. The total central deflection is then calculated by summing the average of the deflections of two opposite column strips with the deflection of the middle strip spanning perpendicularly to these two column strips. According to Bruinette[12] the Equivalent Frame Method yields reasonably good results and in general underestimates instantaneous deflections by a small amount.

Many codes, such as CP110[13], give bending moment coefficients for two-way slabs with varying aspect ratios and edge constraints. These values, however, are based on an elastic analysis of plates and cracking is not taken into account. Cracking cannot be ignored and the amount of moment redistribution that takes place can be significant.

Researchers such as Branson[4] and Gilbert[8] have taken formulae for determining elastic deflections for beams and by introducing an aspect ratio/boundary condition factor have applied them to two-way slabs.

Branson[4] makes use of a method of deflection coefficients:

$$\Delta = K_s \, q \, L^4 / D$$

where

Δ = deflection
K_s = slab deflection coefficient dependent on aspect ratio and boundary conditions
q = uniformly distributed load per unit area
L = Longer span
D = flexural rigidity = $Eh^3 / 12(1-\nu^2)$
where E = Young's Modulus of the Concrete
h = slab thickness
ν = Poisson's ratio
(0.2 for concrete)

This formula, however, ignores the effect of cracking and the factor K_s is only presented for either all four sides of the slab being simply supported or all four sides being fully clamped. No cases in between are considered.

Gilbert[8] makes use of the principle of determining the equivalent load acting on orthogonal beams spanning through the region of maximum deflection. He extends Rangan's[6] expression developed for predicting the deflection Δ of beams.

$$\frac{L}{d} \leq \lambda_1 \lambda_2 \lambda_3 \left[\frac{\Delta}{L} \left(\frac{\alpha \, b_{ef} \, E_c}{k(w_v + c \, w_s)} \right) \right]^{\frac{1}{3}}$$

where

λ_1 = factor accounting for edge conditions of a unit width beam spanning in the short direction
λ_2 = factor accounting for the geometry of the beam section
λ_3 = factor dependent on aspect ratio found in codes
α = factor accounting for the reinforcement ratio and modular ratio (n)
b_{ef} = effective width of compression face of the beam
E_c = Young's Modulus of the concrete

k = portion of uniformly distributed load acting on the beam
w_v = transient load
w_s = long-time sustained load
c = factor accounting for creep and shrinkage
L = effective span of beam under consideration

The formula above uses the method of crossing beam analogies to determine the factor k. As has already been discussed, this method does not take the torsional stiffness of the beam into account.

A model will be proposed in the following chapter that will attempt to determine the load dispersion of a two-way spanning slab system. The concepts of both the Crossing Beam Analogy Method and the Analogous Grid Method will be used. While it is recognised that the proposed model is still only an approximation of the true load dispersion, the short-falls of the aforementioned methods will be minimised. Cracking will also be recognised and incorporated in the analysis. Essentially, the same logic as used by Gilbert[7],[8] in developing his deflection model will be used. The equivalent load acting on a unit width beam is found so that the deflection of that "beam" will be the same as the deflection of the actual two-way slab system.

CHAPTER 3

DEVELOPMENT OF MODELS AND COMPUTER PROGRAM

Two mathematical models are developed in this chapter. For a two-way spanning slab, the equivalent load on a "beam" spanning through the region of maximum deflection is determined. Once this load has been determined, a second model determining the maximum deflection of the "beam" is developed. Section 3.3 deals with the development of the computer program incorporating these two models and predicting the maximum deflection of a slab system. The models are first tested for predicting short-term deflections. If the values look realistic and compare well with expected trends, then the models will be extended to predicting long-term deflections.

3.1 MODEL 1 FOR THE EQUIVALENT LOAD

This model only applies to two-way spanning slabs. The slab is divided up into a number of orthogonal strips in the x- and y-directions and if the proportion of load acting on each strip can be determined, then that strip will deflect the same amount as the portion of slab that it represents.

The slab is divided into 5 strips in each of the x- and y-directions, as shown in the diagram on the following page. Each strip consists of five zones. The outer two zones are of length L/8, while the three inner zones are of length L/4. There is a node at the centre of each of the three inner zones. Each zone has its own stiffness and unique portion of load that it carries. Deflection formulae are set up in terms of unknown load for each strip by integrating the shear force equations three times. These equations have been determined for every support condition that can be encountered by a beam and can be seen in appendix A.

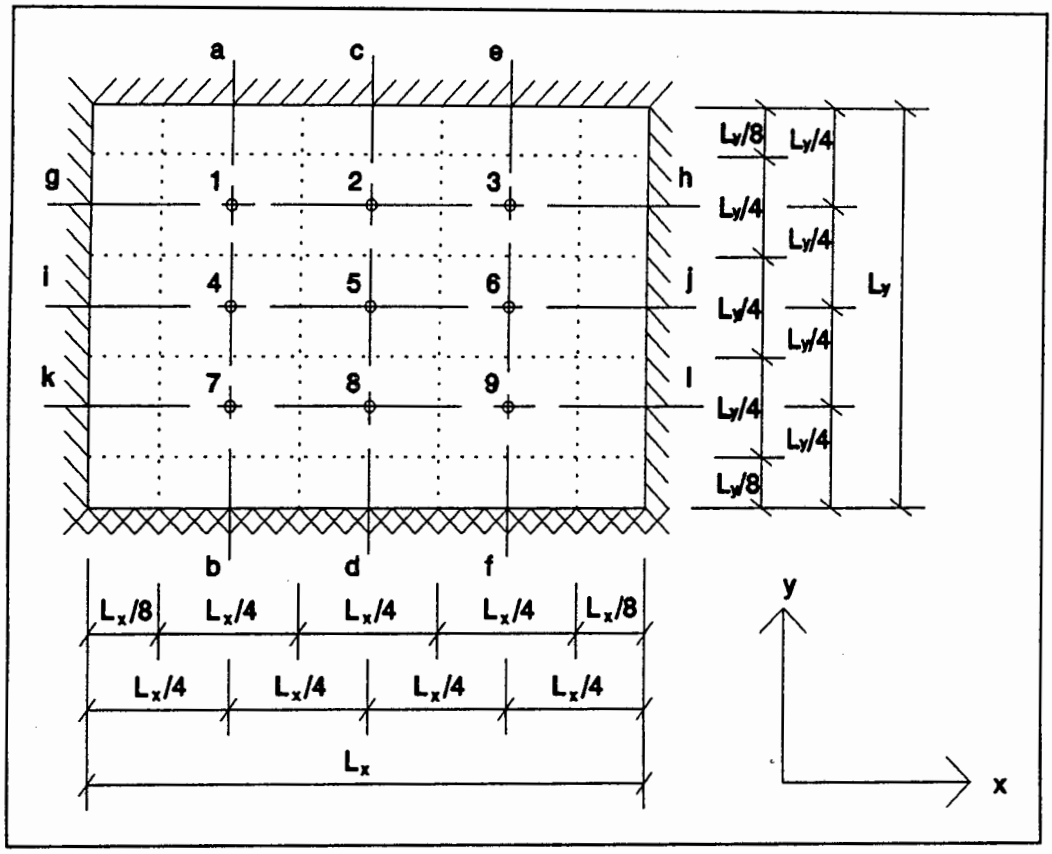

Fig 3.1 - Division of slab into strips (between dotted lines)

The deflection at each of the nine nodes (numbered one to nine in the diagram) must be the same when determined for the strips in the x- and y- directions.

Consider strips a-b and g-h (each strip will have the same support conditions as the portion of slab that it represents).

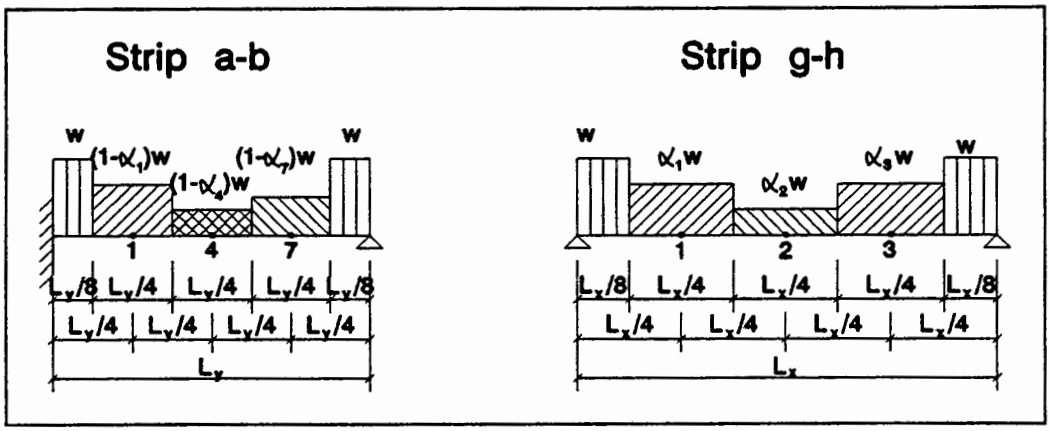

Fig 3.2 - Division of load onto orthogonal strips

The two strips intersect at node 1. If the deflections at node 1 for each strip are equal, then strip g-h will carry α_1 of the load at that node and strip a-b will carry $(1-\alpha_1)$ of the load. Each node governs the load for the zone that it is in. If the deflections in the orthogonal strips at each of the nine nodes are equal, then a grid of load dispersions can be determined.

The two outer zones carry the full load in one direction, while the inner zones carry the portion of load determined as described above. The bending moment can be determined for the loads thus acting on the strip. The cracking moment for each zone is also determined. If the bending moment of a zone exceeds its cracking moment then a new effective stiffness I_{eff} is determined. This stiffness is determined on the following basis:

If the entire zone is cracked, then the moment of inertia I for that zone is determined ignoring concrete in tension.

If the entire zone is uncracked, then the uncracked moment of inertia for that zone is used.

If only a portion of the zone is cracked, then a linear interpolation between the cracked and uncracked moments of inertia is used. This is best described with the use of the following diagram.

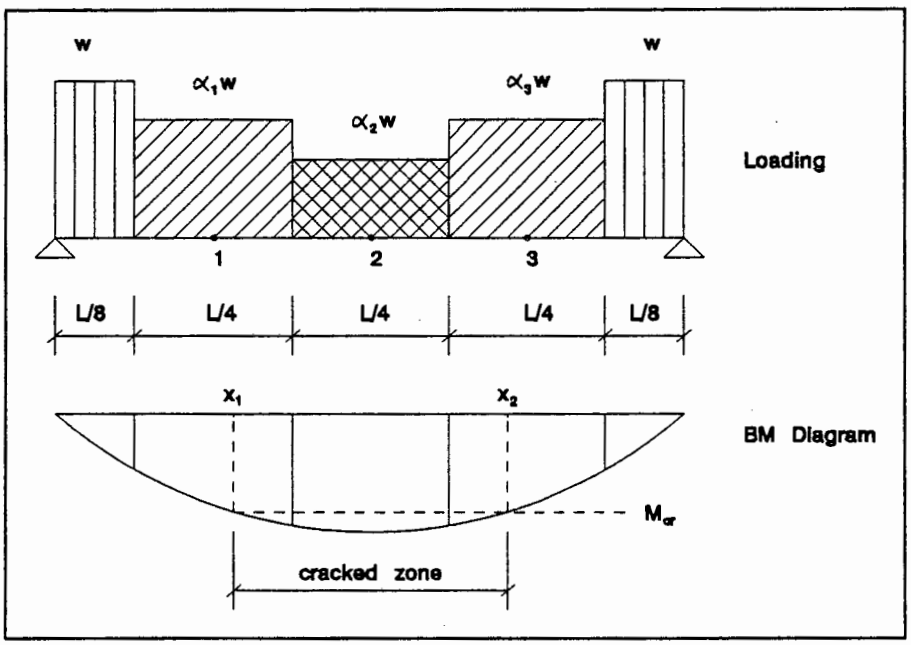

Fig 3.3 - Cracked zone of a beam

The portion of the strip between x_1 and x_2 is cracked. The two outer zones are completely uncracked and the uncracked moment of inertia I_{uncr} can be used. The middle zone (zone governed by node 2) is completely cracked and the cracked moment of inertia I_{cr} is used. The other two zones (zones governed by nodes 1 and 3) are only partially cracked.

$$I_{eff2} = [(x_1 - \frac{L}{8}) I_{uncr} + (\frac{3L}{8} - x_1) I_{cr}] / (\frac{L}{4})$$

AND

$$I_{eff4} = [(\frac{7L}{8} - x_2) I_{uncr} + (x_2 - \frac{5L}{8}) I_{cr}] / (\frac{L}{4})$$

Formulae for determining I_{uncr}, I_{cr}, M_{cr}, etc. can be found in Appendix B.

These new stiffnesses are substituted into the deflection equations and a new load dispersion pattern calculated. Once again a new cracked region is determined, and if this differs considerably from the previous one, then the whole procedure is repeated. This iteration procedure carries on until a stable cracking zone is achieved. This final load dispersion is the one now used to determine deflections.

For those beams that are statically indeterminate, a check must be made on whether the plastic moment at the support(s) is exceeded or not. If it is, then the entire iteration procedure is repeated from the start, but the statically indeterminate beam is now assumed to be discontinuous with the plastic moment M_{pl} as end moment(s). When the bending moment diagram is calculated, the effect of the plastic moment is taken into consideration. This is illustrated in the set of diagrams on the next page. Cracking must now be checked for and if necessary the whole iteration procedure must be repeated.

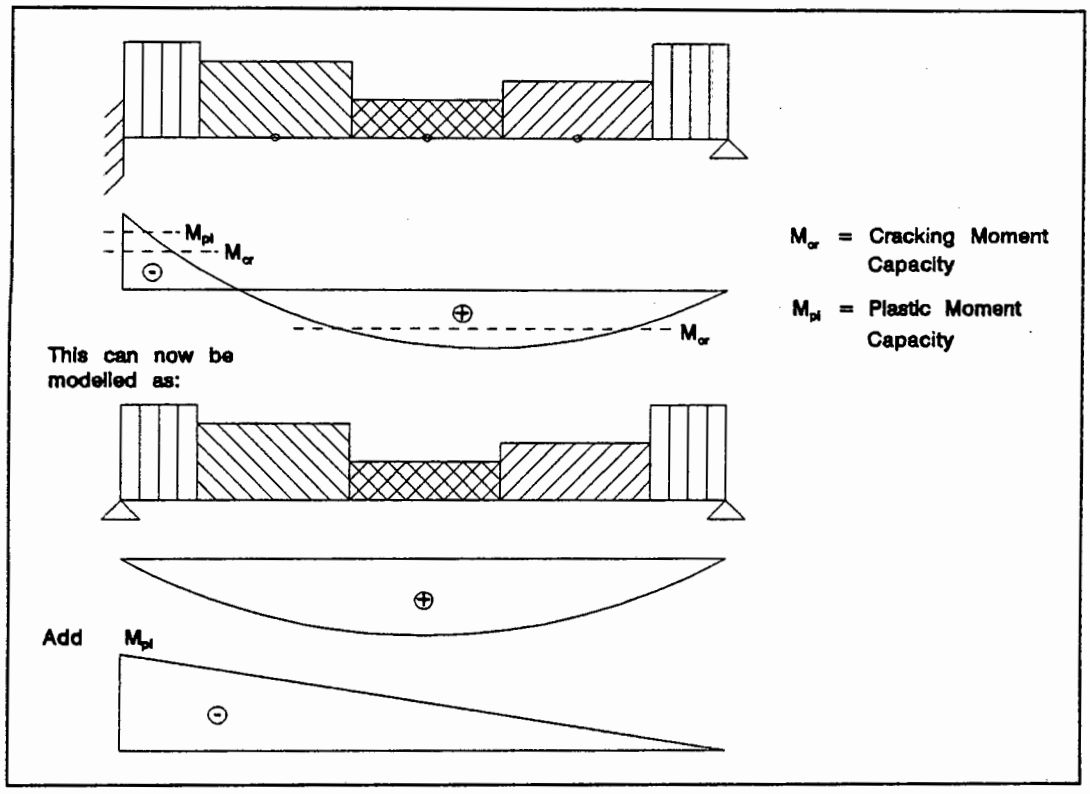

Fig 3.4 - New model for propped cantilever

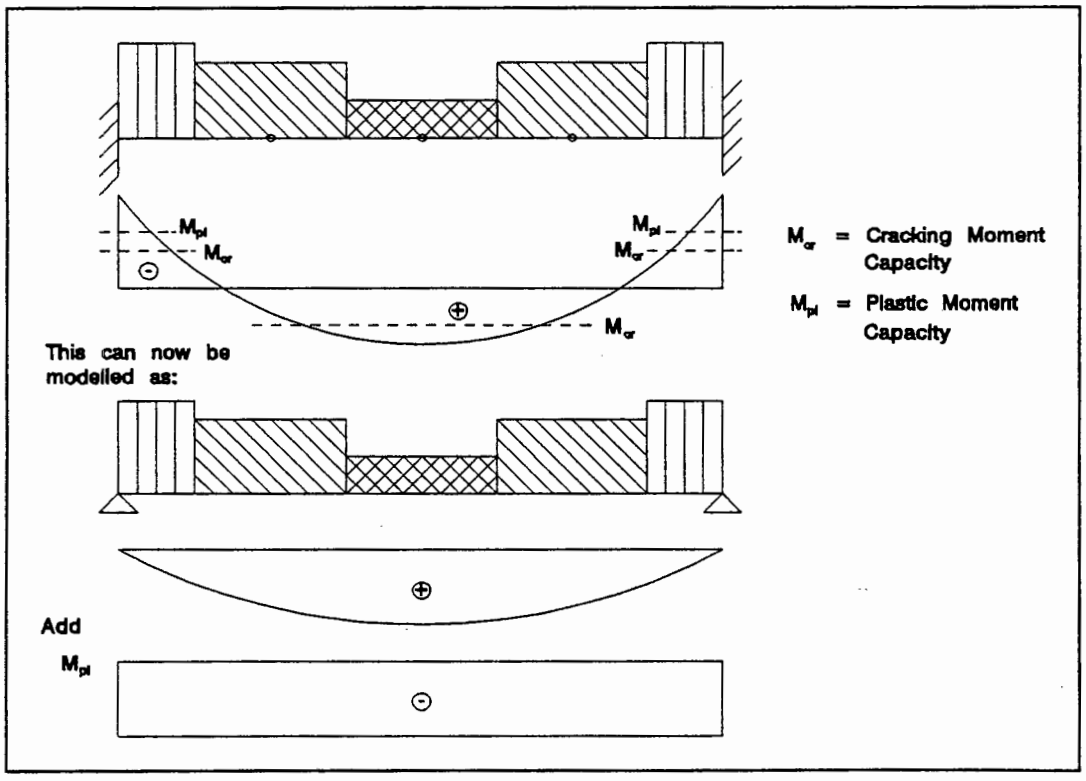

Fig 3.5 - New model for fully encastre beam

This model that is developed is a combination of the Crossing Beam Analogy Method and the Analogous Grid Method described in section 2.4. However, each strip is still separate from the adjacent one and torsional moments are neglected. This factor will be minimized if the slab is divided into more and more strips of smaller width, approaching a type of finite element mesh. For this thesis the number of strips spanning in each direction was kept to five (i.e. nine nodes).

Unfortunately, the model does not hold for slabs supported on only 3 sides and when the side opposite the free edge is only simply supported.

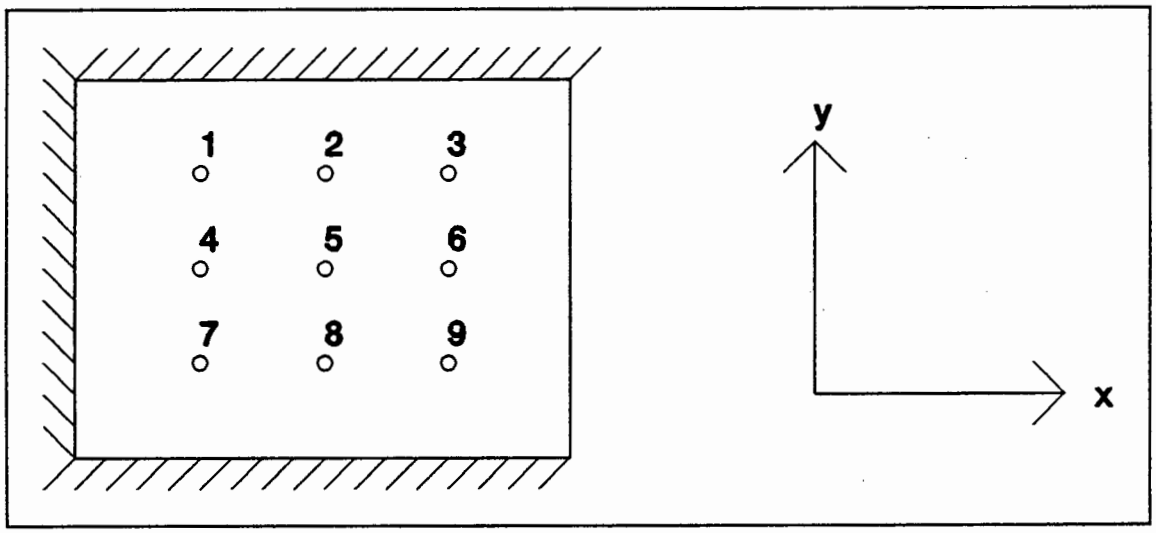

Fig 3.6 - Slab supported on only three sides

A strip running in the x - direction through the middle of the slab (through nodes 4, 5 & 6) would look as follows:

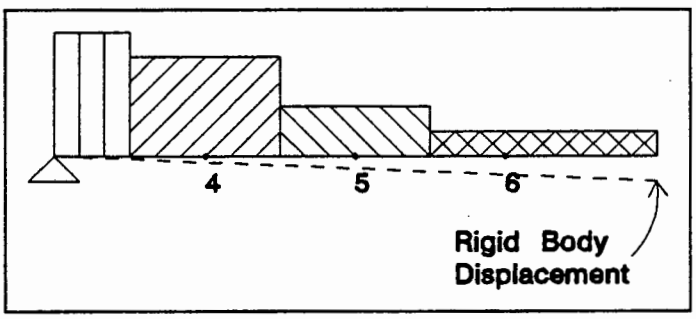

Fig 3.7 - Rigid body displacement

If rigid body displacement due to no moment restraints in the x-direction takes place, then the displacement at node 5 would be twice the displacement at node 4, and the displacement at node 6 would be three times the displacement at node 4. However, none of the displacements at nodes 4, 5 & 6 can be determined independently of the others, since the beam model is a mechanism in the x-direction.

The anticipation of rigid body displacement is also a faulty one, since the beam will curve downwards due to the phenomenon of anticlastic curvature. Anticlastic curvature can best be described by observing the bending pattern of a flat plate of finite thickness.

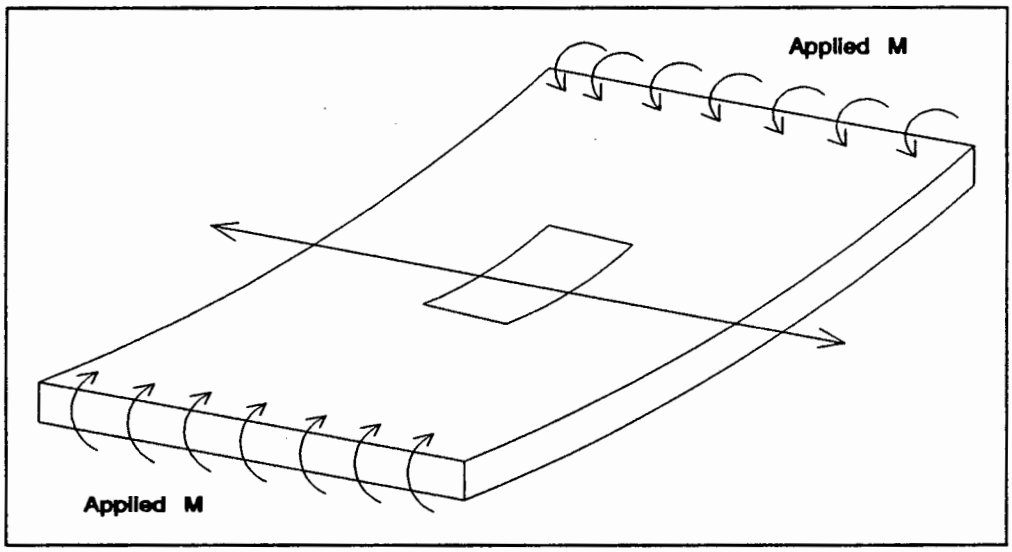

Fig 3.8 - Plate bending about one axis

Assume the plate bends primarily as shown in the figure due to external loads. If the square element on the upper surface of the plate is examined, it will be seen that the element will be in compression in the plane of the bending and will shorten. Due to the Poisson effect, the element will therefore extend or lengthen in the perpendicular plane and will undergo tensile strain in the upper surface.

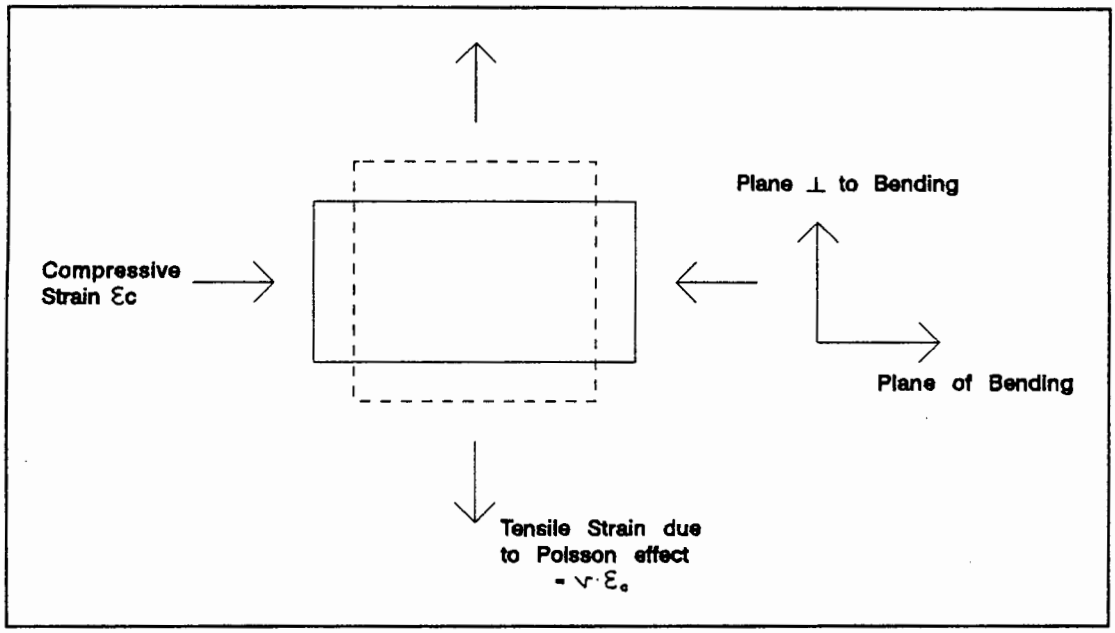

Fig 3.9 - Poisson effect on a small element stressed in the plane of bending only

On the lower surface of the plate, a similar element will undergo the opposite effect. The fibres of plate in the direction of the bending will undergo extension due to the tensile strain. In the plane perpendicular to the bending the fibre will undergo compressive strain due to the Poisson effect in the lower surface. The combined effects of the foregoing will cause the plate to bend in a plane perpendicular to the applied primary moment, but in an opposite sense to that of the plane of the applied primary load.

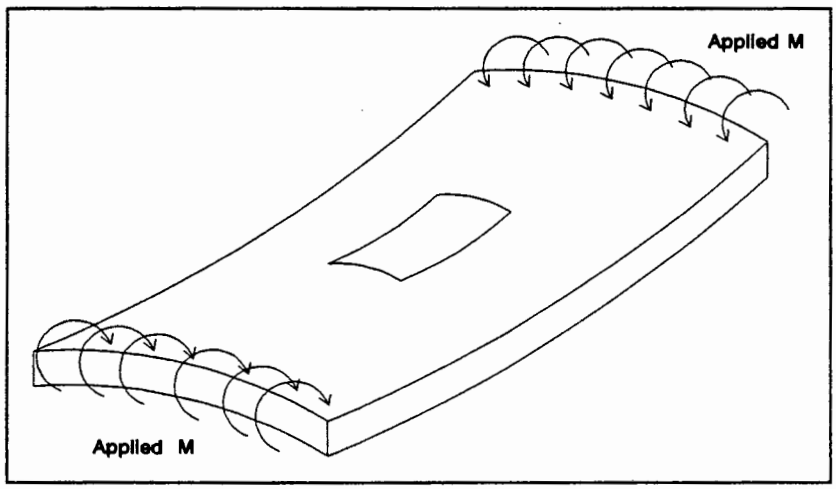

Fig 3.10 - Bending of a plate

This anticlastic curvature will cause the plate considered earlier to curve in a convex manner seen from above. The anticlastic curvature will be compounded by cracking that will occur in the plane of the two opposite supporting edges (y-plane in figure 3.6). No cracking will occur in the x-plane since the plate is a mechanism and cannot carry any moments in this direction.

The phenomenon of anticlastic curvature is present in all the slabs and not only in the case described above. For a horizontal slab subjected to downward loading causing bending about both its two principal axes, the Poisson effect due to the loads about the secondary axes will to a certain degree limit the bending due to the loading about the primary axis. This will result in measured deflections being less than those obtained with the model proposed in this thesis, since this model has not taken the Poisson effect into account.

Another phenomenon also ignored by the proposed model is the effect of the surface-layer shearing action. While this shearing action has been known of for a long time, it is extremely complicated to model and to date has not been successfully modelled.

Looking at a horizontal slab from the tension side, for cracks to occur (as shown) the slab will have to displace slightly outwards at the edges.

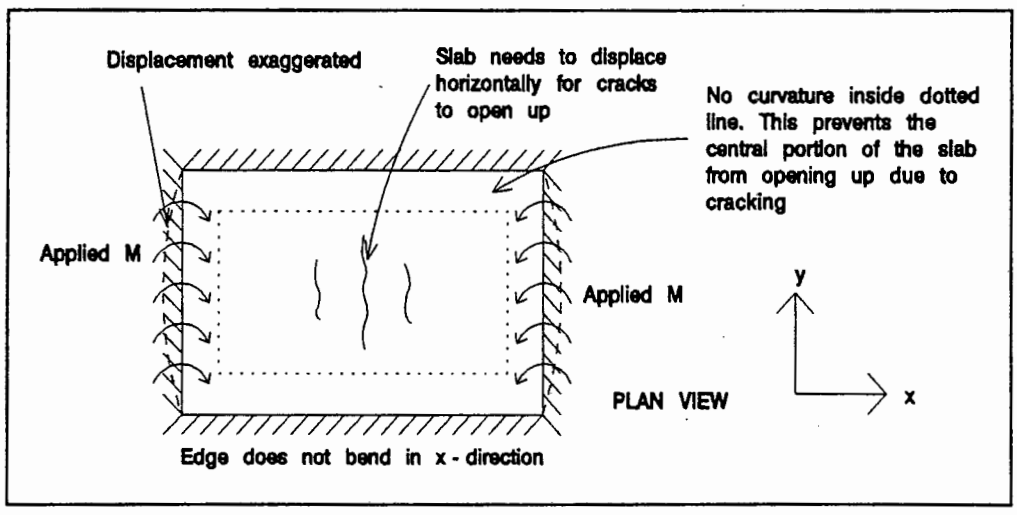

Fig 3.11 - In-plane displacement of a slab

However, the adjacent uncracked portions of the slab will resist this transverse movement. Since the slab is extremely stiff in its own plane, these internal resisting forces can be very high. This will result in cracking long after the unrestrained cracking moment has been exceeded. The edge conditions of the slab are also important factors since this phenomenon will only occur in slabs supported on all four edges, i.e. there has to be an external restraint on all the edges. If all sides of the slab are supported, then the sides will have no curvature and will not be able to extend to allow the cracks to open up.

Membrane action will not be present for the slabs tested in the laboratory, but must be considered for most other in-situ slabs. The slabs tested in the laboratory were supported by a layer of rubber on top of the supporting frame. This rubber is not very stiff in shear and will not provide any restraint against the edge of the slab moving in-plane due to the bending. If the end constraints of the slab prevented in-plane displacement then the deflections would be even less since the slab would physically have to extend on the bottom surface to allow for this deflection. Similarly, the top surface would have to shorten.

The combination of the Poisson effect and the surface-shearing action will always show the observed deflections to be lower than the deflections predicted by the proposed model for slabs supported on all four sides.

3.2 MODEL 2 FOR DEFLECTIONS

When determining the maximum deflection, only the strip of slab ("beam") which will contain this maximum deflection, in each of the x- and y- directions, need be considered. The maximum deflection is determined for the "beam" spanning in each of the x- and y-directions. In the case of the two deflections not being equal, the average of the two deflections may be taken.

In the case of the cracking moment not being exceeded, the deflection is determined using elastic formulae and uncracked moments of inertia. If the cracking moment is exceeded then the following model is proposed.

The deflection of a beam subjected to cracking is made up of two parts. The first contribution will be due to an elastic deflection, while the second contribution is ascribed to cracking. This is illustrated by the next set of diagrams.

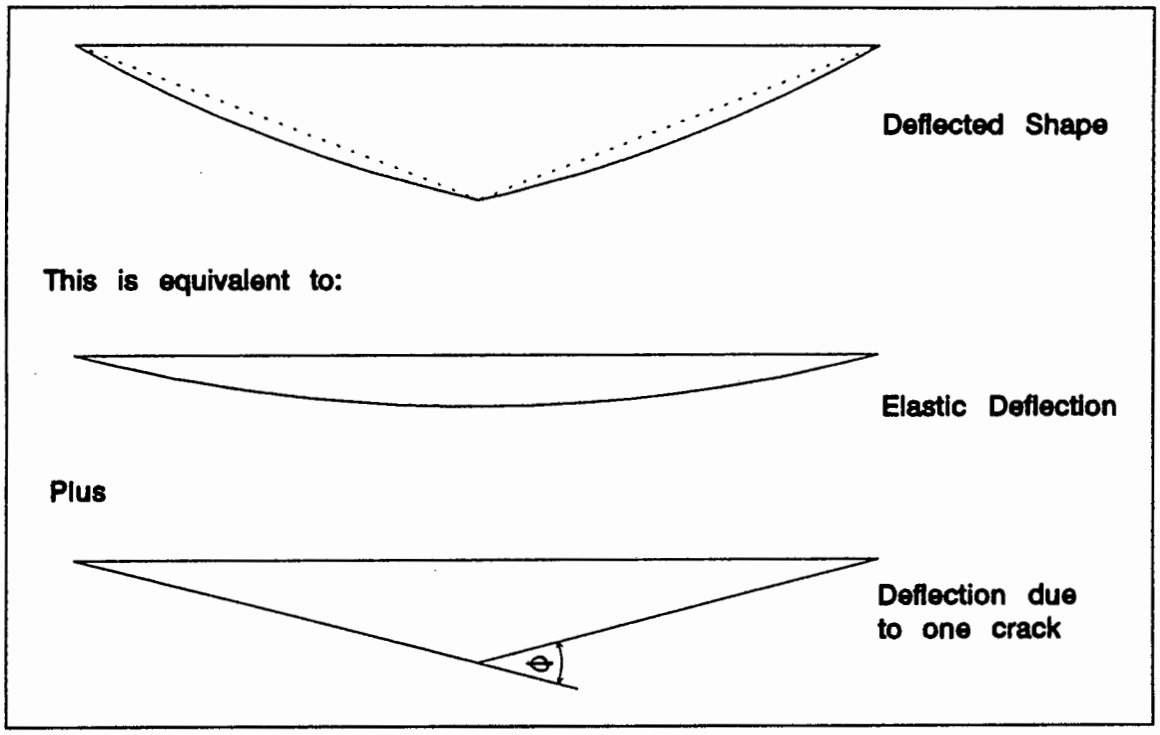

Fig 3.12 - Deflection model

In order to obtain θ, the zone in which cracking occurs needs to be identified. This is the zone in which the bending moment exceeds the cracking moment capacity of the strip.

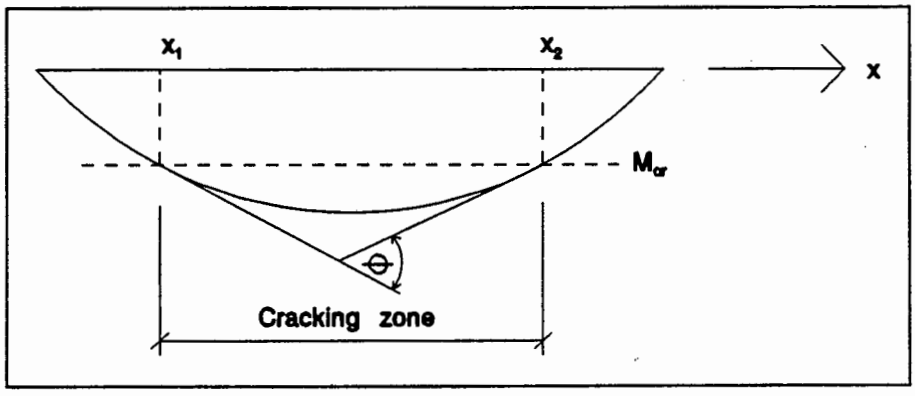

Fig 3.13 - Cracking zone

Assume that all the cracking over this zone is lumped together to form one single crack at the position of maximum moment. The rotation that this "hinge" undergoes is equal to the integral of the curvatures across all cracks in the cracking zone.

In this cracking zone the concrete consists of cracked and uncracked sections. The length of the cracked section in the cracking zone can be determined by the factor ζ. This factor was developed in the Manual on the CEB/FIP Model Code on cracking and deflection[3], as described in Chapter 2.3. Thus, the rotation of the hinge will be equal to the integration of the curvature over this cracked length.

$$\theta = \zeta \int_{x_1}^{x_2} \frac{M}{E\, I_{cr}}\, dx$$

where

$$\zeta = 1 - \beta_1\, \beta_2\, M_{cr}^2/M_m^2$$

M_m = geometric mean of the maximum moment occurring in the cracked zone and the cracking moment

$= (M_{max}\, M_{cr})^{0.5}$

This is similar to the development of the bilinear model proposed in the Manual on the CEB/FIP Model Code[3], except that in the Manual cracking was assumed to occur uniformly over the entire element length.

In the case of statically indeterminate horizontal beams with downward loading (i.e. propped cantilevers or beams built-in at both ends), only the zone in which the sagging moment exceeds the cracking moment needs to be considered. The hogging moment at the supports is always higher and will exceed the cracking moment capacity of the support zone long before the cracking moment capacity in sagging is exceeded at the point of maximum sagging moment. For a cracking "hinge" to occur at midspan, a cracking hinge will always occur at the supports.

Once θ is known, the cracking deflection δ can be easily determined from trigonometry.

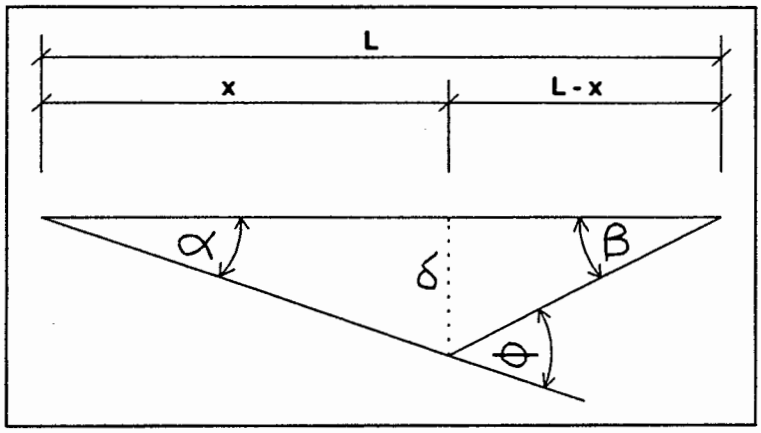

Fig 3.14 - Calculation of deflection due to cracked hinge

The hinge is placed at the position of maximum moment. The distance x is therefore known.

<u>Now:</u> $\tan \alpha = \delta/x$ $\quad\quad$ $\tan \beta = \delta/(L-x)$

$\delta = x \tan \alpha$ $\quad\quad$ $\delta = (L-x) \tan \beta$

therefore $x \tan \alpha = (L-x) \tan \beta$

If small angle theory is used, then $\alpha \approx \tan \alpha$

$\beta \approx \tan \beta$

thus, $x\,\alpha = (L-x)\,\beta$

and $\alpha = [(L-x)/x]\,\beta$ ... eqn 1

but $\alpha+\beta = \theta$

therefore $\beta = \theta-\alpha$

substituting into eqn 1

$\alpha = [(L-x)/x]\,(\theta-\alpha)$

$(\theta-\alpha)/\alpha = x/(L-x)$

$\theta/\alpha - 1 = x/(L-x)$

$\theta/\alpha = x/(L-x) + 1$

$= L/(L-x)$

therefore $\alpha = \theta\,(L-x)/L$

Now $\delta = x \tan \alpha$

$= x \tan (\theta\,(L-x)/L)$

The deflections thus computed are only short-term (instantaneous) deflections.

3.3 DEVELOPMENT OF THE COMPUTER PROGRAM

The computer program is written in True Basic version 3.04. A printout of the program as well as a disk containing the program has been handed in to the department.

The main program consists of three separate files, with the option of using two more for storing data. The first file is called "Main" and determines all the necessary data. Data can either be input by hand or by using the file "Writer". If the file "Writer" is used and run, then all the data is stored in a file called "Data.inp" and is accessed by the first file "Main".

The second file in the main program is called "Sub1". This program determines the load dispersion of the slab taking all the parameters into account. The third file in the main program is called "Sub2". This program determines the extent of cracking, whether the plastic moment is reached and then computes elastic deflections and deflections due to cracking.

The following flow chart best illustrates this:

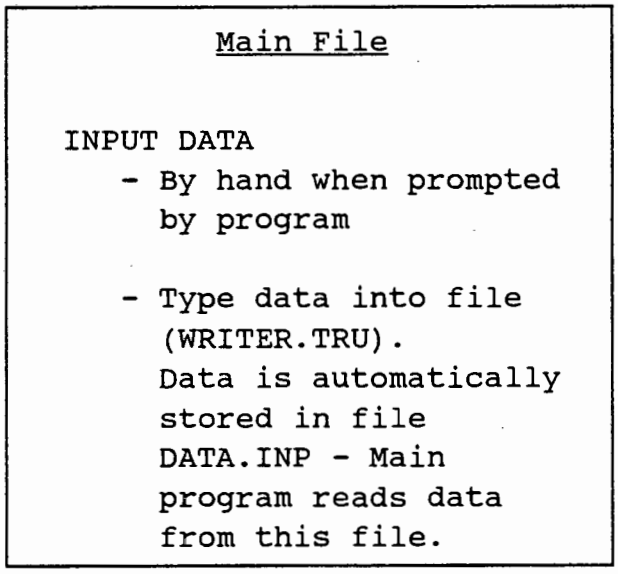

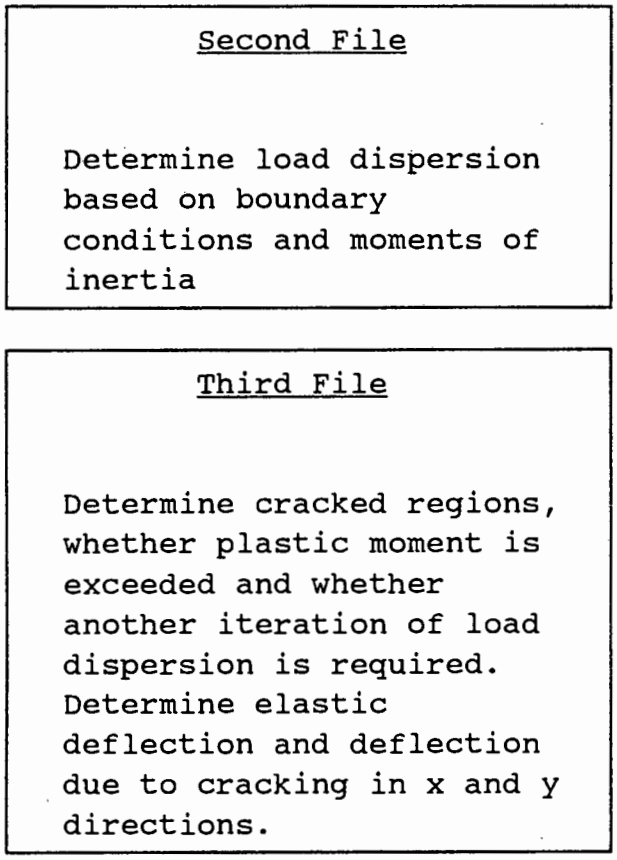

A brief description of each file will follow.

3.3.1 First File - Main

This file requires all the material parameters and dimensions to be input, either by hand or by means of a data file.

The program begins by asking on how many sides the slab is supported (either two, three or four sides). The lengths of the sides are then required, as well as the boundary conditions. The boundary conditions are determined by first looking at the slab spanning in the x-direction and then looking at it spanning in the y-direction. The user has six combinations to choose from. These are:

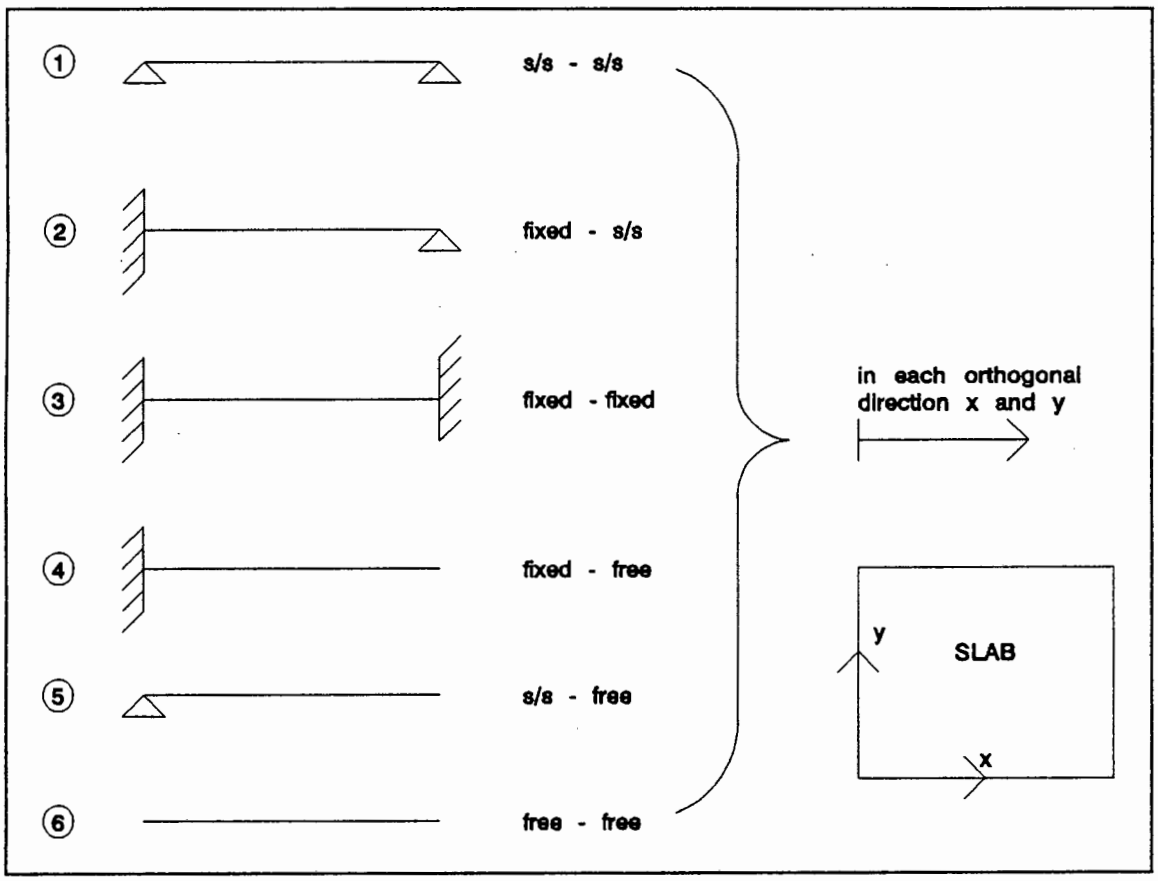

Fig 3.15 - End constraints of strips in slab

It must be noted that in the case of the slab spanning in the x-direction, for the propped cantilever and cantilever cases (case 2 or 4), the clamped edge must be on the datum side (x = 0) of the slab. In the case of the slab spanning in the y-direction, the clamped edge is also the datum side (y = 0) of the slab. Case no 5 (simply-supported edge and free edge) is not used since the model cannot handle that particular set of boundary conditions.

The program now asks for the reinforcement requirements of the slab. The slab is divided into five zones in each of the x- and y-directions. The zones correspond to those described in section 3.1 and can be seen in the next set of diagrams.

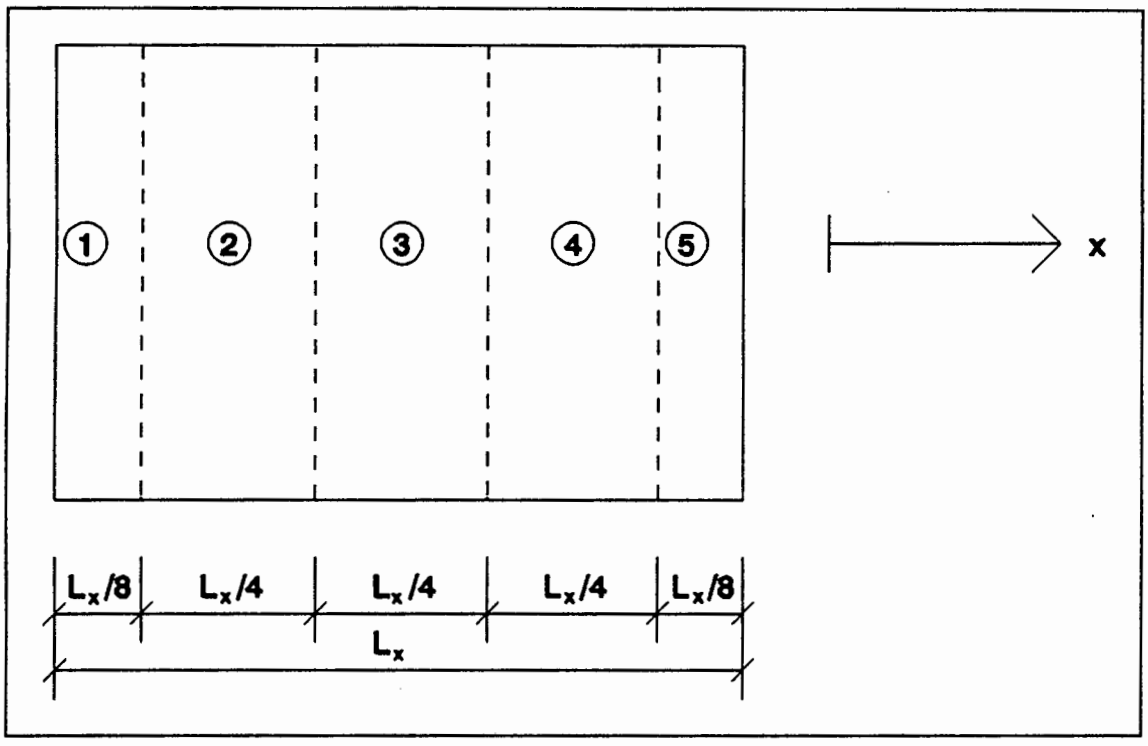

Fig 3.16 - Regions for reinforcement spanning in the x-direction

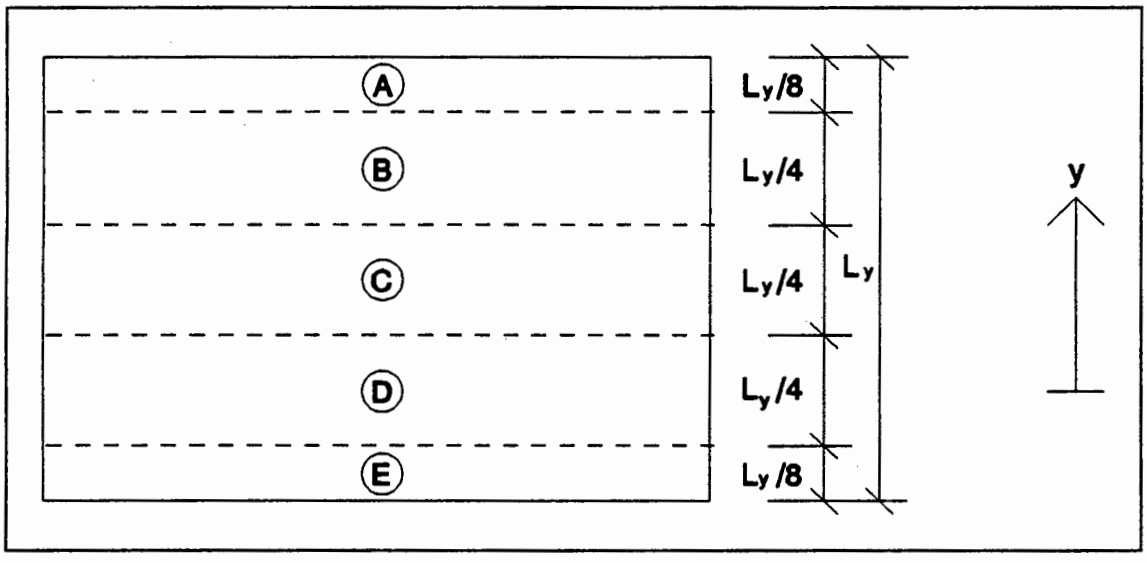

Fig 3.17 - Regions for reinforcement spanning in the y-direction

The following parameters are also required:

f_{cu} - cube strength of the concrete (in MPa)
h - depth of slab (in m)
ddx,ddy - depth to centre of top reinforcement running in the x- and y-directions respectively (in m)
dx, dy - depth to centre of bottom reinforcement running in the x-direction (in m)
wa - service load (in N/m^2)
f_y - ultimate stress of the steel (in MPa)
h or m - high strength or mild steel reinforcing bars
f or l - first time or long-term (cyclic) loading

The program then works out the following parameters:

β_1 - (Beta1) - see section 3.2
β_2 - (Beta2) - see section 3.2
E_c - Young's Modulus of Concrete - see Appendix B
I_{xuncr}, I_{yuncr} - uncracked moment of inertia for strips spanning in the x- and y-directions respectively (one for each zone) - see Appendix B
I_{xcr} , I_{ycr} - cracked moment of inertia in sagging for strips spanning in the x- and y-directions respectively (one for each zone) - see Appendix B
I_{xdcr}, I_{ydcr} - cracked moment of inertia in hogging for strips spanning in the x- and y-directions respectively (one for each zone) - see Appendix B
M_{crx} , M_{cry} - cracking moment capacity in sagging (for each zone) for strips spanning in the x- and y-directions respectively - see Appendix B
M_{crxd}, M_{cryd} - cracking moment capacity in hogging (for each zone) for strips spanning in the x- and y-directions respectively - see Appendix B
M_{plx} , M_{ply} - plastic hogging moment capacity for support zones for strips spanning in the x- and y-directions respectively - see Appendix B

The two files "WRITER.TRU" and "DATA.INP" are included for when many similar slabs need to be analyzed and only one or a few of the parameters are changed every time the program is run. All the data is stored in these files, they are easily accessed and only the relevant changes need to be made.

Once these parameters have all been determined, the program calls the next file "SUB1" into execution.

3.3.2 Second File - SUB1

This program determines the load dispersion on the slab, taking into account the moments of inertia, the boundary conditions and the dimensions of the slab.

The deflection formulae developed in section 3.1 and Appendix A are inserted as part of the program. The deflection at each node is determined in terms of the loads for strips spanning in both the x- and the y-direction. The deflection in the x- and the y-direction are set equal. There are nine nodes, so nine equations are set up. In effect, there are eighteen unknown parameters (there are 2 fractions of load at each node, one for the strip spanning in the x-direction and one for the strip spanning in the y-direction). These eighteen unknown parameters are reduced to nine by the fact that the sum of the two fractions of load at a node must be equal to one, i.e. the full load at the node.

The program then draws a diagram of the slab with associated boundary conditions and the load dispersion at each node is shown. This is reproduced in the next figure.

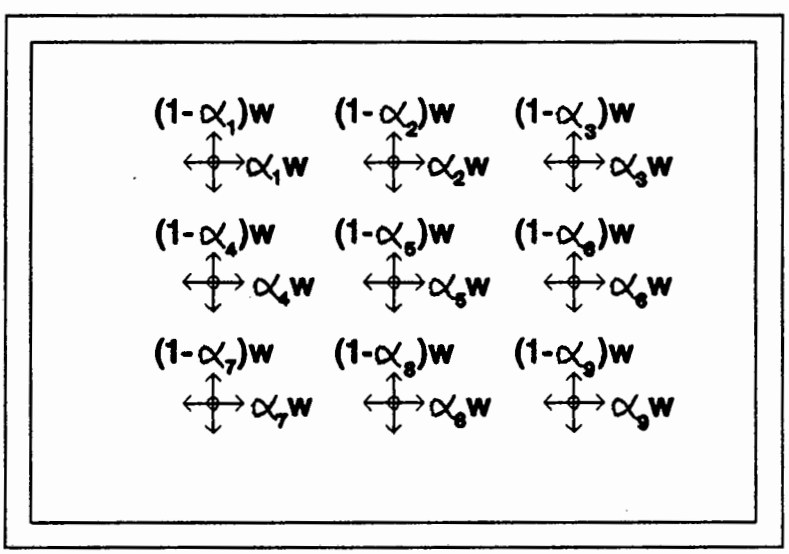

Fig 3.18 - Load dispersion displayed on computer screen

As was mentioned before, the model developed here cannot handle the case of a strip being simply supported on one end and free on the other end. This case is a mechanism without bending moments. Consequently, no deflection equation can be developed. Initially it was decided to include cantilevers and deflection formulae were developed for them (see Appendix A4). A problem arises, however, when the plastic moment at the support of the cantilever is exceeded, the beam then becomes the mechanism described above. The program still works out the load dispersion though, but doesn't execute any further once this has been achieved. By looking at an example of a square slab, the load at the free edge spans completely parallel to the free edge (as shown in the next figure). Since only the region of maximum deflection is of importance, the problem can thus be treated as one-way spanning. The case shown in the figure below is, for a square slab supported on three edges, where the clamped edge opposite the free edge will have the most influence on the load dispersion. The stiffness offered by a strip spanning in the perpendicular direction (y-direction) is the lowest one can get, i.e. a strip simply supported at both ends.

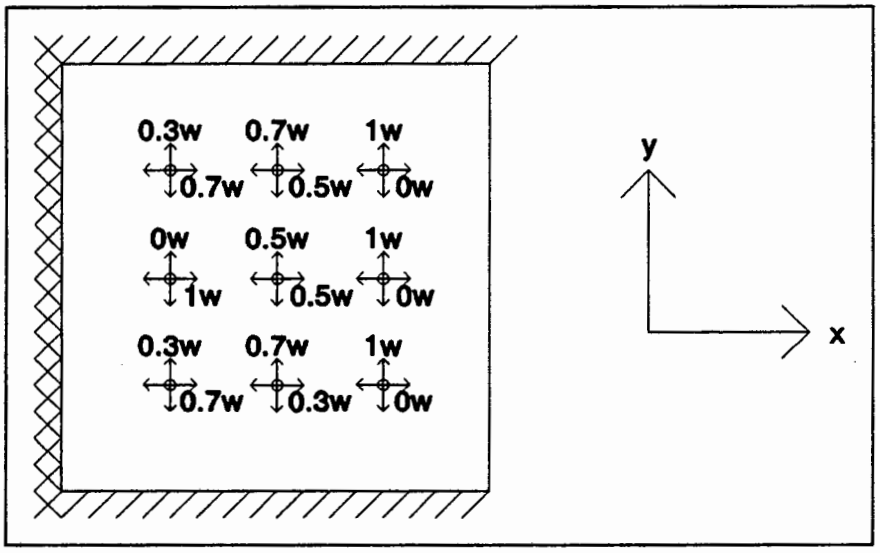

Fig 3.19 - Load dispersion of a slab supported on three edges

All the slabs that were supported on three edges were thus treated as one-way spanning. This assumption, however, becomes inaccurate as the ratio of the length of the side parallel to the free edge to the lengths of the adjacent sides increases.

Once the load dispersion has been determined, the program calls the third file, SUB2, into execution.

3.3.3 Third File - Sub 2

The first function of this file is to determine which sections of the slab are cracked. The bending moments along the entire lengths of the strips spanning in both the x and y-directions are determined. If these bending moments exceed the cracking moment, then the exact position of the cracking zone for each respective strip is calculated. The effective moments of inertia for each of the five zones for each beam are calculated - this procedure was described in section 3.1. The second program, SUB1, is again called into execution to determine the new load dispersion.

It became apparent, however, that this procedure is inappropriate. In most cases only the two middle strips experience cracking under serviceability loading conditions. When their cracked stiffnesses are calculated and the new load dispersion determined, these two middle strips carry minimal load and the other strips carry the majority of the load (as shown in the diagram below). In other words, the strips at quarter span and three-quarter span are now deflecting more than the middle strips, which clearly should not happen.

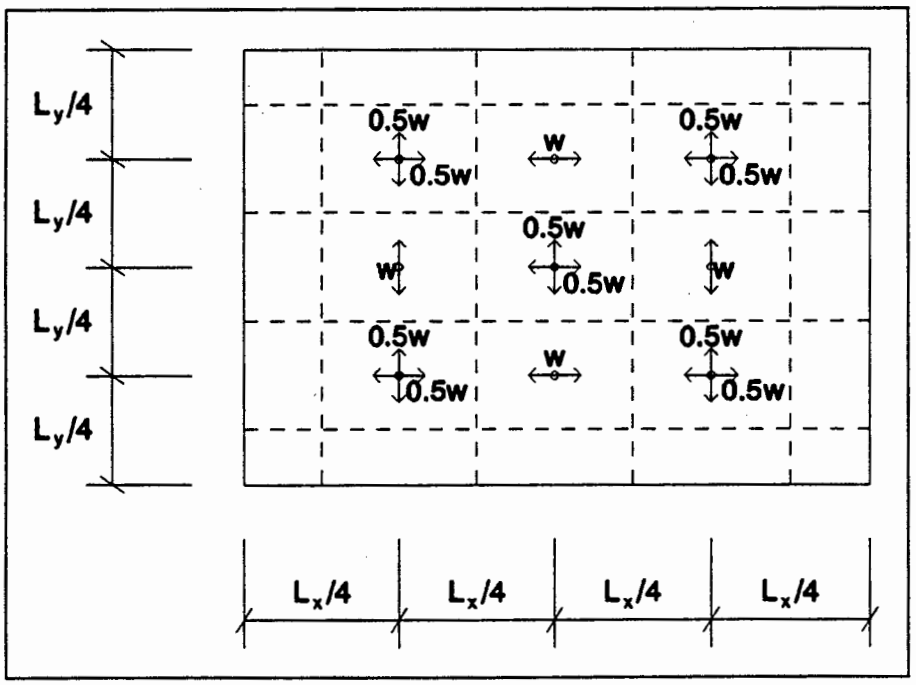

Fig 3.20 - Load dispersion for cracked middle strips

If new stiffnesses are now calculated on this load dispersion, then the strips at quarter span and at three-quarter span become cracked, while the middle strips become uncracked. Once again a new load dispersion is determined, but now the majority of the load is carried by the middle strips and the outer strips carry minimal load - see diagram below.

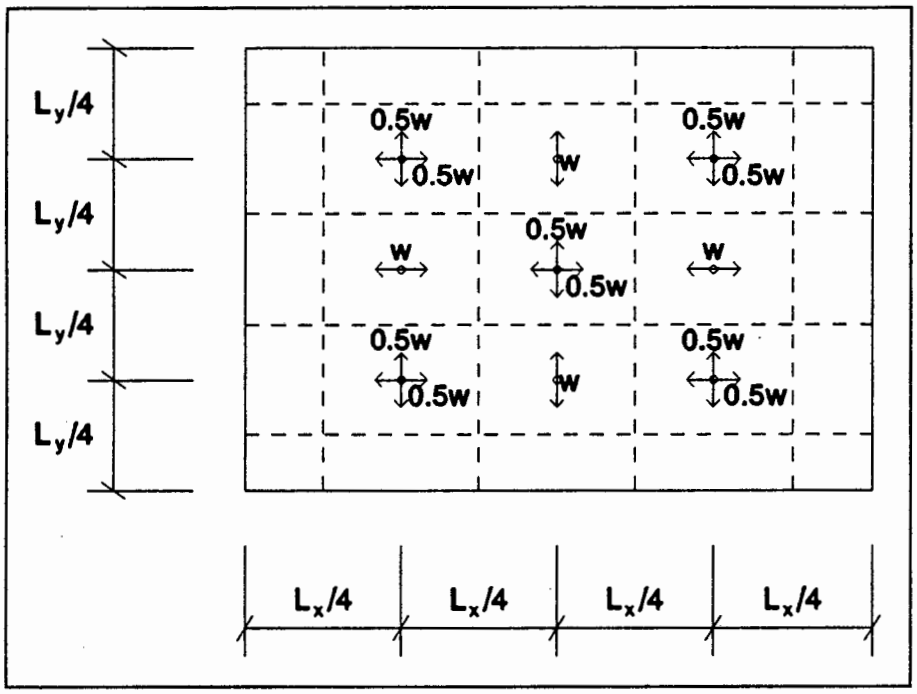

Fig 3.21 - Load dispersion for cracked strips at quarter and three-quarter span

Successive iterations do not yield better load dispersions.

To solve this problem, it was decided to approach the true cracking lengths of each strip asymptotically. To do this, the cracking lengths of each strip are calculated for the load dispersion based on uncracked properties. However, instead of using this full cracked length to determine the new section properties, only half this length is used.

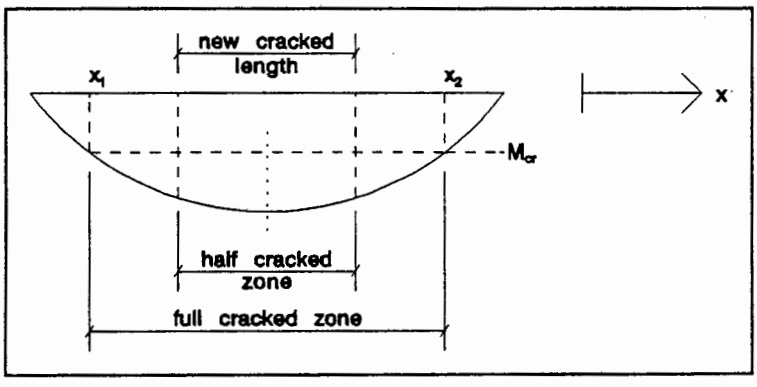

Fig 3.22 - Full and half cracked zones

A new load dispersion is calculated and the new bending moment diagram and cracked zone are calculated. Once again, instead of using the new calculated cracked zone, the average between the previous cracked zone and the new one is used. This procedure is repeated until the difference between the cracked lengths for successive iterations for all strips is less than an eightieth of the span of the strip being considered (i.e. < L/80).

This method appears to be realistic in that the middle strips clearly deflect more than the strips at quarter and three-quarter span. This entire procedure is only applicable to two-way spanning slabs, i.e. slabs supported on all four sides.

From this stage on the program only concerns itself with the two middle strips. The maximum deflection of the slab will fall within the area covered by these two strips when crossing each other.

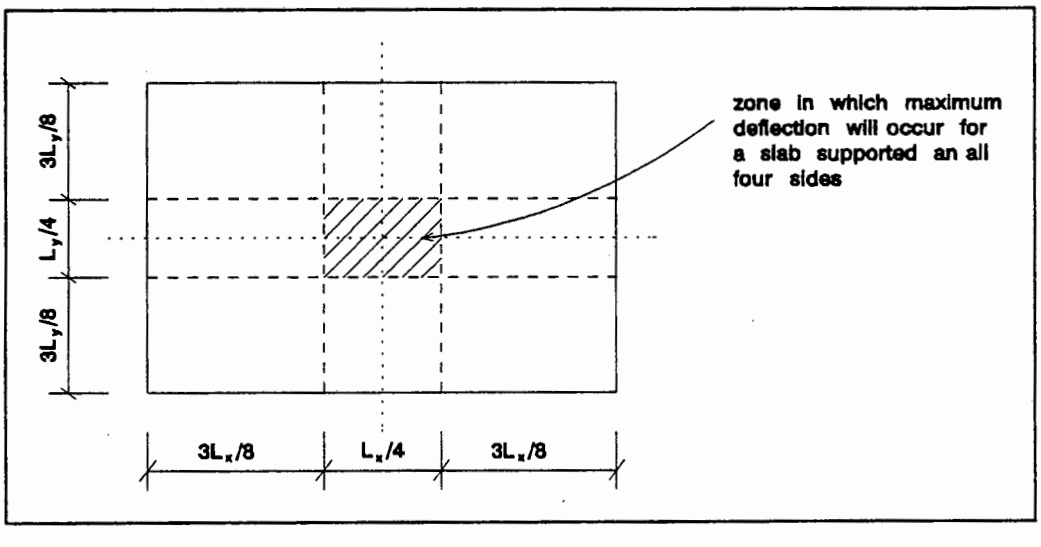

Fig 3.23 - Zone for occurrence of maximum deflection

For a strip that is either simply-supported at both ends or fully fixed at both ends, the maximum deflection will occur at the centre. These two cases are symmetrical about their centres in all respects, including loading. For a propped cantilever (fully fixed at one end and simply-supported at the other), the maximum deflection for a uniformly distributed load occurs at five-eighths of the span (5L/8) from the fixed edge. This is exactly on the boundary of the region bounded by the crossing of the two orthogonal middle strips. However, the equivalent load is not uniformly distributed, it is varying. The clamped or fixed edge will cause more load to be acting on that side of the strip than on the simply-supported side. This will cause the maximum deflection to occur somewhere between half and five-eights of the span from the fixed edge. This is within the zone shown in fig 3.23.

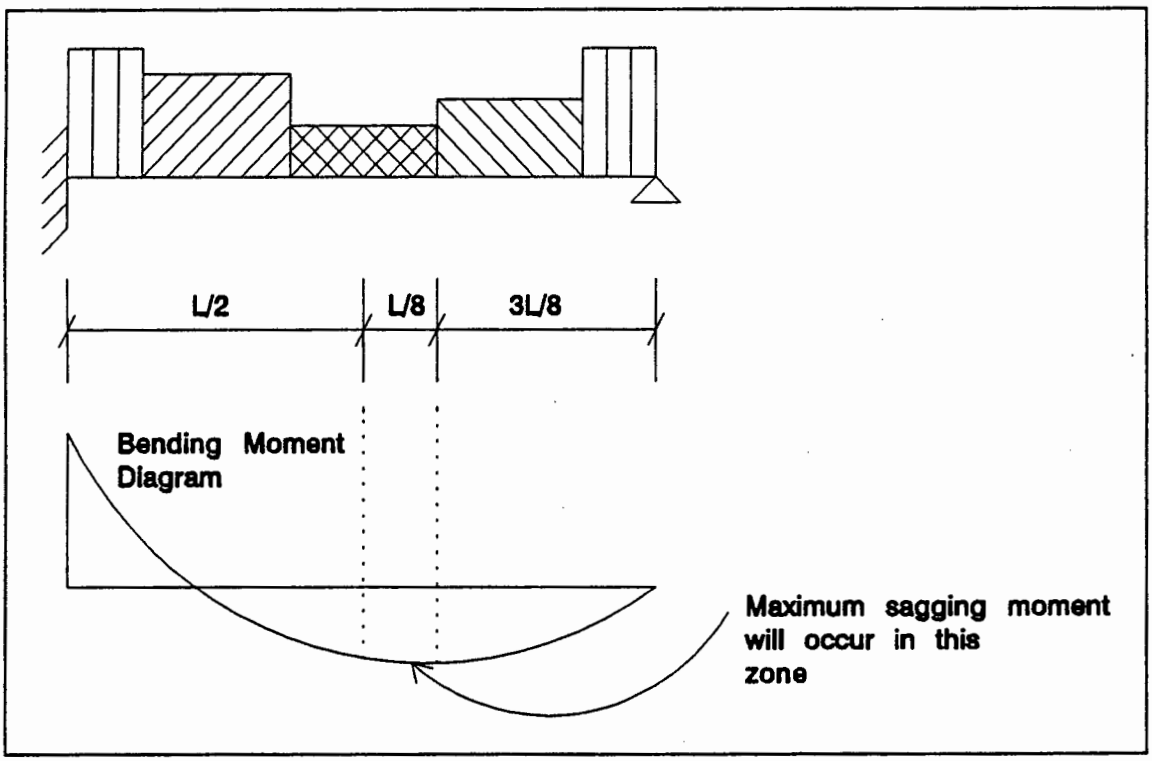

Fig 3.24 - Region of maximum sagging moment for a propped cantilever

It is therefore considered to be a reasonable assumption to only work out the maximum deflection of each of the two orthogonal middle strips.

The program determines the moment at the support for fixed edges. If the plastic moment is exceeded, the relevant changes as described in section 3.1. are made and the entire load dispersion iteration procedure is repeated.

Once the final load dispersion is known, deflections can be calculated. Firstly the elastic deflections are calculated. Elastic deflection formulae have been programmed into the file. For the "beams" simply-supported at both ends or fully fixed at both ends, only the midspan deflection is calculated. For the propped cantilever the deflections from midspan to five-eighths of the span from the support at increments of one-eightieth of the span are calculated. The position of maximum deflection is recorded.

Now cracked deflections are calculated by using the model described in section 3.2. The "cracked hinge" is assumed to occur at midspan for beams simply-supported at both ends or fully fixed at both ends. For the propped cantilever case, the hinge is assumed to occur at the position of maximum elastic deflection.

The elastic deflection and the deflection due to cracking are added for each of the strips spanning in the x- and y-directions. These totals are compared to one another and the average of the two deflections is given.

As a comparison, the deflections are calculated using the formulae developed in Appendix A. These are the deflections that were used to determine the load dispersion at the nine nodes and were developed by integrating the shear force diagrams three times. The maximum deflection for the middle strips spanning in the x- and y-directions are thus given, as well as the average of the two values.

For one-way spanning slabs the whole procedure is the same, except that the load dispersion need not be determined. The entire load spans in the direction of the support. The effect of cracking and plasticity are still taken into account, as previously.

CHAPTER 4

EXPERIMENTAL RESULTS

The results of four undergraduate theses have been used. Each thesis investigated the short-term deflections of various slab configurations under simulated uniformly distributed loads in the laboratory. The edge constraints of the slabs were varied to provide either a simply-supported, fixed or free edge. Deflections of the slab were monitored by a grid of dial gauges placed under the slab. The load was incrementally increased until failure of the slab occurred.

A yield-line analysis was performed for each slab configuration (see Appendix C5 for an example) for comparison and to determine the design ultimate load. This value was then divided by a factor of 1.6 to determine the design serviceability load for that particular slab. The value of 1.6 was arrived at by using only the imposed load factor given in CP 110:Part 1:1972[13] clause 2.3.3.1.(1). Since the dead load of the slabs tested in the laboratory contributes only slightly to the uniformly distributed load (in the order of 1% to 8%) it was decided to ignore the effect of the dead load factor - 1.4 as given in CP 110:Part 1:1972[13] clause 2.3.3.1.(1). The maximum deflection of each slab at this serviceability load was then read from load versus deflection curves drawn up for the respective slabs. These deflections are the ones used for a comparison with the deflections derived by using the model propsed in chapter 3.

The maximum deflection of each slab at a common total load (10 kN or 15 kN) for a given set of slab configurations was determined in the same manner. This maximum deflection at the predetermined load was used as an extra criterion to find any anomalies in the testing of the slabs.

Each undergraduate thesis will now be examined separately and the results analyzed. In the following tables, two deflection values are given for each slab. The first is the maximum deflection at the service load for that particular slab and the second deflection value is the maximum deflection at the predetermined common load for that set of slab configurations. The following key can be used for the figures that follow:

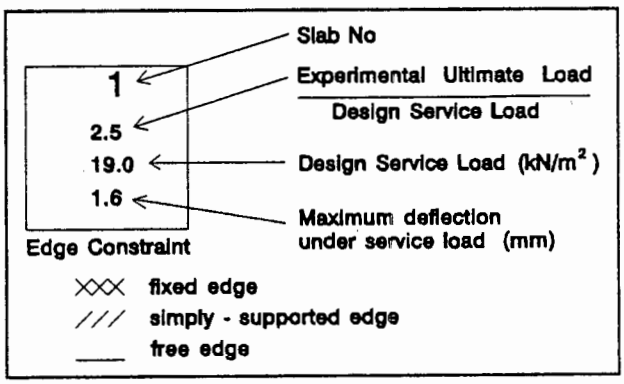

FIG 4.1 - Key for slab lay-outs

4.1 SQUARE SLABS CRUDGE[14]

The slab dimensions are 0.82m by 0.82m by 0.027m.

SQUARE SLABS A
RESULTS OF THESIS BY R. CRUDGE[14] - 1987
fy = 500 MPa

Slab No	f_{cu} (MPa)	Experimental Ultimate Load (kN/m²)	Design Ultimate Load (kN/m²)
1	46.4	24.7	35.3
2	63.9	16.7	17.7
3	52.8	16.7	10.4
4	52.5	14.7	20.8
5	58.9	24.7	26.1
6	66.1	22.7	25.7
7	44.1	20.7	30.5
8	63.5	24.7	21.6
9	62.0	12.7	13.0
10	46.3	16.7	17.7
11	52.5	18.7	16.9
12	54.4	12.7	14.0
13	54.4	4.7	4.4
14	44.1	8.7	8.8
15	53.5	6.7	6.0

Table 4.1

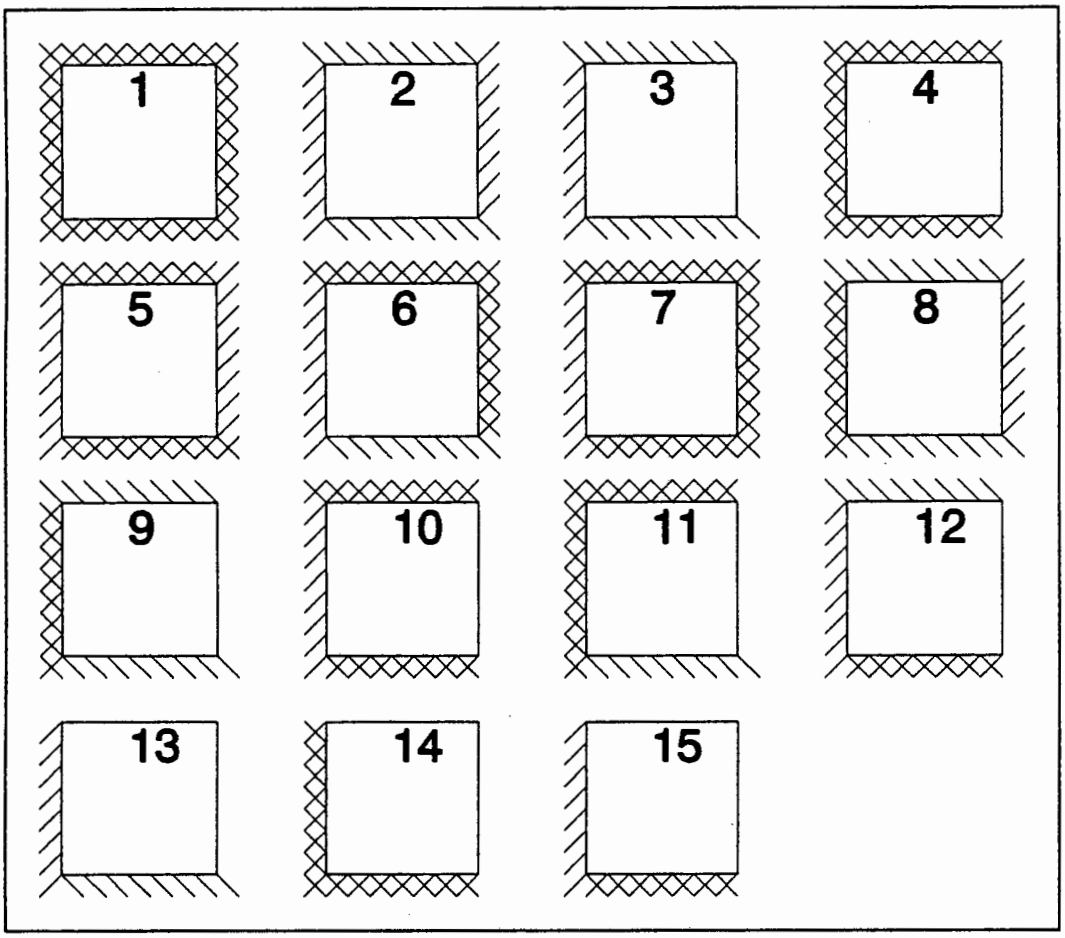

Fig 4.2 - Slab configurations for Square Slabs Crudge

It is not clear, however, at what stage the experimental ultimate load was reached. The student who undertook the testing reported that he tested the slabs until cracks could be seen and assumed this to be the ultimate load. The design ultimate load should always be lower than the experimentally determined ultimate load because of the material factors that take into account the uncertainty of the material parameters of the concrete and the reinforcing steel. As can be seen from table 4.1 this is not so in the majority of cases. It was therefore decided to ignore the results of this thesis. The bar charts of experimental and design ultimate loads can be seen in Appendix C1.

4.2 SQUARE SLABS CHRYSTAL[15]

The slab dimensions are 1.0m by 1.4m by 0.04m.

SQUARE SLABS CHRYSTAL
RESULTS OF THESIS BY A. CHRYSTAL[15] - 1988
fy = 415 MPa

Slab no	f_{cu} (MPa)	Experimental Ultimate Load (kN/m²)	Design Ultimate Load (kN/m²)	Service Load (kN/m²)	Maximum Service Deflection (mm)	Maximum Deflection at 15kN (mm)
1	33.0	47.7	30.4	19.0	1.8	2.0
2	27.3	48.9	37.2	23.3	4.0	2.4
3	21.3	71.1	44.9	28.1	3.5	1.4
4	30.0	60.0	44.3	27.5	3.5	1.7
5	30.0	73.5	52.4	32.8	2.8	0.9
6	30.0	80.0	60.8	37.9	4.0	0.8
7	27.8	28.1	17.9	11.2	2.6	4.4
8	30.0	33.3	22.4	14.0	3.5	2.3
9	30.0	33.7	24.1	15.1	2.4	3.5
10	30.0	36.5	29.0	18.1	5.0	3.3
11	30.0	49.5	30.4	19.0	4.6	2.7
12	30.0	57.5	35.8	22.3	2.1	2.0
13	35.4	18.9	10.1	6.3	1.2	5.3
14	30.0	28.0	14.8	9.2	2.2	4.0
15	30.0	37.0	20.3	12.7	0.9	1.2
16	26.9	13.3	15.2	9.5	11.0	-

Table 4.2

The sixteen slabs were examined in terms of their experimental ultimate loads and maximum deflections at a common load (15 kN). As the degree of fixity of the edge constraints of the slabs increases (i.e. from a free to a simply-supported to a fixed edge) so too should the experimental ultimate load increase. The maximum deflection of the slab at the common load should decrease with increasing fixity. Any slab failing both these two criteria and having any other problems as reported by the student who did

the testing, should be ignored. For these reasons, the results for slabs no. 2, 8 & 16 can be ignored. If a slab only failed one of the above criteria the results are still used.

It was realised that the frame-system supporting the slabs was supported on blocks only at each of its corners, as shown in the figure below.

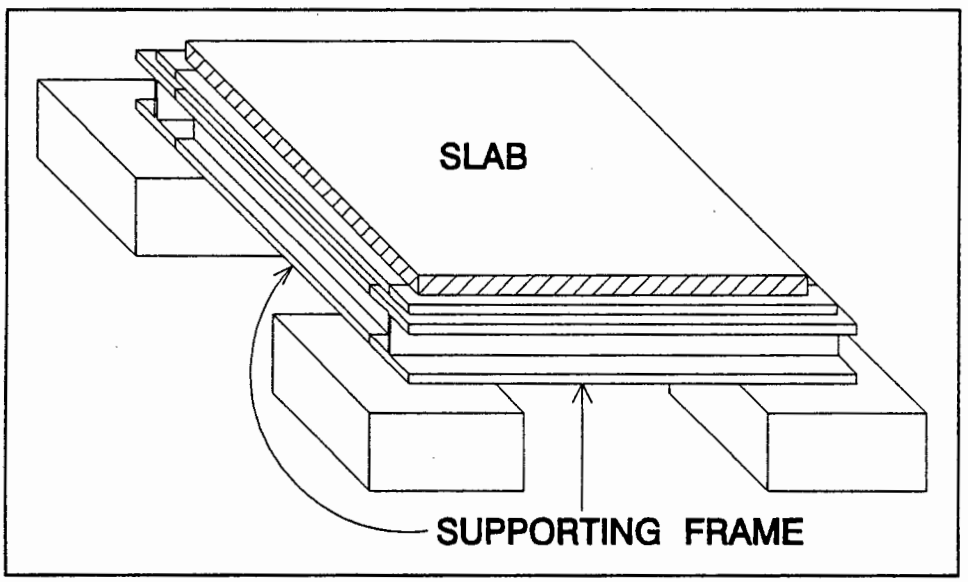

Fig 4.3 - Slab on supporting frame and blocks

This meant that the frame could deflect downwards between corners. This would have caused larger deflections in the slab than would be the case if the frame was completely rigid. Unfortunately the deflections of the frame were not recorded. However, by observing the deflection pattern of the slab some idea of the deflection of the frame can be obtained. The procedure is described below, as well as the method for making allowance for these frame deflections.

The figure on the next page shows a plan view of a slab with the positions of the dial gauges marked in numbers on the slab.

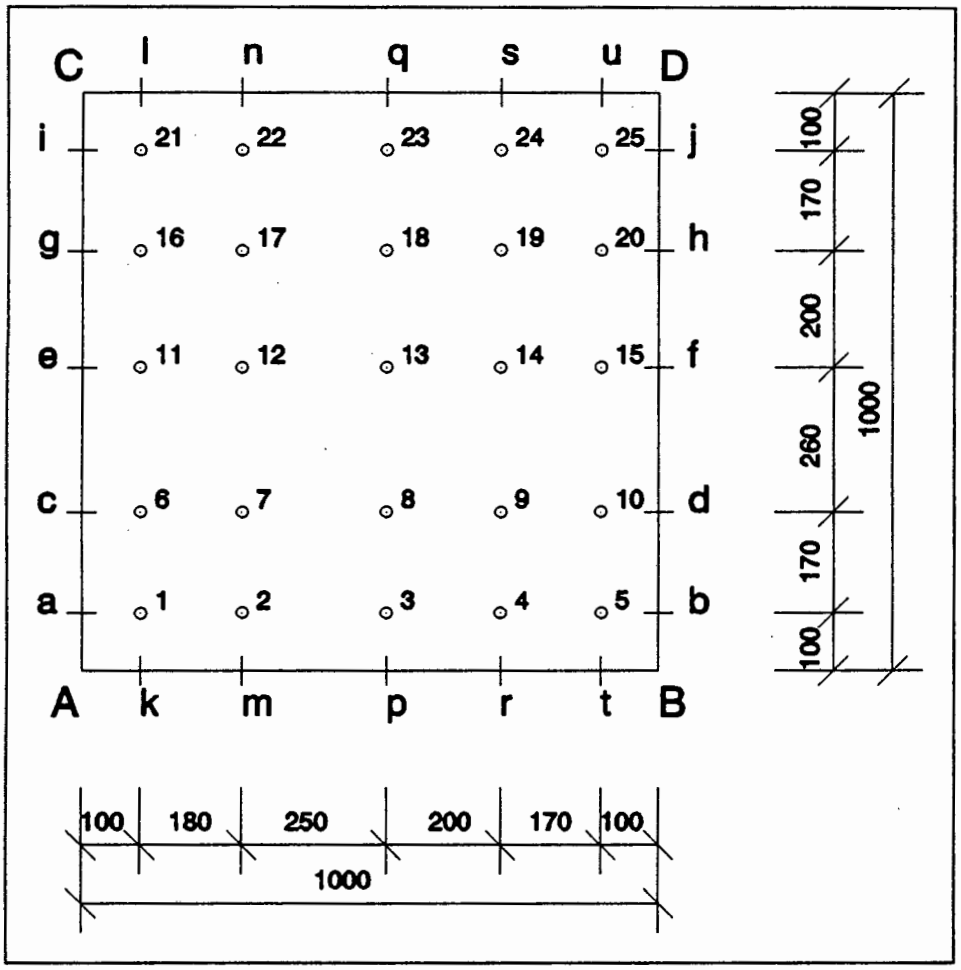

Fig 4.4 - Dial gauge layout for Square Slabs Chrystal

Consider only dial gauges 1, 2, 3, 4 & 5 in one row. A smoothed curve is fitted through the deflection readings and the function extrapolated to give readings for endpoints a & b.

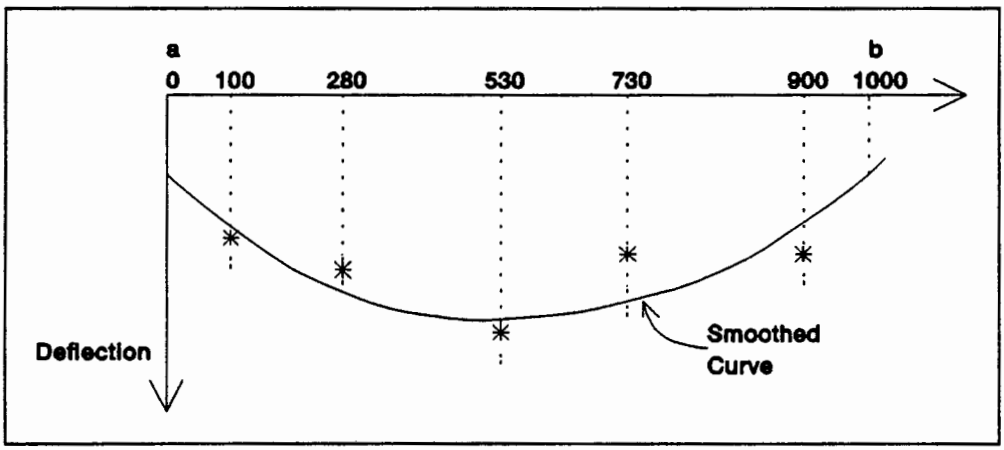

Fig 4.5 - Fitting smoothed curve to dial gauge readings

This procedure is repeated to get readings for endpoints c & d, e & f, g & h and i & j. The procedure is then also used to fit a smoothed curve through points 1, 6, 11, 16 & 21 to give readings at endpoints k & l and likewise for endpoints m & n, p & q, r & s and t & u. Extrapolated dial gauge readings have now been obtained for each of the four frames. Each frame can now be looked at individually and yet another smoothed curve fitted through the five extrapolated points and extrapolated to get deflection values at each of the four corners (labelled A, B, C & D in figure 4.4).

A straight line is then drawn between corner points A & B, C & D, A & C and B & D. Each corner will have two extrapolated readings which are averaged out. A straight line is again drawn between these averaged values. Figure 4.6 shows side C - D of slab 3 in the SQUARE SLABS CHRYSTAL series.

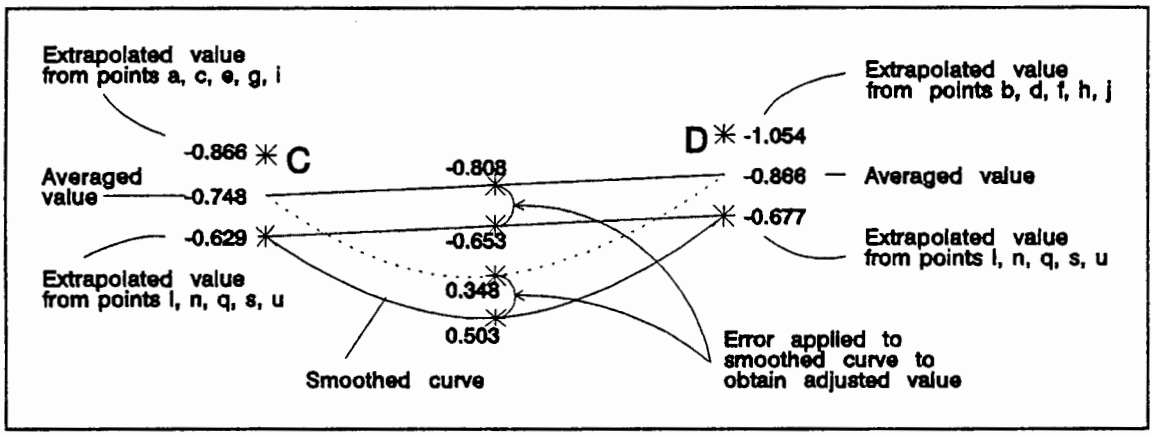

Fig 4.6 - Adjusting smoothed curve

The values on the two baselines as well as on the smoothed curve at the position corresponding to the maximum slab deflection are derived next. The difference in values of the two straight lines is then applied to the smoothed curve. This value now represents the deflection of the frame relative to the zero datum. This procedure is applied to all four side frames. A straight line is drawn between the two opposite sides and the value on the line determined at the position of maximum slab deflection. Another value is obtained from the second pair of opposite sides and an average taken. This average is then subtracted from the maximum deflection to give the final deflection relative to the zero datum. An example is shown in Appendix C6 where slab 3 of SQUARE SLABS CHRYSTAL is analysed.

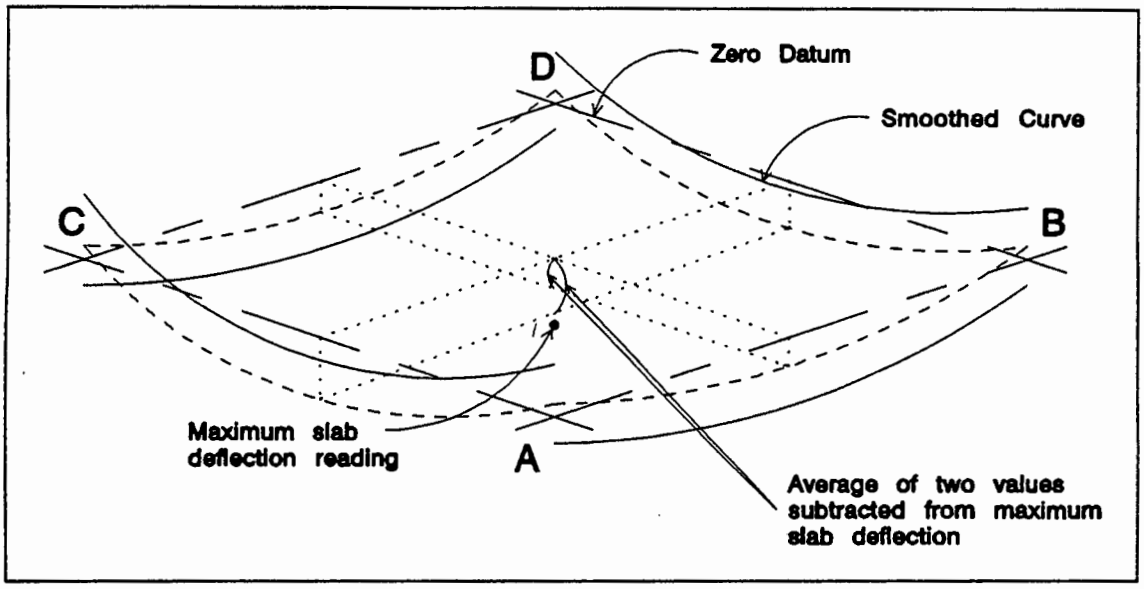

Fig 4.7 - Deflected slab

Using this manipulation it was possible to see which slabs yielded extraordinary deflection patterns and thus could also be ignored. Therefore, in addition to the previously rejected slabs the following slabs can be ignored - slabs no. 6, 7 & 12.

It is known that the deflection of slabs and beams is governed by a fourth order polynomial. There were five dial gauge readings in each line, so theoretically a fourth order polynomial could be fitted through the points. However, it was soon realised that a fourth degree polynomial easily yielded unrealistic results. The reason for this is that if only one dial gauge reading is incorrect then the fourth degree polynomial would be severely affected and would yield unrealistic extrapolated values, as is shown in the diagram. In addition, if a dial gauge reading was rejected for any reason, then there would be too few points to fit the fourth order polynomial.

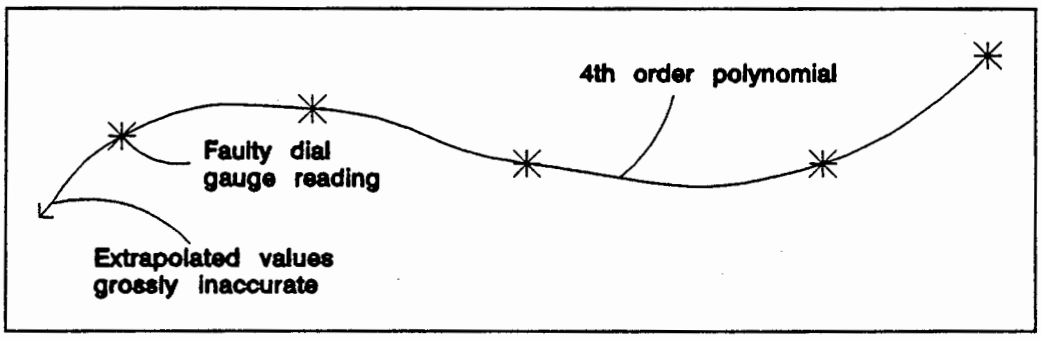

Fig 4.8 - Fourth order polynomial fitted to five points

It was therefore decided to fit a smoothing (least squares) polynomial of second degree through the points. The advantage of using this polynomial is to minimise the effect of any one erroneous dial gauge reading, as can be seen in the diagram.

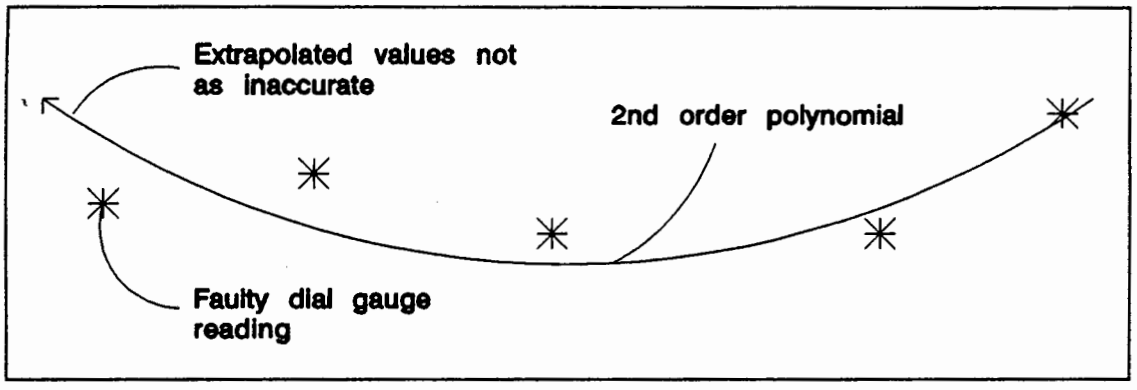

Fig 4.9 - Fitting a second degree polynomial to five points

A problem arises, however, when confronted with a clamped edge, as the deflection shape then reverses curvature. This was overcome by fitting another second order polynomial between the clamped edge and the first dial gauge reading. This polynomial was specified to have zero slope at the clamped edge and the same ordinate and slope as the smoothed polynomial at the position of the first dial gauge.

When considering the supporting frame itself, it was treated as being simply-supported. The frame perpendicular to the one being considered was not regarded as being rigid enough to provide full fixity at the supported end. Thus only one second degree polynomial was fitted through the extrapolated points.

The following set of slab configurations contains the adjusted deflections after the deflection of the supporting frame has been accounted for. The key for the slab configurations can be found on page 52.

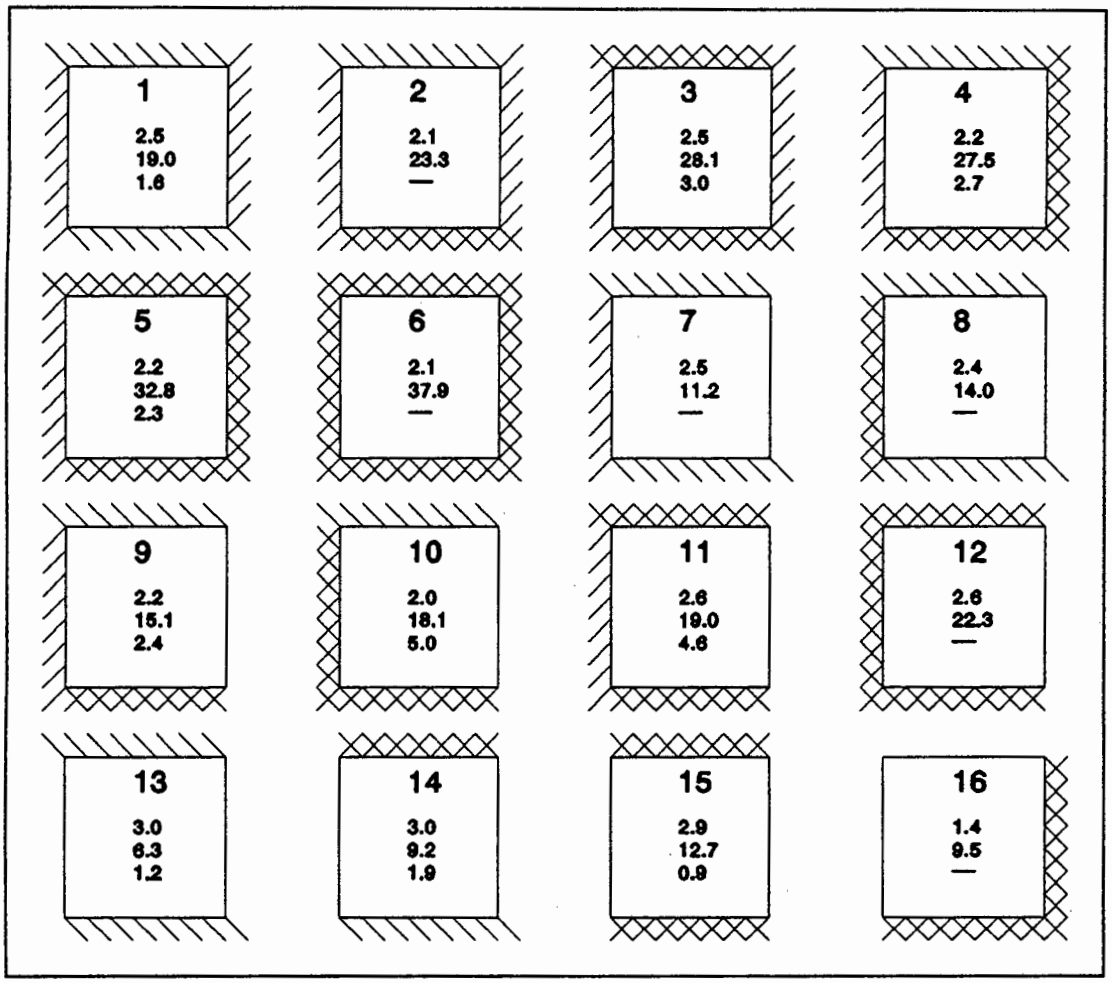

Fig 4.10 - Slab configurations for Square Slabs Chrystal

The bar charts of experimental and design ultimate loads, serviceability loads and maximum deflections at 15 kN can all be seen in Appendix C2.

4.3 RECTANGULAR SLABS ,JACKSON[16]

The slab dimensions are 1.0m by 1.4m by 0.04m.

RECTANGULAR SLABS A
RESULTS OF THESIS BY D. JACKSON[16] - 1989
fy = 522 MPa

Slab No	fcu (MPa)	Experimental Ultimate Load (kN/m^2)	Design Ultimate Load (kN/m^2)	Service Load (kN/m^2)	Maximum Service Deflection (mm)	Maximum Deflection at 10kN (mm)
1	23.2	38.4	27.0	16.9	5.2	2.8
2	25.2	43.7	30.8	19.3	4.9	2.7
3	25.0	40.1	33.2	20.7	6.0	1.8
4	26.0	41.6	40.1	25.0	7.9	2.1
5	21.9	44.4	34.9	21.9	5.6	2.1
6	19.9	47.1	37.1	23.2	5.5	2.0
7	18.3	47.3	41.5	26.0	8.4	2.2
8	18.1	48.7	44.3	27.7	3.9	0.7
9	18.9	59.4	48.9	30.5	3.1	0.5
10	19.8	18.7	18.2	11.3	3.7	2.5
11	18.2	13.3	13.6	8.5	12.6	11.2
12	16.7	17.3	16.7	10.5	11.2	5.2
13	18.5	19.0	17.5	10.9	7.6	4.3
14	18.0	22.8	20.8	13.0	6.7	2.8
15	12.6	34.6	33.0	20.6	3.2	0.7
16	16.6	27.0	24.6	15.3	7.9	3.3

Table 4.3

These sixteen slabs were also examined in terms of their experimental ultimate loads and maximum deflections at a common load of 10 kN, as described in the previous section. The student who tested these slabs plotted their experimentally determined deflected shapes against their deflected shapes as determined by using a finite element program. Slabs no. 3, 7, 13 & 14 exhibited severe distortions and also failed the two criteria mentioned before. They were thus ignored.

The same analysis, as described for SQUARE SLABS CHRYSTAL, was used to compensate for the deflection of the frame-system supporting the slab. The following figure shows a plan view of a typical slab with the layout of the dial gauges.

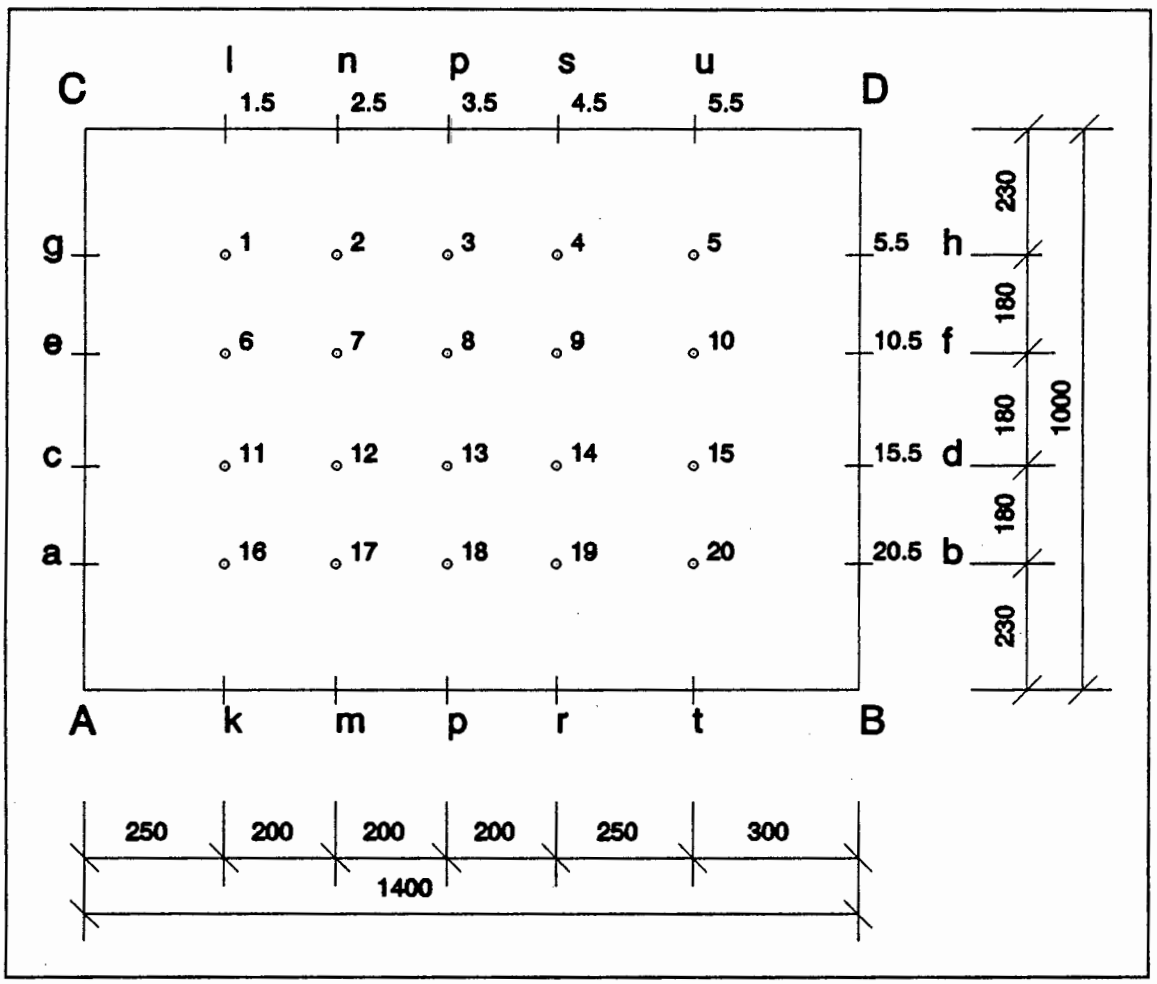

Fig 4.11 - Dial gauge layout for Rectangular Slabs Jackson

Dial gauges were used on the free slab edge at positions 1.5, 2.5, 3.5, 4.5 & 5.5 only for slabs 11, 12, 13, 14 & 16 and at positions 5.5, 10.5, 15.5 & 20.5 for slabs 10 & 15.

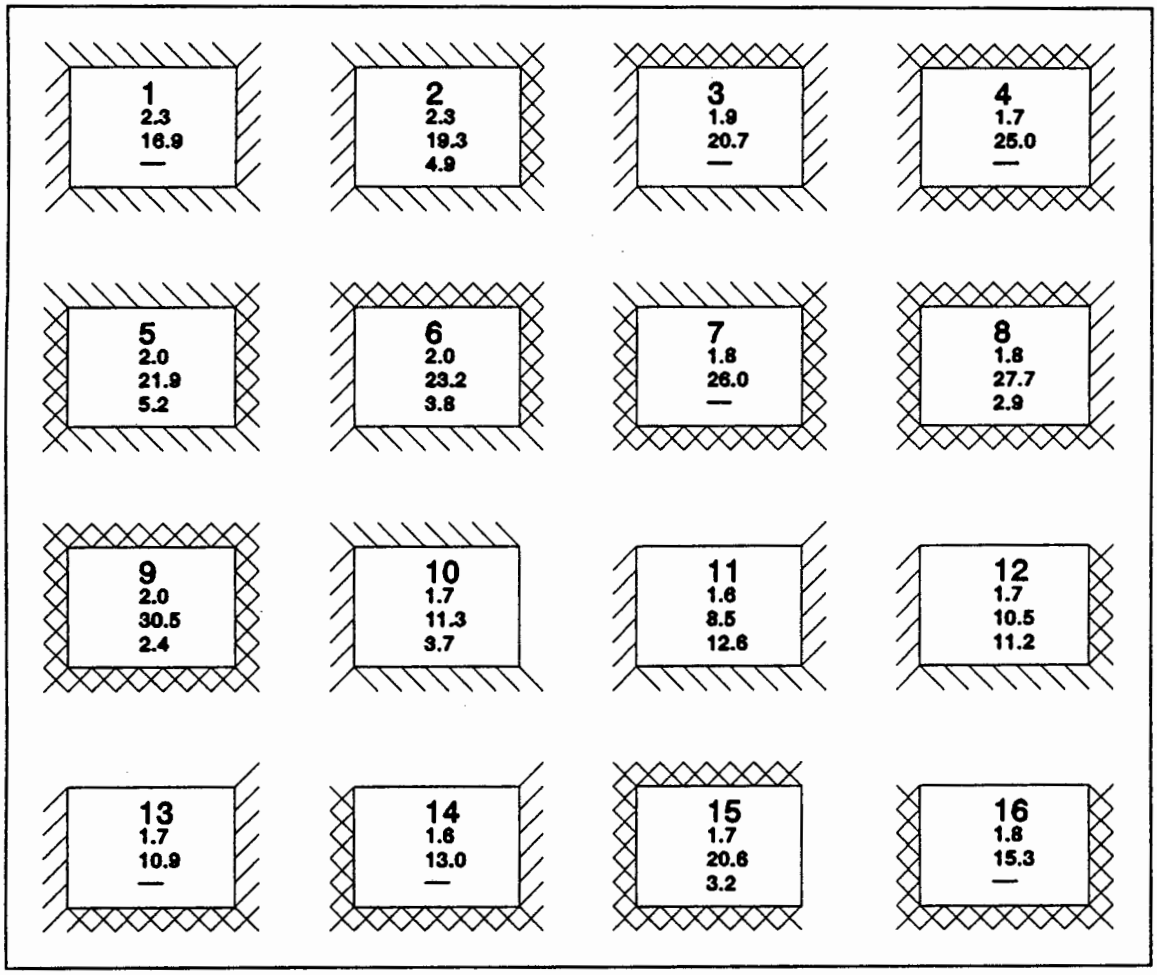

Fig 4.12 - Slab configurations for Rectangular Slabs Jackson

The following slabs yielded extraordinary deflection shapes and can be ignored in addition to those already rejected - slabs no. 1, 4, 7 & 16.

The bar charts of the experimental and design ultimate loads, serviceability loads and maximum deflections at 10 kN can all be seen in Appendix C3.

4.4 RECTANGULAR SLABS COOKE[17]

The slab dimensions are 1.0m by 1.4m by 0.04m.

RECTANGULAR SLABS B
RESULTS OF THESIS BY I.S. COOKE[17] - 1993
fy - 477 MPa

Slab No	fcu (MPa)	Experimental Ultimate Load (kN/m^2)	Design Ultimate Load (kN/m^2)	Service Load (kN/m^2)	Maximum Service Deflection (mm)	Maximum Deflection at 10kN (mm)
1	37.4	44.9	26.4	16.5	2.2	0.7
2	29.1	53.6	32.3	20.2	1.7	0.5
3	30.4	59.9	38.9	24.4	4.2	1.0
4	19.6	59.0	36.1	22.5	2.7	0.6
5	20.5	76.5	47.4	29.6	2.8	0.1
6	39.6	21.8	11.8	7.4	1.4	1.7
7	41.1	27.0	16.2	10.1	3.0	1.4
8	41.4	31.1	21.2	13.2	3.1	1.4
9	32.2	15.1	8.4	5.3	3.8	10.2
10	27.8	17.3	19.7	12.3	14.0	7.7
11	27.0	20.8	20.1	12.6	8.4	4.4
12	34.4	22.3	21.2	13.3	8.3	3.9

Table 4.4

These twelve slabs were examined by the same criteria as the other two sets of slabs, i.e. experimental ultimate loads, maximum deflections at a common load (10kN), severe deviations of experimentally determined deflected shapes from theoretically calculated shapes and any other practical problems reported by the student who tested them. Slabs no. 3, 4, 10 & 11 failed at least three of the above four criteria and were ignored. Slabs no. 10, 11, 12 & 13 are flat slab configurations with column supports at each of the corners. The corners were either simply supported (as indicated by three parallel lines) or clamped (as indicated by cross-hatching). These results were not used for the purposes of this thesis.

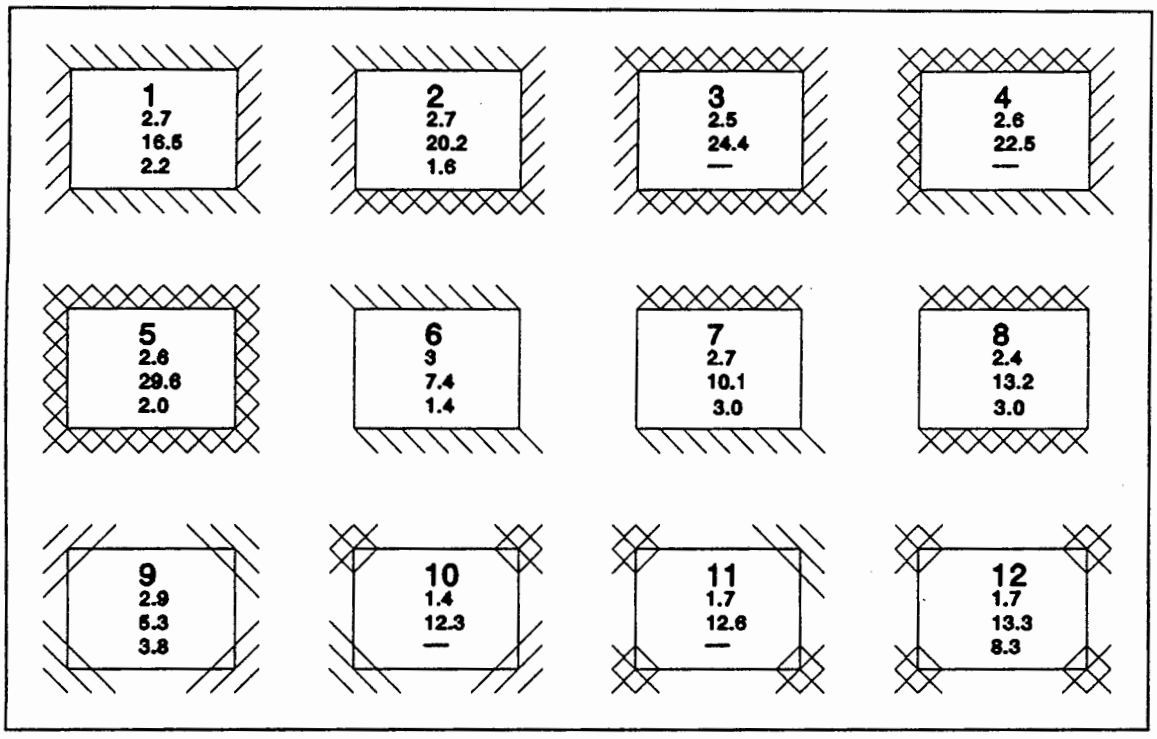

Fig 4.13 - Slab configurations for Rectangular Slabs Cooke

The same analysis as described for SQUARE SLABS CHRYSTAL was used to compensate for the deflection of the frame supporting the slab. This procedure was only applied to the first eight slabs as the last four slabs are flat slab configurations that are only supported at their corners. The figure on the following page shows a plan view of a typical slab with the positions of the dial gauges.

The following slabs yielded unusual deflection shapes and can be rejected in addition to those already rejected - slabs no. 3 & 4.

The bar charts of experimental and design ultimate loads, serviceability loads and maximum deflections at 10 kN can all be seen in Appendix C4.

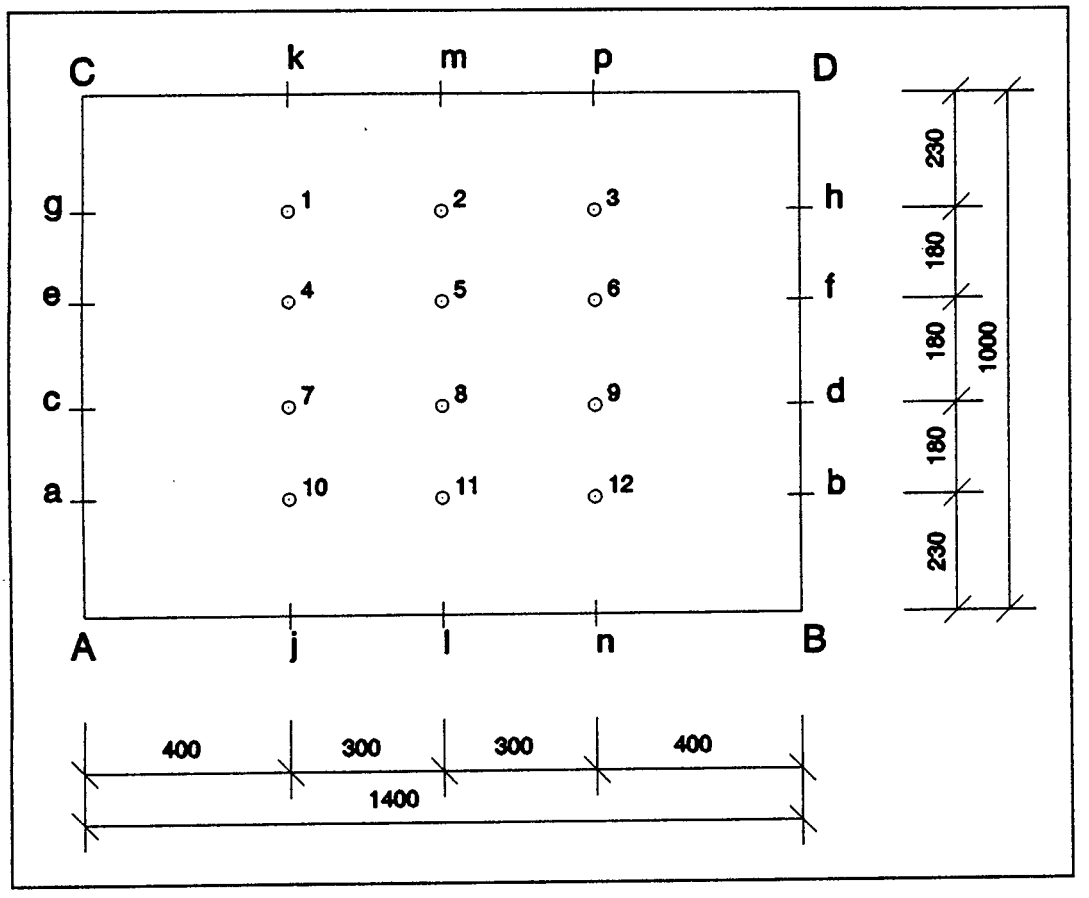

Fig 4.14 - Dial gauge layout for Rectangular Slabs Cooke

CHAPTER 5

ANALYSIS OF RESULTS AND DISCUSSION

Tables 5.1, 5.2 and 5.3 on the next few pages show the values of deflection at the maximum service loads. Table 5.1 corresponds to the slab configurations of SQUARE SLABS CHRYSTAL, table 5.2 to RECTANGULAR SLABS JACKSON and table 5.3 to RECTANGULAR SLABS COOKE.

SQUARE SLABS CHRYSTAL													
Slab No (1)	Exp. Defl. (mm) (2)	Elas. Defl. x (mm) (3)	Crack Defl. x (mm) (4)	Total Defl. x (mm) (5)	Elas. Defl. y (mm) (6)	Crack Defl. y (mm) (7)	Total Defl. y (mm) (8)	Ave. Defl. (mm) (9)	Ave ÷ Exp (10)	Form. Defl. x (mm) (11)	Form. Defl. y (mm) (12)	Ave. Defl. (mm) (13)	Ave ÷ Exp (14)
1	1.6	0.9	4.3	5.2	0.9	4.3	5.2	5.2	3.3	4.8	4.8	4.8	3.0
2	-	0.8	3.8	4.7	1.1	3.1	4.2	4.4	-	4.3	4.1	4.2	-
3	3.0	1.1	9.8	10.9	1.8	4.1	5.9	8.4	2.8	7.9	8.0	7.9	2.6
4	2.7	1.3	5.2	6.5	1.3	5.2	6.5	6.5	2.4	5.9	5.9	5.9	2.2
5	2.3	1.6	8.0	9.6	1.7	4.1	5.8	7.7	3.3	7.8	7.9	7.8	3.4
6	-	1.9	5.3	7.2	1.9	5.3	7.2	7.2	-	9.1	9.1	9.1	-
7	-				0.9	4.8	5.7	5.7	-		4.9	4.9	-
8	-				1.1	7.9	8.9	8.9	-		7.1	7.1	-
9	2.4				1.1	3.5	4.6	4.6	1.9		5.2	5.2	2.2
10	5.0				1.4	6.4	7.8	7.8	1.6		6.4	6.4	1.3
11	4.6				1.4	2.0	3.4	3.4	0.7		6.4	6.4	1.4
12	-				1.7	3.3	5.0	5.0	-		7.9	7.9	-
13	1.2				0.5	0.0	0.5	0.5	0.4		0.5	0.5	0.4
14	1.9				0.3	0.0	0.3	0.3	0.2		0.4	0.4	0.2
15	0.9				0.2	0.0	0.2	0.2	0.2		0.3	0.3	0.3
16	-	-	-	-	-	-	-	-	-	-	-	-	-

Table 5.1

The first column in each table refers to the slab configuration as shown in figures 4.10, 4.12 and 4.13. The second column refers to the experimentally observed maximum deflection at the maximum service load for each particular slab. The next three columns (3, 4 & 5) refer in turn to the calculated maximum elastic deflection, the maximum deflection due to cracking and the total deflection (sum of elastic and cracked deflections) for a strip spanning in the x-direction. The three columns thereafter (6, 7 & 8) are similar, but are for a strip spanning in the y-direction. The following two columns (9 & 10) are the average of the two total deflections and the ratio of this average total deflection to the experimentally observed deflection respectively.

The last four columns (11, 12, 13 & 14) form an independent set. These values are the deflections as obtained by the formulae developed in Appendix A. These deflections were used to determine the load dispersion at the nine nodes, as described in section 3.1. The last four columns, in order, are the maximum deflection as calculated for a strip spanning in the x-direction, the maximum deflection as calculated for a strip spanning in the y-direction, the average of these two deflections and the ratio of this average to the experimentally observed maximum deflection at the service load. These last four columns were included as a comparison for the other readings and a comparison can also be made for the deflections in each of the orthogonal directions.

Each one of the three sets of slabs (i.e. 1 to 6; 7 to 12; 13 to 16) is arranged in the order of increasing support restraint.

Considering table 5.1, a number of interesting facts can be observed. Slabs 1 to 6 are supported on all four edges and the predicted maximum deflection is always higher than the experimentally observed maximum deflection. Slabs 7 to 12 are supported on three sides and it can be seen that the ratio of computed maximum deflection to experimentally observed maximum deflection is closer to 1.0. Slabs 13, 14 and 15 are one-way spanning slabs and the proposed model has predicted deflections much lower than the observed deflections. Slab 16 cannot be modelled and is ignored.

For the two-way spanning slabs (slabs 1 to 6) the proposed model predicts deflections much higher than the observed deflections. The restraining effects of the surface-shearing action and the Poisson effect (as described in section 3.1) are responsible for a portion of this over-prediction. The proposed model does not include these effects and would consequently over-estimate deflections. For slabs supported on only two opposite sides the effect of the surface-shearing action no longer exists, while for slabs supported on three sides the surface-shearing action is present to some extent. Consequently the deflections predicted by the proposed model should be closer to the experimentally observed maximum deflections for these latter two cases of slab configurations. This fact is observed (although only slightly) for the slabs supported on three edges (slabs 7 to 12). When considering two-way spanning slabs, the ratio of predicted to observed maximum deflections (values in column 10) range from 2.4 to 3.3 with an average value of 2.95. For the slabs supported on three edges the ratio varies from 0.7 to 1.9 with an average value of 1.4. While these values do support the expected trend, it is appreciated that there are not enough results to verify them statistically. The results of the experiments are also not reliable enough to attach importance to them individually, but as a group they can be analyzed. The Poisson effect will be present in the slabs that are supported on only three sides and will affect the observed maximum deflections. This explains the high ratio of predicted to observed deflections. However, the extent of both the Poisson effect and the surface-shearing action cannot be quantified easily. As was also discussed in section 3.1, membrane action is not present in the slabs tested in the laboratory because of the low shear resistance of the rubber supports.

For the one way spanning slabs (13, 14 & 15), the proposed model has predicted deflections well below those that were observed. A careful examination of the computed results shows that at the serviceability limit state the cracking moment has not been exceeded and consequently there is no deflection due to cracking. If pre-cracking has occurred, then the experimentally observed deflections would be much higher than what would have occurred if no pre-cracking has taken place. This is explained clearly with the following diagram, which is based on the deflection model discussed in the Manual on the CEB/FIP Model Code[3].

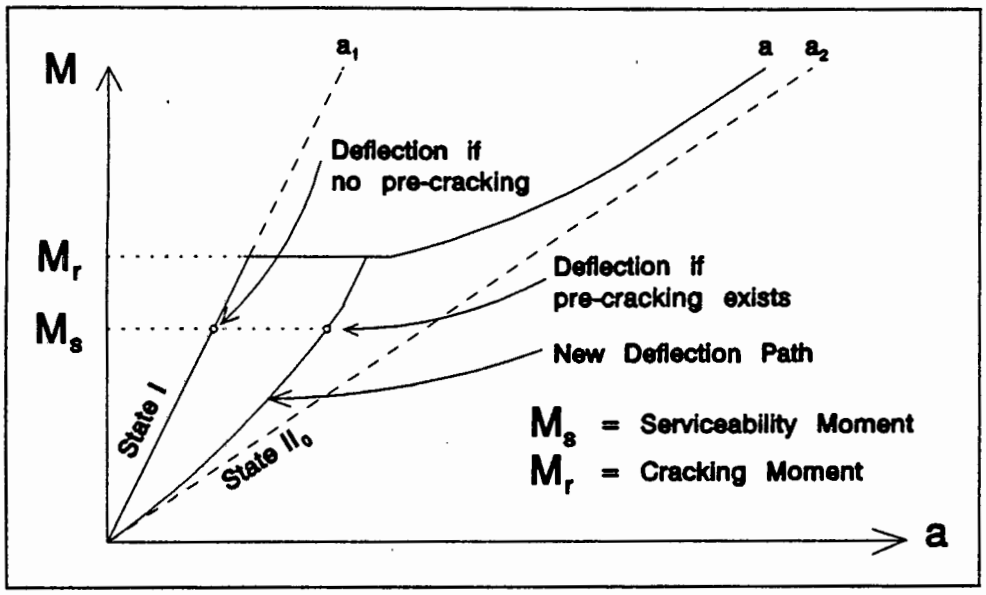

Fig 5.1 - Influence of pre-cracking on deflection

A close examination of the method used by each of the undergraduate students showed that one day after having been cast, the slabs were lifted off the ground and stripped of their shuttering, as shown below.

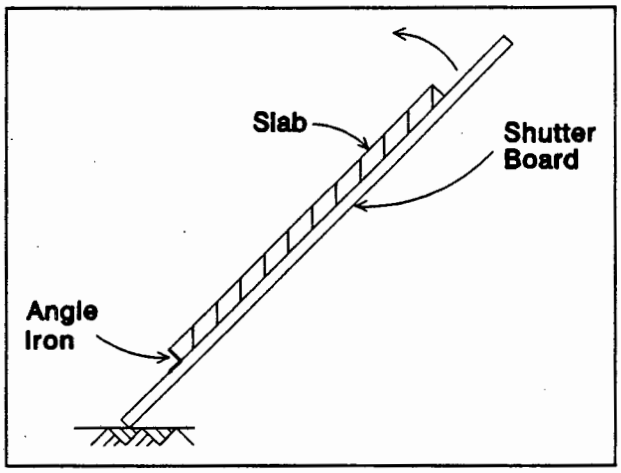

Fig 5.2 - Lifting of day-old slabs off the floor

At age one day, the slabs would not have gained much strength and the shutter board would have to carry the full weight as they are levered off the ground. Since the stiffness (EI) of the shutter board is not very high, enough deflection could take place for

micro-cracks to occur in the slabs. Upon loading, the cracks would open up at a load much lower than what would normally cause cracking, creating higher deflections. Unfortunately, if pre-cracking was present, the extent cannot be determined.

The effect of this pre-cracking would be more pronounced in the slabs, tested for this thesis, that are one-way spanning. With all the other slabs, the cracking moment has been reached and the effect of the pre-cracking will have been cancelled or minimized.

RECTANGULAR SLABS JACKSON

Slab No (1)	Exp. Defl. (mm) (2)	Elas. Defl. x (mm) (3)	Crack Defl. x (mm) (4)	Total Defl. x (mm) (5)	Elas. Defl. y (mm) (6)	Crack Defl. y (mm) (7)	Total Defl. y (mm) (8)	Ave. Defl. (mm) (9)	Ave ÷ Exp (10)	Form. Defl. x (mm) (11)	Form. Defl. y (mm) (12)	Ave. Defl. (mm) (13)	Ave ÷ Exp (14)
1	-	1.5	8.8	10.3	1.2	11.0	12.2	11.2	-	8.8	8.8	8.8	-
2	4.9	2.4	9.0	11.4	1.4	12.9	14.3	12.8	2.6	10.4	10.1	10.3	2.1
3	-	1.4	8.1	9.5	1.6	7.4	9.0	9.2	-	8.6	7.6	8.1	-
4	-	1.6	12.3	13.9	1.9	4.3	6.3	10.1	-	11.5	9.0	10.2	-
5	5.2	2.7	2.3	5.0	1.6	16.0	17.6	11.3	2.2	11.9	11.9	11.9	2.3
6	3.8	2.6	9.8	12.4	1.7	8.2	9.9	11.2	2.9	10.9	8.1	9.5	2.5
7	-	2.6	1.1	3.7	2.1	11.8	14.0	8.8	-	10.6	10.6	10.6	-
8	2.9	2.6	10.4	13.0	2.3	6.1	8.3	10.7	3.7	11.3	10.6	10.9	3.8
9	2.4	2.9	2.5	5.5	2.5	7.9	10.4	7.9	3.3	12.3	12.3	12.3	5.1
10	3.7				0.9	8.0	8.9	8.9	2.4		6.6	6.6	1.8
11	12.6	2.7	25.6	28.3				28.3	2.2	19.2		19.2	1.5
12	11.2	3.4	16.7	20.1				20.1	1.8	16.0		16.0	1.4
13	-	3.5	34.0	37.4				37.4	-	24.6		24.6	-
14	-	4.1	23.4	27.6				27.6	-	21.0		21.0	-
15	3.2				0.4	2.3	2.6	2.6	0.8		3.0	3.0	0.9
16	-	4.9	14.2	19.1				19.1	-	24.5		24.5	-

Table 5.2

The facts observed previously can also be seen upon examination of the results for Rectangular Slabs Jackson and Rectangular Slabs Cooke. For Rectangular Slabs Jackson the two-way spanning slabs are numbered from 1 to 9. The ratio of predicted to experimentally observed maximum deflections (values in column 10) varies from 2.2 to 3.7. The average value for the ratio is 2.94. Slabs supported on only three edges are numbered from 10 to 16. The ratio varies from 0.8 to 2.4 with an average value of 1.8.

RECTANGULAR SLABS COOKE													
Slab No (1)	Exp. Defl. (mm) (2)	Elas. Defl. x (mm) (3)	Crack Defl. x (mm) (4)	Total Defl. x (mm) (5)	Elas. Defl. y (mm) (6)	Crack Defl. y (mm) (7)	Total Defl. y (mm) (8)	Ave. Defl. (mm) (9)	Ave ÷ Exp (10)	Form. Defl. x (mm) (11)	Form. Defl. y (mm) (12)	Ave. Defl. (mm) (13)	Ave ÷ Exp (14)
1	2.2	1.4	4.7	6.1	1.1	7.2	8.4	7.2	3.3	7.0	7.1	7.0	3.2
2	1.6	1.4	6.8	8.2	1.5	7.1	8.6	8.4	5.3	7.9	7.3	7.6	4.8
3	-	1.7	10.6	12.2	1.8	4.3	6.2	9.2	-	10.6	8.6	9.6	-
4	-	2.5	9.8	12.3	1.6	7.4	9.0	10.6	-	10.6	7.4	9.0	-
5	2.0	2.9	3.5	6.4	2.4	8.3	10.7	8.5	4.3	12.3	12.1	12.2	6.1
6	1.4				0.5	0.0	0.5	0.5	0.4		0.5	0.5	0.4
7	3.0				0.3	0.0	0.3	0.3	0.1		0.3	0.3	0.1
8	3.0				0.2	0.0	0.2	0.2	0.1		0.2	0.2	0.1

Table 5.3

For Rectangular Slabs Cooke the two-way spanning slabs are numbered 1 to 5. The ratio of predicted to experimentally observed maximum deflection varies from 3.3 to 5.3 with an average value of 4.3. The average ratio for two-way spanning slabs is considerably higher than the corresponding average ratios for Square Slabs Chrystal and Rectangular Slabs Jackson. For one-way spanning slabs, numbered 6 to 8, the proposed model once again predicts maximum deflections well below the observed maximum deflections. This is in accordance with Square Slabs Chrystal and can be explained by the presence of pre-cracking.

The results for the two-way spanning slabs (1 to 6) of Square Slabs Chrystal will now be examined again. The computed deflections using the proposed model for the x- and y-directions (values in columns 5 and 8) generally compare very well, except for slab 3. An interesting phenomenon is observed with slabs 2, 3 & 5. In each of these cases the strip spanning in the x-direction is not as rigidly supported as the strip spanning in the y-direction. As a result of this, the strip spanning in the y-direction attracts more of the load than the strip in the x-direction, as is expected. This is confirmed by the maximum elastic deflection in the y-direction being higher than that in the x-direction (columns 6 vs. 3). However, the deflection due to cracking is much higher for the strip less rigidly supported than the more rigidly supported strip! This phenomenon, where the more rigidly supported strip attracts more of the load and has a higher elastic deflection but has a lower deflection due to cracking than the less rigidly supported strip, is also observed in Rectangular Slabs Jackson (with the exception of slab 8) and Rectangular Slabs Cooke (with the exception of slab 2).

The model that was developed in section 3.2 to determine the deflection due to cracking is based on the relationship

$$\theta = \zeta \int_{x_1}^{x_2} \frac{M}{EI_{cr}} dx$$

For two strips that are of equal length and stiffness and have the same maximum moment in sagging, then the strip that is less rigidly supported will have a longer cracked length ($x_2 - x_1$) - see figure 3.3. The factor ζ will be the same for both cases, so consequently the strip less rigidly supported will have a higher θ and thus a higher deflection due to cracking. If, on the other hand, the two strips of equal length and stiffness have the same cracked lengths ($x_2 - x_1$), then the less rigidly supported slab will have a lower maximum moment in sagging. The value of the integral will therefore be lower. In addition, the factor ζ is defined as shown on the next page:

$$\zeta = 1 - \beta_1\beta_2\frac{M_{cr}^2}{M_m^2}$$

$$\text{where } M_m = \sqrt{M_{max}\, M_{cr}}$$

$$\therefore \zeta = 1 - \beta_1\beta_2\frac{M_{cr}}{M_{max}}$$

Therefore, the smaller the value of M_{max} (for sagging) the lower the value of ζ. This will lead to a smaller θ and thus a lower deflection due to cracking.

Depending on which of the two cases described above is more applicable to each individual slab, it is possible for the less rigidly supported strip to attract less load, but to have a higher deflection due to cracking. This is the case for the majority of the slabs tested. The apparent anomalies observed with slab 8 of Rectangular Slabs Jackson and slab 4 of Rectangular Slabs Cooke can be explained by the second case. A solution to this problem would be to redefine M_m in the formula. If M_m can be taken as some lower value than its present definition, then the contribution of the deflection due to cracking will be less. In addition to this, M_m must be defined as a value that will not vary (decrease) as much as at present as the degree of fixity of the supports increases. The absolute maximum moment (hogging or sagging) of the strip will not vary as much as the maximum moment in sagging as the fixity of the supports increases for a strip carrying the same load. The cracking moment capacity will also have to be included in the definition since it is a measure of the beam's ability to withstand concrete flexural tensile stresses. A suggestion is to take a fraction of the geometric mean of the maximum moment (whether hogging or sagging) of the strip and its cracking moment capacity.

$$e.g. \quad M_m = \frac{1}{2}\sqrt{M_{abs.\ max} \cdot M_{cr}}$$

It was now decided to investigate the effect of increasing aspect ratio on the predicted maximum deflections. Tables 5.4, 5.5 and 5.6 show the calculated results of increasing the aspect ratio for a slab simply-supported on all four edges, for a slab clamped on all four edges and for a slab with two adjacent edges clamped and simply-supported on the other two, respectively.

accordance with most Codes of Practice that recommend that slabs with an aspect ratio of 2 or more be treated as one-way spanning. The value for deflection in the table above for a slab spanning in only one direction is very similar to the values for two-way spanning slabs with high aspect ratios. The elastic deflection is the same, but the deflection due to cracking is slightly different. The reason for this is the incremental changing of the cracked length for two-way spanning slabs, as described in section 3.3.3. An interesting observation is that for aspect ratios less than 2.5, the strip spanning in the x-direction has a lower elastic deflection but a higher deflection due to cracking than the strip spanning in the y-direction.

The next table is for a slab clamped on all four edges. The properties and dimensions are the same as for the previous slab, but with:

$d' = 0.005$ m (x- and y-directions)
$A_s' = 100$ mm^2/m (x- and y-directions)
$w_a = 30\ 000$ N/m^2

SLAB CLAMPED ON ALL FOUR EDGES							
L_y ÷ L_x	Elastic Defl. x (mm)	Cracked Defl. x (mm)	Total Defl. x (mm)	Elastic Defl. y (mm)	Cracked Defl. y (mm)	Total Defl. y (mm)	Average Defl. (mm)
1.0	0.3	0.0	0.3	0.3	0.0	0.3	0.3
1.1	1.3	0.4	1.7	1.5	0.0	1.5	1.6
1.2	1.6	3.7	5.3	1.7	1.5	3.1	4.2
1.3	1.7	3.9	5.6	1.9	0.9	2.8	4.2
1.4	2.2	7.5	9.7	2.4	2.6	5.1	7.4
1.5	2.2	7.4	9.6	2.8	2.6	5.4	7.5
1.6	2.2	7.3	9.5	3.2	2.8	6.0	7.8
1.7	2.2	7.3	9.5	3.4	2.3	5.7	7.6
1.8	2.2	7.3	9.5	3.5	1.2	4.7	7.1
1.9	2.2	7.3	9.5	3.6	0.0	3.6	6.6
2.0	2.2	7.3	9.5	3.7	0.0	3.6	6.6
One-way	2.2	6.6	8.8	-	-	-	-

Table 5.5

The computed results for the deflection due to cracking are even more erratic than for the previous two cases. For this slab configuration, the two-way spanning slab can be treated as one-way spanning once the aspect ratio increases above 1.6. The results show a decrease in deflection for aspect ratios of 1.7 and 1,8 and any aspect ratio higher than 1.8 could not be handled by the computer program (this is explained below). The results for a one-way spanning slab compare favourably with the two-way spanning slab with an aspect ratio of 1.6. The same trend as with the other two slabs has been observed. Generally the shorter span (span in the x-direction) has a lower elastic deflection, but a higher deflection due to cracking.

Some of the results of the computer program are encouraging, while others are not. For the two-way spanning slabs, the deflections computed in the two orthogonal directions compared favourably with each other for slabs that are simply-supported on all four edges or have only one edge clamped. However, for slabs with more than one edge clamped, the deflections begin to differ considerably, especially as the aspect ratio increases. This is true not only for the total maximum deflection, but also for the elastic deflection and deflection due to cracking.

In table 5.6, which shows the results of increasing aspect ratio on the predicted deflections for a slab clamped on two adjacent edges and simply-supported on the other two, there are no results for aspect ratios of 1.9 and 2.0. The reason for this is that once the cracking length of the middle strip has been found to increase by less than an eightieth of the span for two successive iterations, the computer checks to see what portion of the load is acting on the middle strip and what portion is acting on the other two strips. If the middle strip (the strip spanning through the region of maximum deflection) is found to have a lower maximum moment in sagging than either of the other two strips, then the computer performs another iteration on the cracking length. In the above case, when the computer performs the next iteration, the cracking length has changed by more than an eightieth and more iterations are necessary. When the increase in cracking length is less than an eightieth of the span, then the maximum moment in sagging of the middle strip is less than that of the other two strips and the whole process is repeated.

There are cases where, when the middle strip has a lower maximum sagging moment than that of either of the other two strips, successive iterations successfully solve the load dispersion. The above problem arises as a result of the strips in one direction acting individually and not as a set. This can be solved by increasing the number of strips spanning in each direction and therefore producing better continuity between the strips.

For these reasons it was concluded that the proposed model does not predict short-term maximum deflections accurately enough. It was therefore decided not to expand the computer program to predict long-term deflections as well.

CHAPTER 6

CONCLUSIONS AND RECOMMENDATIONS

The literature review showed the short-falls of the various Design Codes. While it is appreciated that the purpose of these design formulations is to simplify the design process, some of them are over-conservative and many aspects influencing the deflections of slabs have been ignored. The formulation in the Manual on the CEB/FIP Model Code[3] is the most sound. The design processes suggested by the Manual were found to contain too many simplifications. It was therefore decided to develop a design method using the theory stated in the Manual.

In this thesis two models have been developed. Model no. 1 predicts the load dispersion at various positions on the slab and thus the equivalent load acting on a strip spanning through the region of maximum deflection of the slab. Model no. 2 proposes a method for predicting the maximum deflection of this strip. Both models have their shortcomings.

Model no. 1 predicts the load dispersion at only nine points on the slab. At the time of development, it was hoped that these nine points would be enough. If the slab can be divided into a greater number of orthogonal strips with more intersection points then a more accurate reflection of the load dispersion can be made. The number of intersection points increases exponentially with the increase in orthogonal strips. Thus, only an extra strip or two still need to be added in each orthogonal direction. The continuity between strips spanning in the same direction will be improved vastly with the addition of extra strips in that direction. The inclusion of torsion in this model would also be a significant improvement.

The analysis of slabs supported on three edges as a one-way spanning slab is not always an accurate one. For a rectangular slab which has the free edge spanning in the longer direction, this assumption becomes invalid as the slab acts almost entirely as a cantilever. The load dispersion model therefore needs to be

expanded to include this case. This can only be done if torsion is recognised in the load dispersion model (model no. 1).

Model no. 2 is based on the theory in the Manual on the CEB/FIP Model Code[3]. The deflection due to cracking is determined from the formula

$$\delta = x \cdot \tan\theta$$

$$\text{where } \theta = \zeta \int_{x_1}^{x_2} \frac{M}{EI_{cr}}\, dx$$

The coefficient ζ determines the contribution of the tension stiffening effect of the concrete to the overall deflection. This coefficient is inaccurate for the proposed model. The results of the computer program, as shown in Chapter 5, indicate that the deflection due to cracking for the strip with a lower moment is higher than for the strip with the higher moment. This coefficient is proportional to M_m, which has been defined as the geometric mean of the cracking moment capacity in sagging and the maximum bending moment in sagging. The higher the value for M_m, the higher ζ becomes. M_m needs to be redefined as some lower value, and one that will not change too much as the degree of fixity of the edge constraints increases. A recommendation is that M_m be defined as a fraction (eg. 1/2) of the geometric mean of the maximum moment of the strip (whether hogging or sagging) and the cracking moment capacity of the strip. This will have two effects. Firstly, the overall contribution of the deflection due to cracking to the total deflection will decrease. This will result in a lower predicted maximum deflection. Secondly, as the degree of fixity of the edge constraints of the strip increases, the value of ζ will not decrease by as much as at present.

The results in chapter 5 have shown the computer program does not predict realistic deflections. As the degree of fixity of the two orthogonal strips varies and the aspect ratio increases, so the deflections calculated in the orthogonal directions differ. It must then be concluded that the models in their present form are not acceptable and therefore the computer program was not expanded to determine the long-term deflections.

The experimental results are not reliable. The slabs that were tested were too small. With a depth of only 40 mm, any slight deviation in the effective depth of the slab will result in significant changes in the area properties of the slab. The slab configurations vary too much, i.e. too much emphasis has been placed on variety and too little on consistency. Concrete is a very unpredictable material and a single deflection test on one type of slab cannot provide an accurate or reliable answer. There is a definite need for a large number of tests on each type of slab. A statistical analysis can then be made on the collection of results for each particular slab.

The computer program containing the two proposed models does not predict deflections accurately enough at the present moment. However, if the above improvements are made to the two models it can be used as a useful design aid. A sensitivity analysis can be run for different slab depths and this can be used as a starting point to obtain dimensions for the design. If reliable experimental results can be used, then a ratio of computed to actual deflection can be obtained. This ratio will quantitatively express the effect of the surface-shearing action and the Poisson effect. This ratio can then be incorporated in the design process as a factor for appropriately reducing the computed deflections.

LIST OF REFERENCES

1. BS 8110 "British Standard. Structural use of concrete (Part 1 and Part 2).", British Standards Institution, 1985.

2. AMERICAN CONCRETE INSTITUTE "Building Code Requirements for Reinforced Concrete", (ACI 318M - 83), American Concrete Institution, June 1984.

3. CEB MANUAL "Cracking and Deformation", Comité Euro-International du Beton (CEB), Swiss Federal Institute of Technology, CH 1015, Lausanne, 1985.

4. BRANSON, D.E. "Deformation of Concrete Structures", McGraw Hill, USA, 1977.

5. AMERICAN CONCRETE INSTITUTE "Commentary on Building Code Requirements for Reinforced Concrete (ACI 318M - 83)", ACI 318RM - 83, American Concrete Institute, June 1984.

6. RANGAN, B.V. "Maximum Allowable Span/Depth Ratios for Reinforced Concrete Beams", Research Report, University of New South Wales, Kensington, NSW, Australia, 1981.

7. GILBERT, R.I. "Deflections of Reinforced Concrete Beams - A Design Approach", Research Report, University of New South Wales, Kensington, NSW, Australia, 1982, pg1.

8. GILBERT, R.I. "A Serviceability Approach to Reinforced Concrete Slab Design", Research Report, University of New South Wales, Kensington, NSW, Australia, 1983, pg 2.

9. SCHOLZ, H. "Appraisal of Deflection and Cracking Models for Partially Prestressed Members", Die Siviele Ingenieur in Suid-Afrika, January 1990, pgs 23-33.

10. BAKOSS, S.L., GILBERT, R.I., FAULKES, K.S. & PULMANO, V.A. "Long-term Deflections of Reinforced Concrete Beams", Magazine of Concrete Research: Vol 34, No 121; December 1982, pgs 203 - 212.

11. GHALI, A. & FAVRE, R. "Concrete Structures: Stresses and Deformations", Chapman and Hall, London, 1986.

12. BRUINETTE, K.E. "Deflection of Concrete Slabs", Symposium, Concrete Design for the 80s, Concrete Society of Southern Africa.

13. CP 110:PART 1 "Code of practice for the structural use of concrete: Part 1. Design, materials and workmanship.", British Standards Institution, London, 1972.

14. CRUDGE, R. "The Effect of Cracks on Deflected Shapes", B.Sc (Eng) Thesis No. 24, University of Cape Town, 1987.

15. CHRYSTAL, A. "Concrete Slab Deflections", B.Sc (Eng) Thesis No. 11, University of Cape Town, 1988.

16. JACKSON, D. "Concrete Slab Deflections", B.Sc (Eng) Thesis No. 6, University of Cape Town, 1989.

17. COOKE, I.S. "Reinforced Concrete Slab Deflections", B.Sc (Eng) Thesis No. 52, University of Cape Town, 1993.

18. HIPPO QUARRIES TECHNICAL PUBLICATION "Properties of Aggregate in Concrete", Part (1), Hippo Quarries, Sandton.

19. LOEDOLFF, G.F. & CHAMBERS, S.L. "Die indirekte treksterkte of splytoets van beton gemaak met 19 mm gebreekte klip van Malmesbury Skalie", Technical Paper, Concrete/Beton no. 71, Concrete Society of South Africa, Johannesburg, 1994, Pgs 8 - 14.

APPENDIX A1

DEFLECTION FORMULAE FOR A BEAM SIMPLY - SUPPORTED AT BOTH ENDS

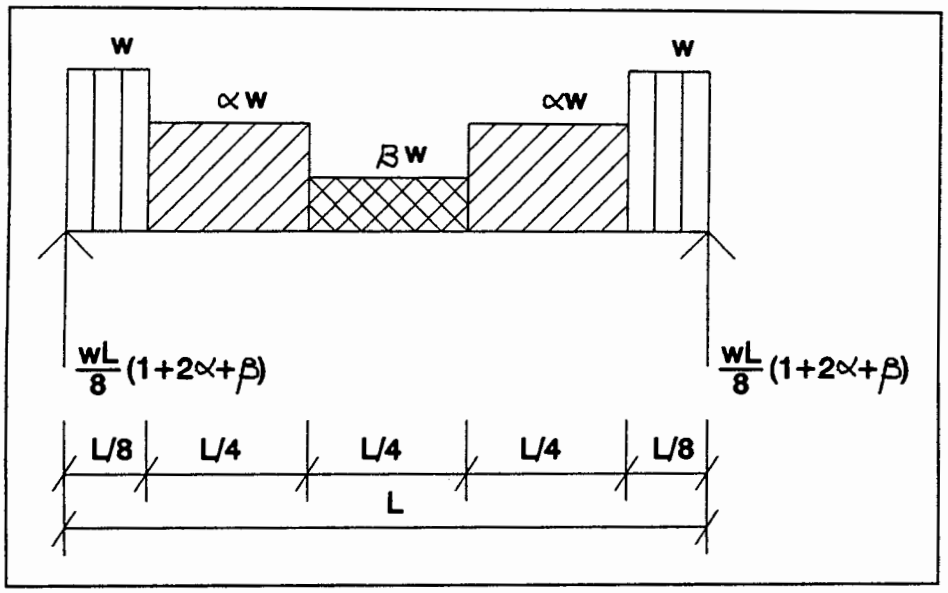

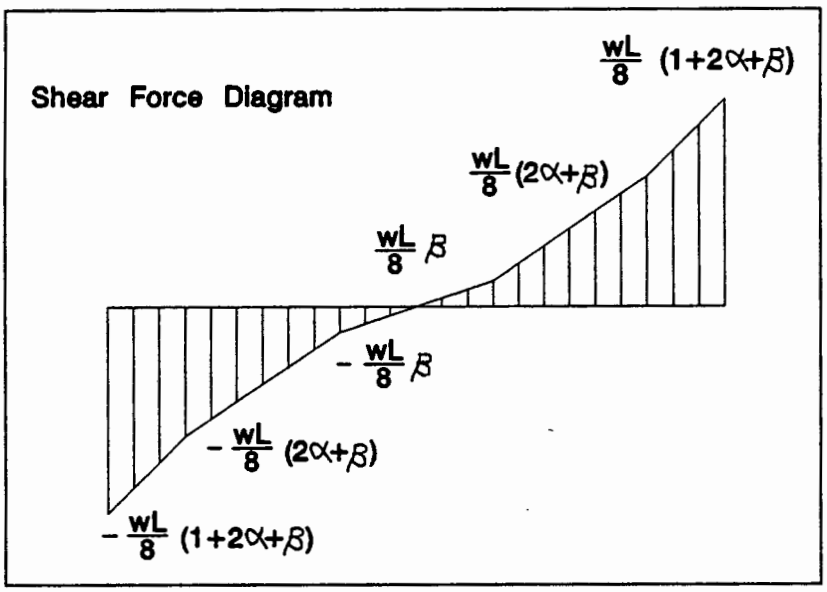

$$S(x) = wx - \frac{wL}{8}(1 + 2\alpha + \beta) \quad \text{for} \quad 0 < x < \frac{L}{8}$$

$$S(x) = \alpha wx - \frac{wL}{8}(3\alpha + \beta) \quad \text{for} \quad \frac{L}{8} < x < \frac{3L}{8}$$

$$S(x) = \beta w(x - \frac{L}{2}) \quad \text{for} \quad \frac{3L}{8} < x < \frac{5L}{8}$$

$$S(x) = \alpha wx + \frac{wL}{8}(\beta - 5\alpha) \quad \text{for} \quad \frac{5L}{8} < x < \frac{7L}{8}$$

$$S(x) = wx + \frac{wL}{8}(2\alpha + \beta - 7) \quad \text{for} \quad \frac{7L}{8} < x < L$$

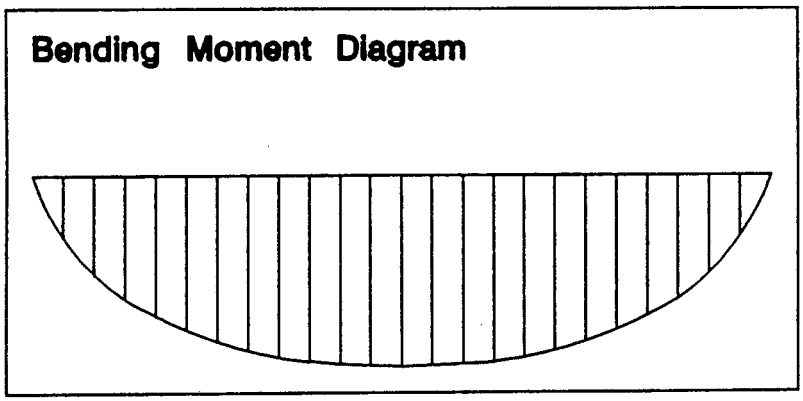

$$M(x) = -\int S(x)\,dx$$

for $0 < x < \frac{L}{8}$

$$M(x) = -\frac{wx^2}{2} + \frac{wLx}{8}(1 + 2\alpha + \beta) + C_1$$

$$\text{At } x = 0,\ M(x) = 0$$

$$\therefore C_1 = 0$$

$$\therefore M(x) = -\frac{wx^2}{2} + \frac{wLx}{8}(1 + 2\alpha + \beta)$$

---

for $\frac{L}{8} < x < \frac{3L}{8}$

$$M(x) = -\frac{\alpha w x^2}{2} + \frac{wLx}{8}(3\alpha + \beta) + C_2$$

$$\text{At } x = \frac{L}{8},\ M(x) = M(x)$$

$$-\frac{w}{2}\frac{L^2}{64} + \frac{wL}{8}\frac{L}{8}(1 + 2\alpha + \beta) = -\frac{\alpha w}{2}\frac{L^2}{64} + \frac{wL}{8}\frac{L}{8}(3\alpha + \beta) + C_2$$

$$\therefore C_2 = \frac{wL^2}{128}(1 - \alpha)$$

$$\therefore M(x) = -\frac{\alpha w x^2}{2} + \frac{wLx}{8}(3\alpha + \beta) + \frac{wL^2}{128}(1 - \alpha)$$

---

for $\frac{3L}{8} < x < \frac{5L}{8}$

$$M(x) = -\beta w\left(\frac{x^2}{2} - \frac{Lx}{2}\right) + C_3$$

At $x = \frac{3L}{8}$, $M(x) = M(x)$

$$-\frac{\alpha w}{2}\frac{9L^2}{64} + \frac{wL}{8}\frac{3L}{8}(3\alpha + \beta) + \frac{wL^2}{128}(1 - \alpha)$$

$$= -\frac{\beta w}{2}\left(\frac{9L^2}{64} - \frac{3L^2}{8}\right) + C_3$$

$$\therefore C_3 = \frac{wL^2}{128}(1 + 8\alpha - 9\beta)$$

$$\therefore M(x) = -\frac{\beta w}{2}(x^2 - Lx) + \frac{wL^2}{128}(1 + 8\alpha - 9\beta)$$

---

for $\frac{5L}{8} < x < \frac{7L}{8}$

$$M(x) = -\frac{\alpha w x^2}{2} - \frac{wLx}{8}(\beta - 5\alpha) + C_4$$

At $x = \frac{5L}{8}$, $M(x) = M(x)$

$$-\frac{\beta w}{2}\left(\frac{25L^2}{64} - \frac{5L^2}{8}\right) + \frac{wL^2}{128}(1 + 8\alpha - 9\beta)$$

$$= -\frac{\alpha w}{2}\frac{25L^2}{64} - \frac{wL}{8}\frac{5L}{8}(\beta - 5\alpha) + C_4$$

$$\therefore C_4 = \frac{wL^2}{128}(1 - 17\alpha + 16\beta)$$

$$\therefore M(x) = \frac{-\alpha w x^2}{2} - \frac{wLx}{8}(\beta - 5\alpha) + \frac{wL^2}{128}(1 - 17\alpha + 16\beta)$$

---

for $\frac{7L}{8} < x < L$

$$M(x) = -\frac{wx^2}{2} - \frac{wLx}{8}(2\alpha + \beta - 7) + C_5$$

At $x = \frac{7L}{8}$, $M(x) = M(x)$

$$-\frac{\alpha w}{2}\frac{49L^2}{64} - \frac{wL}{8}\frac{7L}{8}(\beta - 5\alpha) + \frac{wL^2}{128}(1 - 17\alpha + 16\beta)$$

$$= -\frac{w}{2}\frac{49L^2}{64} - \frac{wL}{8}\frac{7L}{8}(2\alpha + \beta - 7) + C_5$$

$$\therefore C_5 = \frac{wL^2}{128}(-48 + 32\alpha + 16\beta)$$

$$\therefore M(x) = -\frac{wx^2}{2} - \frac{wLx}{8}(2\alpha + \beta - 7) + \frac{wL^2}{128}(-48 + 32\alpha + 16\beta)$$

Deflections

$\kappa = M/EI$ & $\kappa = d^2v/dx^2$ $\rightarrow$ $d^2v/dx^2 = M/EI$

for $0 < x < \frac{L}{8}$

$$\frac{dv}{dx} = \frac{1}{EI_1}\left[-\frac{wx^3}{6} + \frac{wLx^2}{16}(1 + 2\alpha + \beta) + C_6\right]$$

$$v(x) = \frac{1}{EI_1}\left[-\frac{wx^4}{24} + \frac{wLx^3}{48}(1 + 2\alpha + \beta) + C_6x + C_7\right]$$

At $x = 0$, $v(x) = 0$

$$\therefore C_7 = 0$$

$$\therefore v(x) = \frac{1}{EI_1}\left[-\frac{wx^4}{24} + \frac{wLx^3}{48}(1 + 2\alpha + \beta) + C_6x\right]$$

---

for $\frac{L}{8} < x < \frac{3L}{8}$

$$\frac{dv}{dx} = \frac{1}{EI_2}\left[-\frac{\alpha wx^3}{6} + \frac{wLx^2}{16}(3\alpha + \beta) + \frac{wL^2x}{128}(1 - \alpha) + C_8\right]$$

$$v(x) = \frac{1}{EI_2}\left[-\frac{\alpha wx^4}{24} + \frac{wLx^3}{48}(3\alpha + \beta) + \frac{wL^2x^2}{256}(1 - \alpha) + C_8x + C_9\right]$$

At $x = \frac{L}{8}$, $v(x) = v(x)$

$$\frac{1}{EI_1}\left[-\frac{w}{24}\frac{L^4}{4096} + \frac{wL}{48}\frac{L^3}{512}(1 + 2\alpha + \beta) + \frac{L}{8}C_6\right]$$

$$= \frac{1}{EI_2}\left[-\frac{\alpha w}{24}\frac{L^4}{4096} + \frac{wL}{48}\frac{L^3}{512}(3\alpha + \beta) + \frac{wL^2}{256}\frac{L^2}{64}(1 - \alpha) + \frac{L}{8}C_8 + C_9\right]$$

$$\therefore C_9 = \frac{I_2}{I_1}\frac{wL^4}{98304}(-5 - 16\alpha - 8\beta) + \frac{wL^4}{98304}(6 + 15\alpha + 8\beta)$$

---

for $\frac{3L}{8} < x < \frac{5L}{8}$

$$\frac{dv}{dx} = \frac{1}{EI_3}\left[-\frac{\beta w}{2}\left(\frac{x^3}{3} - \frac{Lx^2}{2}\right) + \frac{wL^2x}{128}(1 + 8\alpha - 9\beta) + C_{10}\right]$$

At $x = \frac{L}{2}$, $\frac{dv}{dx} = 0$

$$-\frac{\beta w}{2}\left(\frac{L^3}{24} - \frac{L^3}{8}\right) + \frac{wL^3}{256}(1 + 8\alpha - 9\beta) + C_{10} = 0$$

$$\therefore C_{10} = \frac{wL^3}{768}(-3 - 24\alpha - 5\beta)$$

At $x = \frac{3L}{8}$, $\frac{dv}{dx} = \frac{dv}{dx}$

$$\frac{1}{EI_2}\left[-\frac{\alpha w}{6}\frac{27L^3}{512} + \frac{wL}{16}\frac{9L^2}{64}(3\alpha + \beta) + \frac{wL^2}{128}\frac{3L}{8}(1 - \alpha) + C_8\right]$$

$$= \frac{1}{EI_3}\left[-\frac{\beta w}{2}\left(\frac{1}{3}\frac{27L^3}{512} - \frac{L}{2}\frac{9L^2}{64}\right) + \frac{wL^2}{128}\frac{3L}{8}(1 + 8\alpha - 9\beta) + C_{10}\right]$$

$$\therefore C_8 = \frac{I_2}{I_3}\left[\frac{wL^3}{3072}(-3 - 24\alpha - 20\beta)\right] - \left[\frac{wL^3}{1024}(3 + 15\alpha + 9\beta)\right]$$

At $x = \frac{L}{8}$, $\frac{dv}{dx} = \frac{dv}{dx}$

$$\frac{1}{EI_1}\left[-\frac{w}{6}\frac{L^3}{512} + \frac{wL}{16}\frac{L^2}{64}(1 + 2\alpha + \beta) + C_6\right]$$

$$= \frac{1}{EI_2}\left[-\frac{\alpha w}{6}\frac{L^3}{512} + \frac{wL}{16}\frac{L^2}{64}(3\alpha + \beta) + \frac{wL^2}{128}\frac{L}{8}(1 - \alpha) + C_8\right]$$

$$\therefore C_6 = \frac{I_1}{I_2}\frac{wL^3}{3072}(-6 - 40\alpha - 24\beta) + \frac{I_1}{I_3}\frac{wL^3}{3072}(-3 - 24\alpha - 20\beta) - \frac{wL^3}{3072}(2 + 6\alpha + 3\beta)$$

$$v(x) = \frac{1}{EI_3}\left[-\frac{\beta w}{2}\left(\frac{x^4}{12} - \frac{Lx^3}{6}\right) + \frac{wL^2x^2}{256}(1 + 8\alpha - 9\beta) + C_{10}x + C_{11}\right]$$

At $x = \frac{3L}{8}$, $v(x) = v(x)$

$$\frac{1}{EI_2}\left[-\frac{\alpha w}{24}\frac{81L^4}{4096} + \frac{wL}{48}\frac{27L^3}{512}(3\alpha + \beta) + \frac{wL^2}{256}\frac{9L^2}{64}(1 - \alpha) + \frac{3L}{8}C_8 + C_9\right]$$

$$= \frac{1}{EI_3}\left[-\frac{\beta w}{2}\left(\frac{1}{12}\frac{81L^4}{4096} - \frac{L}{6}\frac{27L^3}{512}\right) + \frac{wL^2}{256}\frac{9L^2}{64}(1 + 8\alpha - 9\beta) + \frac{3L}{8}C_{10} + C_{11}\right]$$

$$\therefore C_{11} = \frac{I_3}{I_2}\frac{wL^4}{98304}(-48 - 336\alpha - 208\beta) + \frac{I_3}{I_1}\frac{wL^4}{98304}(-5 - 16\alpha - 8\beta) + \frac{wL^4}{98304}(54 + 432\alpha + 135\beta)$$

---

for $\frac{5L}{8} < x < \frac{7L}{8}$

$$\frac{dv}{dx} = \frac{1}{EI_4}\left[-\frac{\alpha w x^3}{6} - \frac{wLx^2}{16}(\beta - 5\alpha) + \frac{wL^2x}{128}(1 - 17\alpha + 16\beta) + C_{12}\right]$$

At $x = \frac{5L}{8}$, $\frac{dv}{dx} = \frac{dv}{dx}$

$$\frac{1}{EI_3}\left[-\frac{\beta w}{2}\left(\frac{1}{3}\frac{125L^3}{512} - \frac{L}{2}\frac{25L^2}{64}\right) + \frac{wL^2}{128}\frac{5L}{8}(1 + 8\alpha - 9\beta) + C_{10}\right]$$

$$= \frac{1}{EI_4}\left[-\frac{\alpha w}{6}\frac{125L^3}{512} - \frac{wL}{16}\frac{25L^2}{64}(\beta - 5\alpha) + \frac{wL^2}{128}\frac{5L}{8}(1 - 17\alpha + 16\beta) + C_{12}\right]$$

$$\therefore C_{12} = \frac{I_4}{I_3}\frac{wL^3}{3072}(3 + 24\alpha + 20\beta) - \frac{wL^3}{3072}(15 - 5\alpha + 165\beta)$$

$$v(x) = \frac{1}{EI_4}\left[-\frac{\alpha w x^4}{24} - \frac{wLx^3}{48}(\beta - 5\alpha) + \frac{wL^2x^2}{256}(1 - 17\alpha + 16\beta) + C_{12}x + C_{13}\right]$$

At $x = \frac{5L}{8}$, $v(x) = v(x)$

$$\frac{1}{EI_3}\left[-\frac{\beta w}{2}\left(\frac{1}{12}\frac{625L^4}{4096} - \frac{L}{6}\frac{125L^3}{512}\right) + \frac{wL^2}{256}\frac{25L^2}{64}(1 + 8\alpha - 9\beta) + \frac{5L}{8}C_{10} + C_{11}\right]$$

$$= \frac{1}{EI_4}\left[-\frac{\alpha w}{24}\frac{625L^4}{4096} - \frac{wL}{48}\frac{125L^3}{512}(\beta - 5\alpha) + \frac{wL^2}{256}\frac{25L^2}{64}(1 - 17\alpha + 16\beta) + \frac{5L}{8}C_{12} + C_{13}\right]$$

$$\therefore C_{13} = \frac{I_4}{I_3}\frac{wL^4}{98304}(-96 - 768\alpha - 640\beta) + \frac{I_4}{I_2}\frac{wL^4}{98304}(-48 - 336\alpha - 208\beta) + \frac{I_4}{I_1}\frac{wL^4}{98304}(-5 - 16\alpha - 8\beta) + \frac{wL^4}{98304}(150 + 575\alpha + 1400\beta)$$

---

for $\frac{7L}{8} < x < L$

$$\frac{dv}{dx} = \frac{1}{EI_5}\left[-\frac{wx^3}{6} - \frac{wLx^2}{16}(2\alpha + \beta - 7) + \frac{wL^2x}{128}(-48 + 32\alpha + 16\beta) + C_{14}\right]$$

At $x = \frac{7L}{8}$, $\frac{dv}{dx} = \frac{dv}{dx}$

$$\frac{1}{EI_4}\left[-\frac{\alpha w}{6}\frac{343L^3}{512} - \frac{wL}{16}\frac{49L^2}{64}(\beta - 5\alpha) + \frac{wL^2}{128}\frac{7L}{8}(1 - 17\alpha + 16\beta) + C_{12}\right]$$

$$= \frac{1}{EI_5}\left[-\frac{w}{6}\frac{343L^3}{512} - \frac{wL}{16}\frac{49L^2}{64}(\beta - 5\alpha) + \frac{wL^2}{128}\frac{7L}{8}(-48 + 32\alpha + 16\beta) + C_{14}\right]$$

$$\therefore C_{14} = \frac{I_5}{I_4}\frac{wL^3}{3072}(6 + 40\alpha + 24\beta) + \frac{I_5}{I_3}\frac{wL^3}{3072}(3 + 24\alpha + 20\beta) - \frac{wL^3}{3072}(-1351 + 1407\alpha + 189\beta)$$

$$v(x) = \frac{1}{EI_5}\left[-\frac{wx^4}{24} - \frac{wLx^3}{48}(2\alpha + \beta - 7) + \frac{wL^2x^2}{256}(-48 + 32\alpha + 16\beta) + C_{14}x + C_{15}\right]$$

At $x = \frac{7L}{8}$, $v(x) = v(x)$

$$\frac{1}{EI_4}\left[-\frac{\alpha w}{24}\frac{2401L^4}{4096} - \frac{wL}{48}\frac{343L^3}{512}(\beta - 5\alpha) + \frac{wL^2}{256}\frac{49L^2}{64}(1 - 17\alpha + 16\beta) + \frac{7L}{8}C_{12} + C_{13}\right]$$

$$= \frac{1}{EI_5}\left[-\frac{w}{24}\frac{2401L^4}{4096} - \frac{wL}{48}\frac{343L^3}{512}(2\alpha + \beta - 7) + \frac{wL^2}{256}\frac{49L^2}{64}(-48 + 32\alpha + 16\beta) + \frac{7L}{8}C_{14} + C_{15}\right]$$

$$\therefore C_{15} = \frac{I_5}{I_4}\frac{wL^4}{98304}(-144 - 944\alpha - 560\beta) + \frac{I_5}{I_3}\frac{wL^4}{98304}(-96 - 768\alpha - 640\beta) + \frac{I_5}{I_2}\frac{wL^4}{98304}(-48 - 336\alpha - 208\beta) + \frac{I_5}{I_1}\frac{wL^4}{98304}(-5 - 16\alpha - 8\beta) + \frac{wL^4}{98304}(-30919 + 32732\alpha + 1960\beta)$$

$$v\left(\frac{L}{4}\right) = \frac{1}{EI_2}\left[-\frac{\alpha w}{24}\frac{L^4}{256} + \frac{wL}{48}\frac{L^3}{64}(3\alpha + \beta) + \frac{wL^2}{256}\frac{L^2}{16}(1 - \alpha) + \frac{L}{4}C_8 + C_9\right]$$

$$= \frac{1}{EI_2}\left[\frac{I_2}{I_3}\frac{wL^4}{12288}(-3 - 24\alpha - 20\beta) + \frac{I_2}{I_1}\frac{wL^4}{98304}(-5 - 16\alpha - 8\beta) - \frac{wL^4}{98304}(42 + 289\alpha + 176\beta)\right]$$

$$v\left(\frac{L}{2}\right) = \frac{1}{EI_3}\left[-\frac{\beta w}{2}\left(\frac{1}{12}\frac{L^4}{16} - \frac{L}{6}\frac{L^3}{8}\right) + \frac{wL^2}{256}\frac{L^2}{4}(1 + 8\alpha - 9\beta) + \frac{L}{2}C_{10} + C_{11}\right]$$

$$= \frac{1}{EI_3}\left[\frac{I_3}{I_2}\frac{wL^4}{98304}(-48 - 336\alpha - 208\beta) + \frac{I_3}{I_1}\frac{wL^4}{98304}(-5 - 16\alpha - 8\beta) + \frac{wL^4}{98304}(-42 - 336\alpha + 281\beta)\right]$$

$$v\left(\frac{3L}{4}\right) = \frac{1}{EI_4}\left[-\frac{\alpha w}{24}\frac{81L^4}{256} - \frac{wL}{48}\frac{27L^3}{64}(\beta - 5\alpha) + \frac{wL^2}{256}\frac{9L^2}{16}(1 - 17\alpha + 16\beta) + \frac{3L}{4}C_{12} + C_{13}\right]$$

$$= \frac{1}{EI_4}\left[\frac{I_4}{I_3}\frac{wL^4}{98304}(-24 - 192\alpha - 160\beta) + \frac{I_4}{I_2}\frac{wL^4}{98304}(-48 - 336\alpha - 208\beta) + \frac{I_4}{I_1}\frac{wL^4}{98304}(-5 - 16\alpha - 8\beta) + \frac{wL^4}{98304}(6 + 47\alpha + 32\beta)\right]$$

The formulae for the other three cases, viz a beam simply-supported at one end and fully fixed at the other end (Appendix A2), a beam fully fixed at both ends (Appendix A3) and a cantilever (Appendix A4), have not been included in this document, but have been handed in to the department.

APPENDIX B

FORMULAE FOR YOUNG'S MODULUS OF CONCRETE, CRACKED AND UNCRACKED MOMENTS OF INERTIA, TENSILE CAPACITY OF CONCRETE AND THE CRACKING AND PLASTIC MOMENT CAPACITIES OF CONCRETE SECTIONS

Young's Modulus (E_c of Concrete)

This formula is taken from the publication on aggregate properties in South African concrete[18] and is for concrete composed of Malmesbury Shale aggregate.

$$E_c = 24 + 0.25\ f_{cu}$$

where E_c = Young's Modulus of the Concrete (in GPa)
f_{cu} = Cube Strength of the Concrete (in MPa)

Moments of Inertia

I_{uncr} refers to the uncracked (gross) transformed all-concrete moment of inertia.

I_{cr} refers to the cracked transformed all-concrete moment of inertia for a section subjected to a sagging moment.

I_{cr}' refers to the cracked transformed all-concrete moment of inertia for a section subjected to a hogging moment.

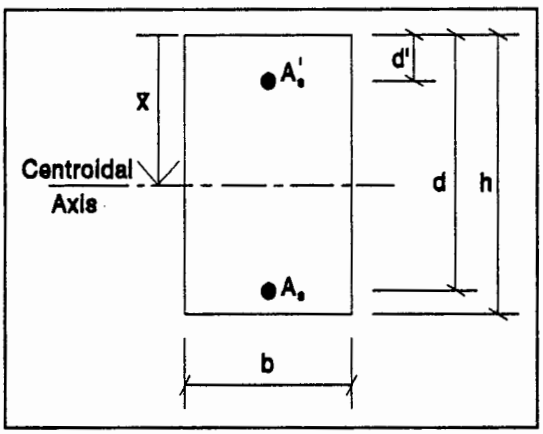

For an uncracked section

$$\bar{x} = \frac{\frac{b \cdot h^2}{2} + (\alpha_e - 1)(A_s' \cdot d' + A_s \cdot d)}{b \cdot h + (\alpha_e - 1)(A_s' + A_s)}$$

$$I_{uncr} = \frac{b \cdot h^3}{12} + b \cdot h \left(\bar{x} - \frac{h}{2}\right)^2 + (\alpha_e - 1)\left[A_s'(\bar{x} - d')^2 + A_s(d - \bar{x})^2\right]$$

For a section cracked in sagging

$$\bar{x} = -\left[\frac{\alpha_e A_s + (\alpha_e - 1)A_s'}{b}\right] + \sqrt{\left(\frac{\alpha_e A_s + (\alpha_e - 1)A_s'}{b}\right)^2 + \frac{2}{b}\left[\alpha_e A_s d + (\alpha_e - 1)A_s' d'\right]}$$

$$I_{cr} = \frac{b\bar{x}^3}{3} + \alpha_e A_s (d - \bar{x})^2 + (\alpha_e - 1)A_s'(\bar{x} - d')^2$$

For a section cracked in hogging

$$\bar{x} = -\left[\frac{\alpha_e A_s' + (\alpha_e - 1)A_s}{b}\right] + \sqrt{\left(\frac{\alpha_e A_s' + (\alpha_e - 1)A_s}{b}\right)^2 + \frac{2}{b}\left[\alpha_e A_s'(h - d') + (\alpha_e - 1)A_s(h - d)\right]}$$

$$I_{cr} = \frac{b\bar{x}^3}{3} + \alpha_e A_s'(h - d' - \bar{x})^2 + (\alpha_e - 1)A_s(\bar{x} - h + d)^2$$

Tensile Capacity of Concrete

The following formula is used to determine the tensile capacity of the concrete and was obtained from a recent technical article in Concrete/Beton[19].

$$f_{ct} = 0.192 \times f_{cu}^{0.802}$$

Cracking Moment Capacities

M_{cr} refers to the cracking moment capacity of a beam subjected to a sagging moment, while M_{cr}' refers to the cracking moment capacity of a beam subjected to a hogging moment.

$$M_{cr} = \frac{f_{ct} \cdot I_{uncr}}{h - \bar{x}}$$

$$M_{cr}' = \frac{f_{ct} \cdot I_{uncr}}{\bar{x}}$$

where $\bar{x}$ is the distance to the centroid for an uncracked section and is measured from the top of the beam.

Plastic Moment Capacities

M_{pl} refers to the plastic moment capacity of a beam subjected to a hogging moment.

$$x = \frac{f_y \cdot A_s'}{0.6 \cdot b \cdot fcu}$$

$$M_{pl} = f_y \cdot A_s' (h - d' - \frac{x}{2})$$

In the formula for x a value of 0.6 was used in the numerator instead of 0.4 as recommended in the design codes for a rectangular stress block. The value of 0.6 was chosen so as to exclude the material factor (1.5) since the **actual** plastic moment capacity is required and not a **design** value.

APPENDIX C1

BAR CHARTS FOR SQUARE SLABS CRUDGE

SQUARE SLABS CRUDGE

EXPERIMENTAL & DESIGN ULTIMATE LOADS

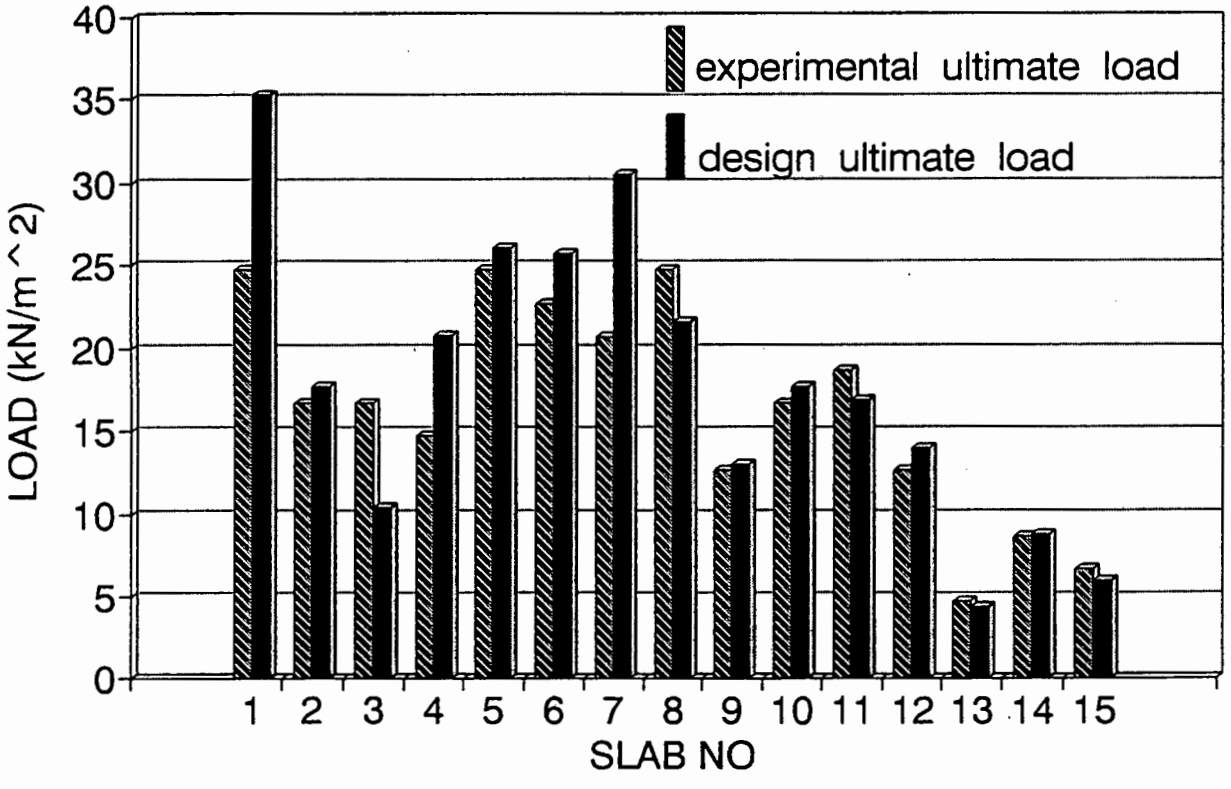

APPENDIX C2

BAR CHARTS FOR SQUARE SLABS CHRYSTAL

SQUARE SLABS CHRYSTAL

EXPERIMENTAL & DESIGN ULTIMATE LOADS

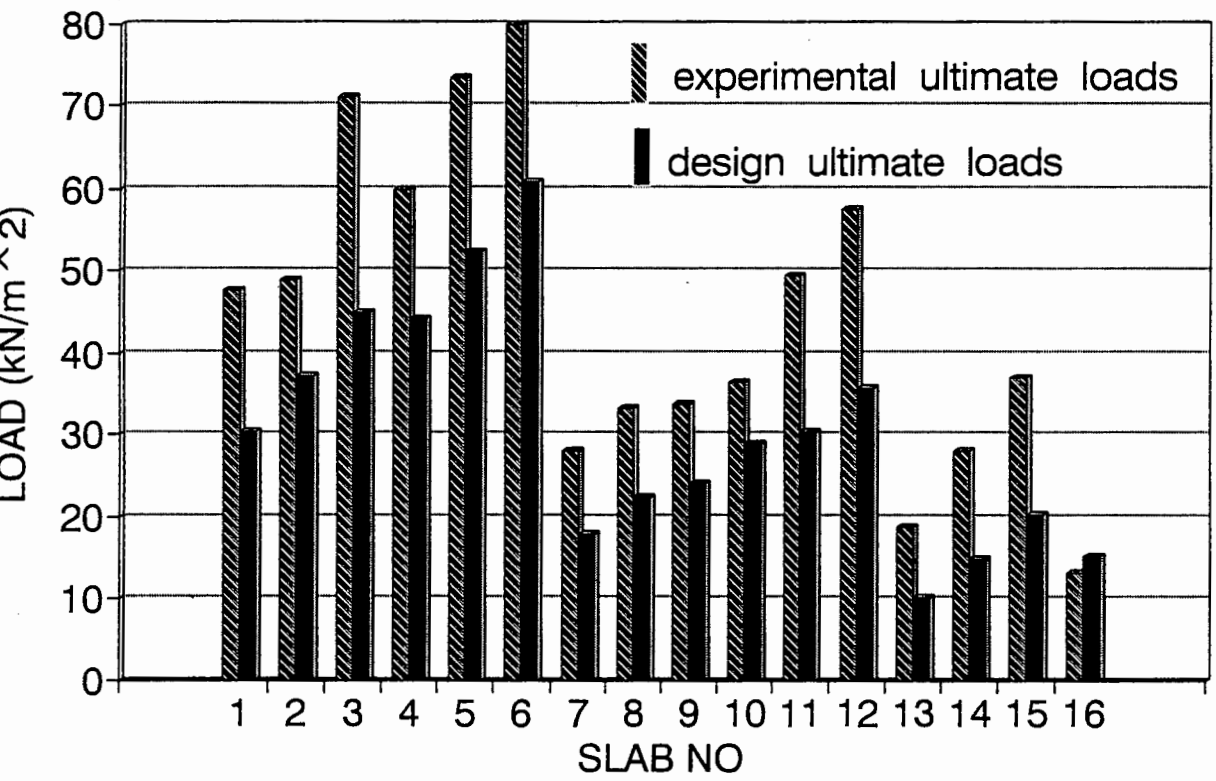

SQUARE SLABS CHRYSTAL

SERVICEABILITY LOADS

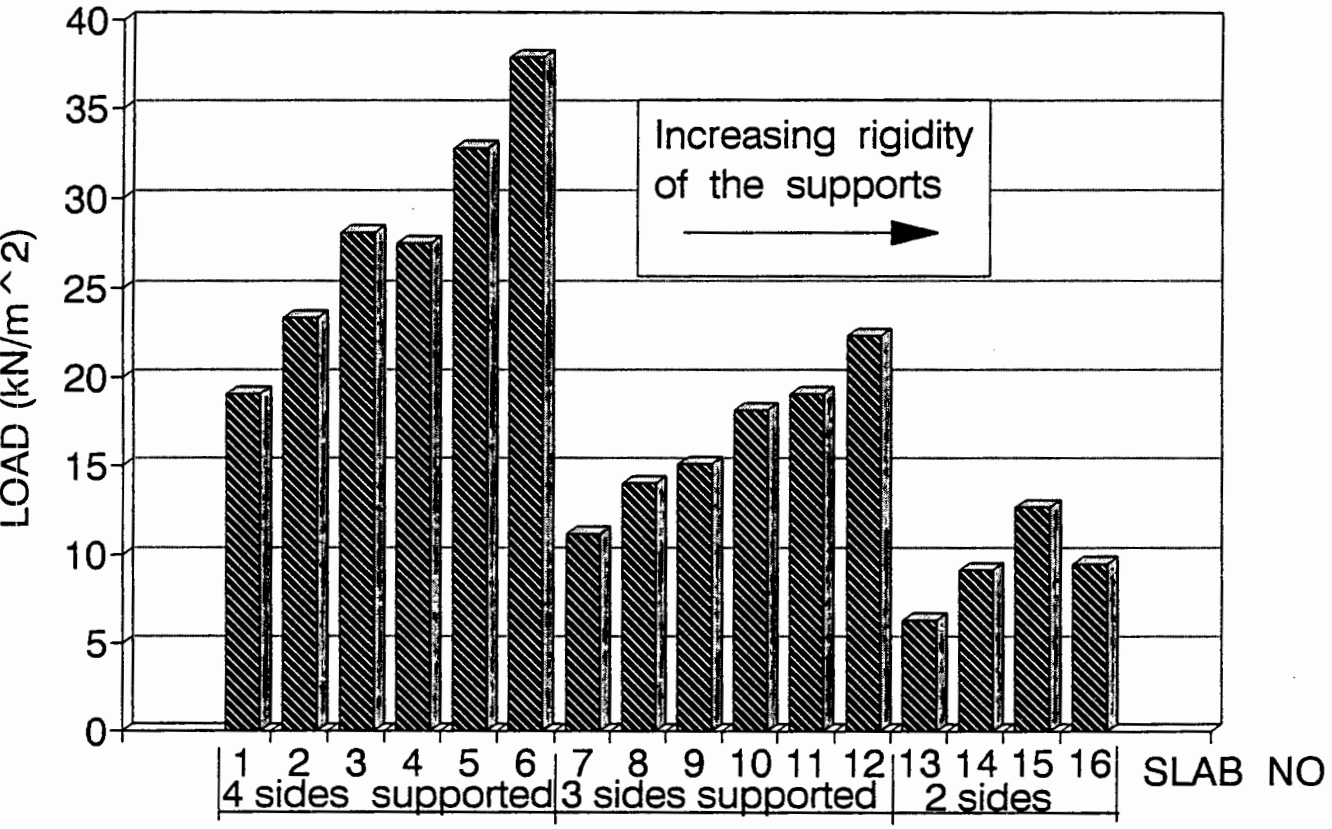

APPENDIX C3

BAR CHARTS FOR RECTANGULAR SLABS JACKSON

RECTANGULAR SLABS JACKSON

EXPERIMENTAL & DESIGN ULTIMATE LOADS

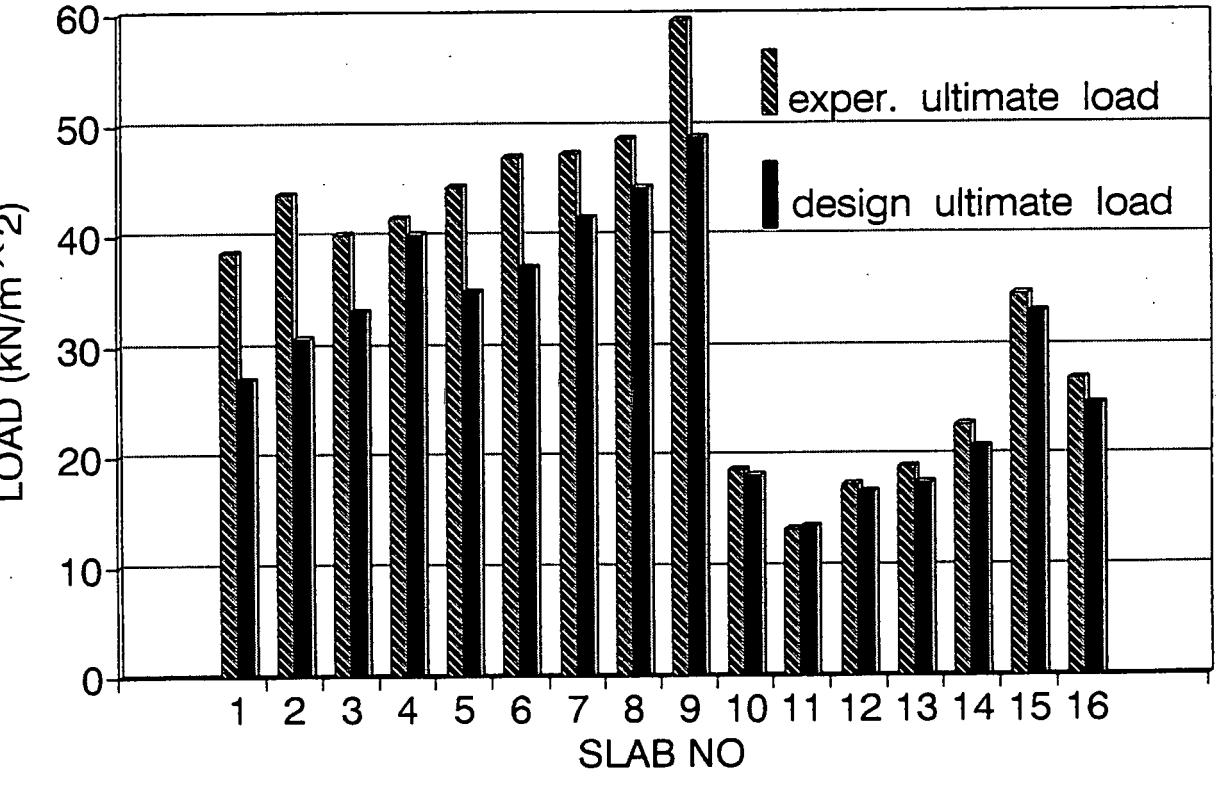

RECTANGULAR SLABS JACKSON
SERVICEABILITY LOADS

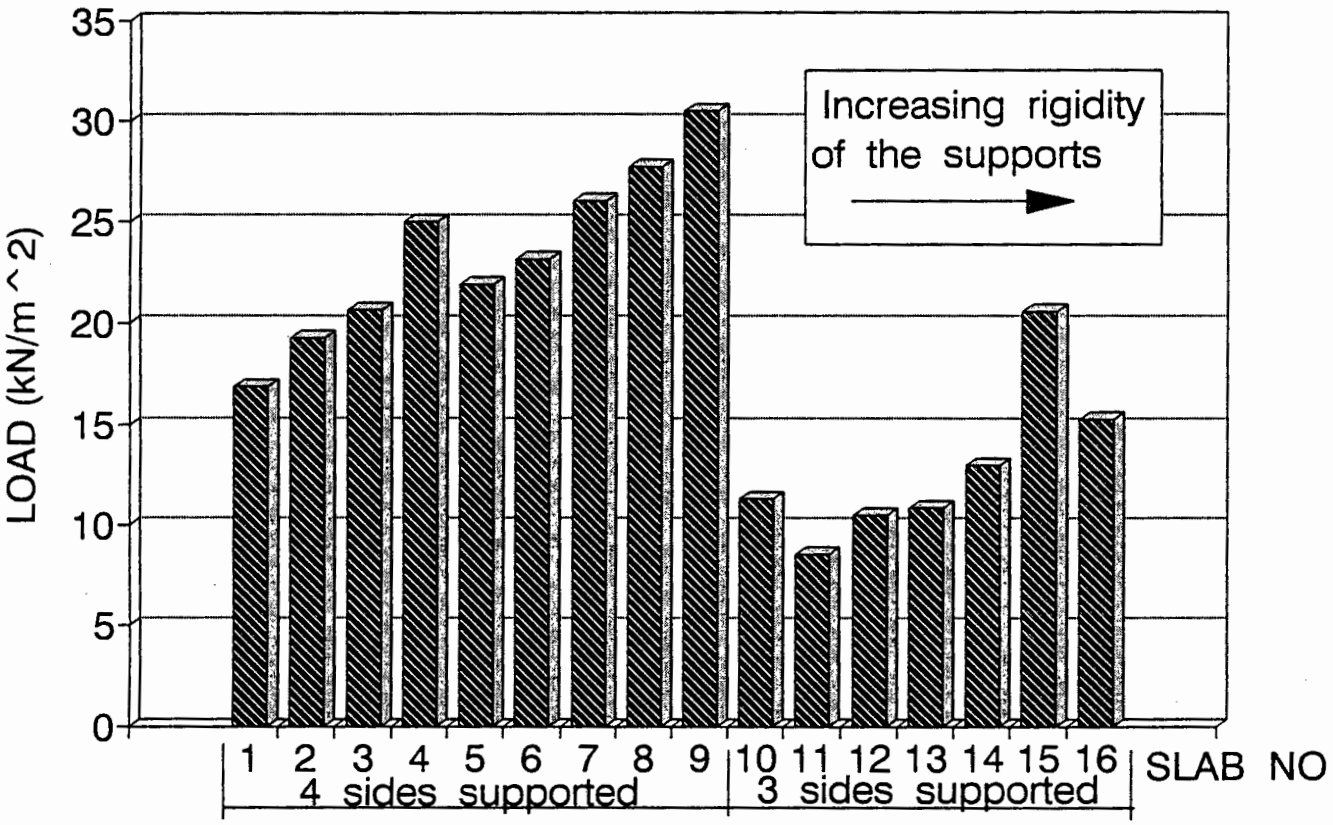

APPENDIX C4

BAR CHARTS FOR RECTANGULAR SLABS COOKE

RECTANGULAR SLABS COOKE

EXPERIMENTAL & DESIGN ULTIMATE LOADS

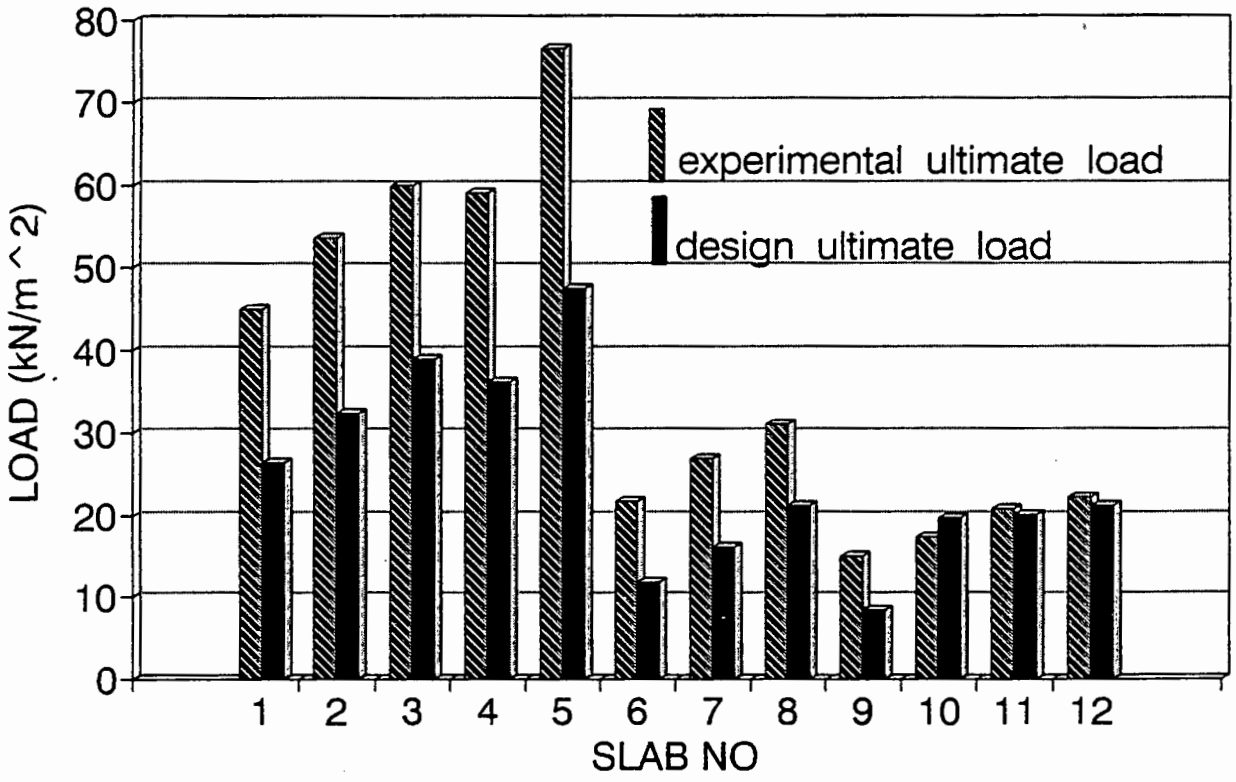

RECTANGULAR SLABS COOKE
SERVICEABILITY LOADS

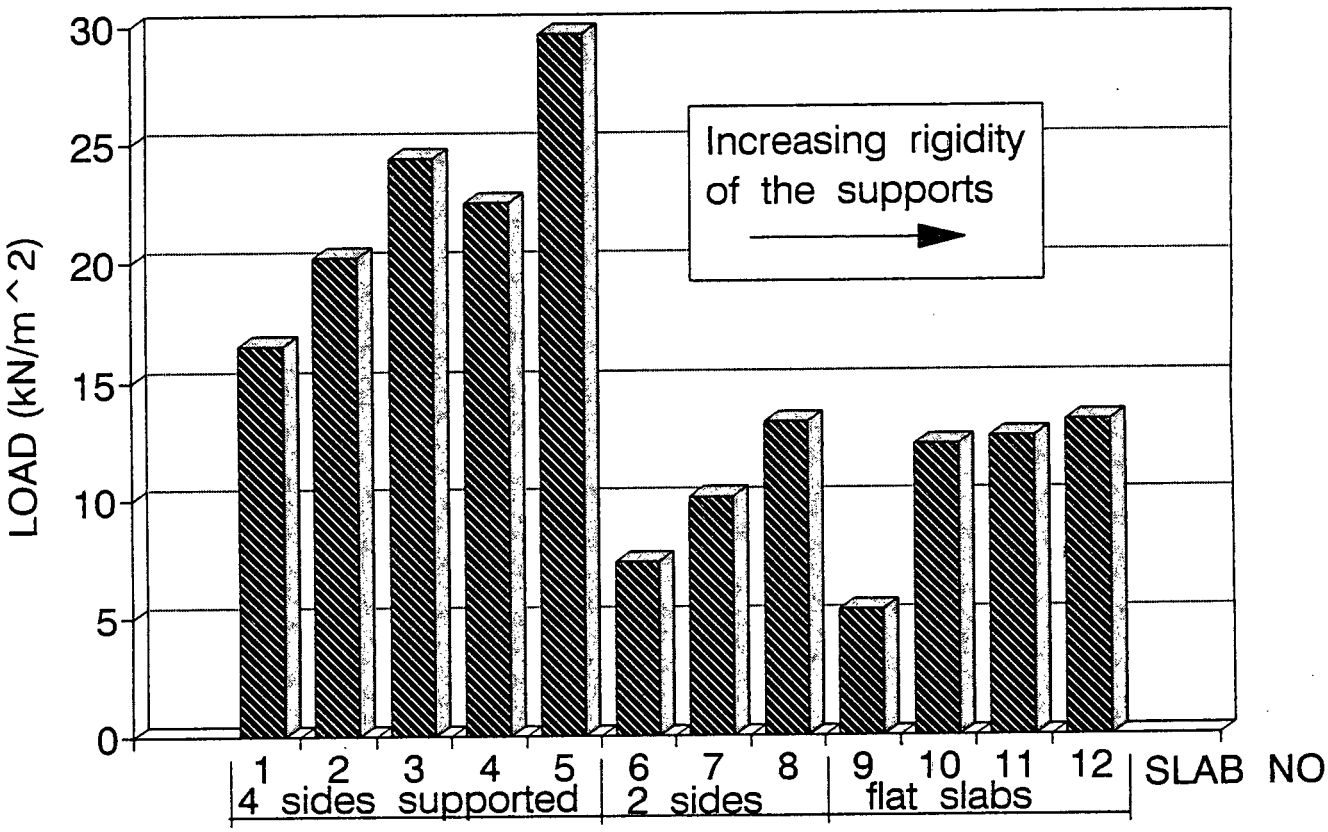

RECTANGULAR SLABS COOKE

DEFLECTIONS @ 10 kN

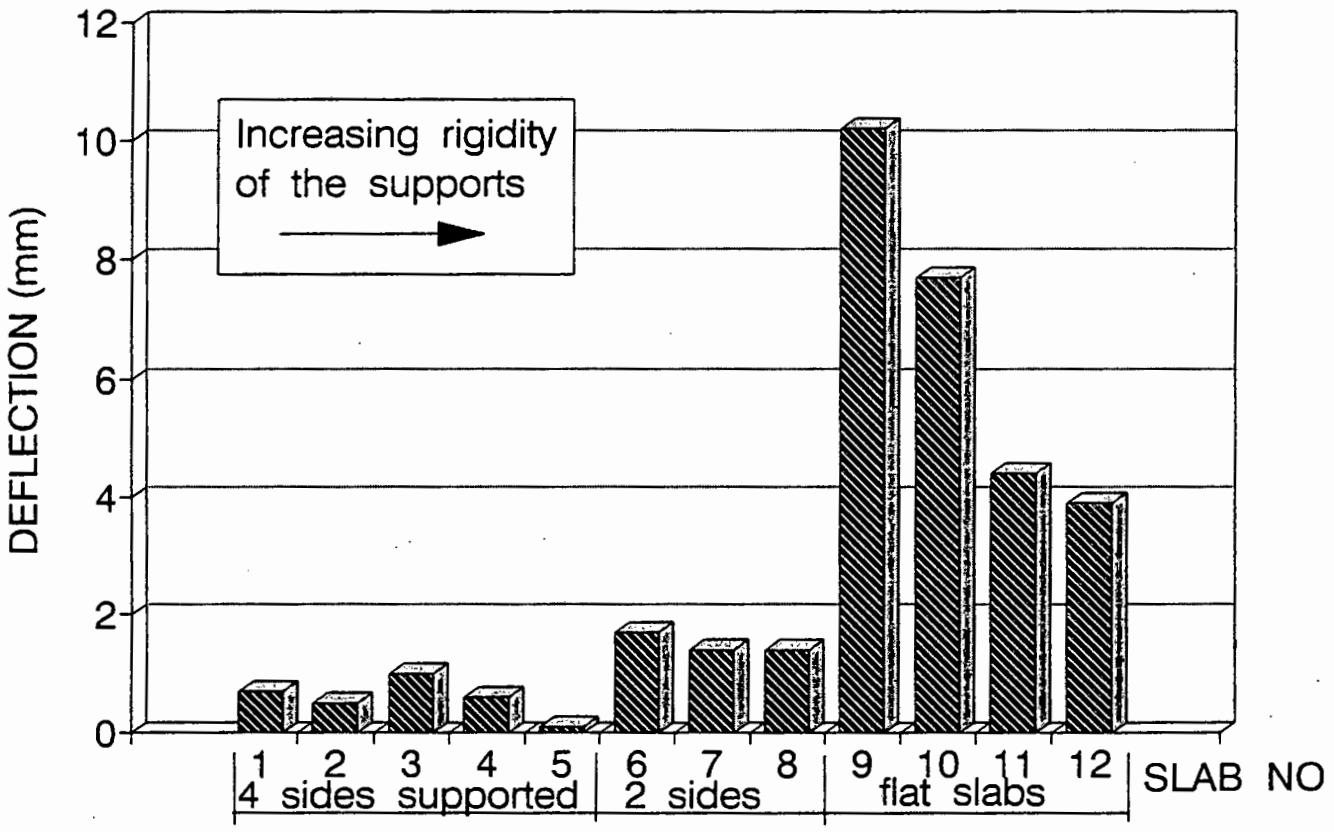

APPENDIX C5

YIELD LINE ANALYSIS OF A TYPICAL SLAB

Slab No 6 - Rectangular Slabs Jackson

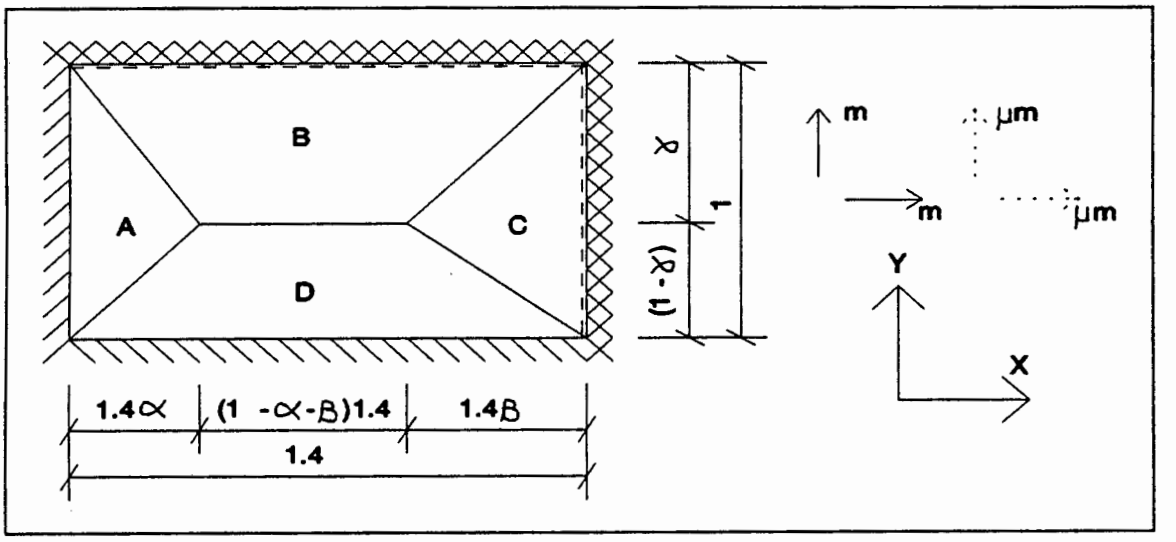

Element	θ_x	θ_y	L_x	L_y	m_x	m_y	$M\theta$
A	0	$1/1.4\alpha$	2.8α	1	m	m	$m/1.4\alpha$
B (pos)	$1/\gamma$	0	1.4	2γ	m	m	$1.4m/\gamma$
(neg)	$1/\gamma$	0	1.4	0	μm	μm	$1.4\mu m/\gamma$
C (pos)	0	$1/1.4\beta$	2.8β	1	m	m	$m/1.4\beta$
(neg)	0	$1/1.4\beta$	0	1	μm	μm	$\mu m/1.4\beta$
D	$1/(1-\gamma)$	0	1.4	$(1-\gamma)2$	m	m	$1.4m/(1-\gamma)$

$$\Sigma M\theta = m/1.4\alpha + 2.543m/\gamma + 1.8102m/1.4\beta + 1.4m/(1-\gamma)$$

Internal Work Done = External Work Done

$$m\frac{\gamma\beta(1-\gamma) + 3.5480\alpha\beta(1-\gamma) + 1.8102\alpha\gamma(1-\gamma) + 1.96\alpha\beta\gamma}{1.4\alpha\beta\gamma(1-\gamma)}$$

$$= w\cdot\frac{1}{2}\cdot 1\cdot 1.4\alpha\cdot\frac{1}{3} + w\cdot\frac{1}{2}\cdot 1.4\alpha\cdot\gamma\cdot\frac{1}{3} + w\cdot(1-\alpha-\beta)\cdot 1.4\cdot\gamma\frac{1}{2}$$

$$+ w\cdot\frac{1}{2}\cdot 1.4\beta\cdot\gamma\frac{1}{3} + w\cdot\frac{1}{2}\cdot 1\cdot 1.4\beta\cdot\frac{1}{3} + w\cdot\frac{1}{2}\cdot 1.4\beta\cdot(1-\gamma)\cdot\frac{1}{3}$$

$$+ w\cdot(1-\alpha-\beta)\cdot 1.4\cdot(1-\gamma)\cdot\frac{1}{2} + w\cdot\frac{1}{2}\cdot 1.4\alpha(1-\gamma)\cdot\frac{1}{3}$$

$$= w(0.2333\alpha + 0.2333\alpha\gamma + 0.7\gamma - 0.7\gamma\alpha - 0.7\gamma\beta + 0.2333\gamma\beta + 0.2333\beta - 0.2333\gamma\beta + 0.7 - 0.7\alpha - 0.7\beta - 0.7\gamma + 0.7\alpha\gamma + 0.7\gamma\beta + 0.2333\alpha - 0.2333\alpha\gamma)$$

$$= w(0.7 - 0.2333\alpha - 0.2333\beta)$$

$$m = \frac{0.3267w\alpha\beta\gamma(1 - \gamma)(3 - \alpha - \beta)}{\gamma\beta(1 - \gamma) + 3.5480\alpha\beta(1 - \gamma) + 1.8102\alpha\gamma(1 - \gamma) + 1.96\alpha\beta\gamma}$$

Optimising

α	β	γ	ANS	α	β	γ	ANS
0.3	0.3	0.4	0.1116	0.3	0.47	0.58	0.12410
		0.5	0.1177	0.4		0.57	0.12431
		0.6	0.1189	0.5			0.12204
		0.7	0.1145	0.35			0.124633
		0.55	0.1190	0.37			0.12459
		0.57	0.11911	0.36	0.47		0.124627
		0.58	0.11910	0.34			0.1246
		0.56	0.11906	0.35	0.47	0.56	0.124579
	0.4	0.57	0.12338			0.58	0.124625
	0.5		0.12404		0.46	0.57	0.124608
	0.6		0.12257		0.48		0.12463318
	0.45		0.12404	0.35	0.47	0.57	0.12463315
	0.47		0.124113				
	0.48		0.124111				
	0.47	0.56	0.12406				

Therefore the optimum values are $\alpha = 0.35$, $\beta = 0.48$ and $\gamma = 0.57$

$\rightarrow m = 0.0407\ w$

$\rightarrow w = 37.14\ kN/m^2$ - design ultimate load

APPENDIX C6

SMOOTHING OF MEASURED DEFLECTIONS ON A TYPICAL SLAB

Slab No 3 - Square Slabs Chrystal

This appendix must be read in conjunction with the procedure described on pages 55 to 58 in Chapter 4.2.

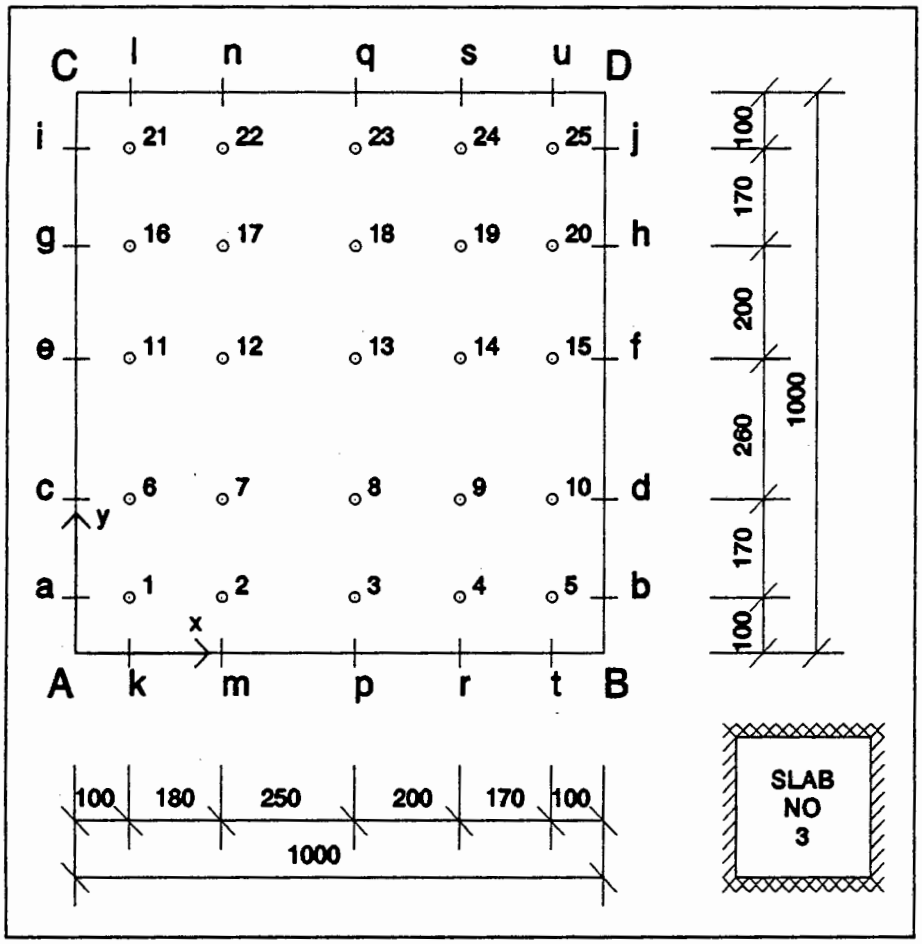

Dial gauge layout for a slab simply-supported on two opposite edges and clamped on the other two edges

In the table below, the twenty-five dial gauge readings for the sevice load can be found in columns 2 to 6 and rows 2 to 6. These dial gauge readings correspond to their positions in the figure above. The row bounding this region above and below and the column to the left and right contain the extrapolated readings, i.e. the readings on the support frame. The four blocks with two sets of readings are the corner points and contain the extrapolated readings from the deflections of the support frame sides. The last two columns and the last two rows contain the maximum deflection for that row/column as well as the position of maximum slab deflection.

-0.629 -0.866	-0.220	0.343	0.319	0.459	-0.338	-0.677 -1.054	0.504	490
-0.338	0.19	0.64	0.89	1.01	0.14	-0.182	0.998	520
0.017	1.09	2.18	2.84	2.52	1.15	0.281	2.876	510
0.631	1.74	2.95	3.53	3.24	1.75	0.819	**3.618**	**510**
0.977	1.65	1.25	2.52	2.28	1.70	1.601	2.201	590
0.631	0.79	0.95	0.96	0.76	0.45	0.212	0.991	400
0.563 0.656	0.560	0.130	0.223	0.128	0.197	0.047 0.312	0.656	0
0.828	1.810	2.603	**3.544**	3.202	1.878	1.147		
280	450	510	**500**	510	470	410		

Corners A and B deflect slightly downwards - not quite what is expected. Corners C and D deflect upwards, which is what is expected. Maximum deflection occurs at the position (510;500) which is very close to the centre of the slab. There are no dial gauge readings at that position, so an interpolation between the existing dial gauge readings for the deflections at service load will have to be made.

a = 3.544 mm - is the maximum deflection on x = 530 @ y = 500
b = 3.618 mm - is the maximum deflection on y = 530 @ x = 510
c is the maximum deflection @ x = 510 & y = 500
d_1 is the value on x = 530 @ y = 530 → 3.532 mm
d_2 is the value on y = 530 @ x = 530 → 3.613 mm
- average is 3.573 mm

Now c/b = a/d
Therefore c = 3.544 * 3.618 / 3.573
= 3.589 mm.

Thus, the maximum deflection (rounded of to one decimal point) is 3.6 mm.

The procedure that follows on the next few pages is the smoothing procedure applied to the support frames to counter their deflections.

Value on smoothed support frame curve AB at x = 510 is 0.128 mm.

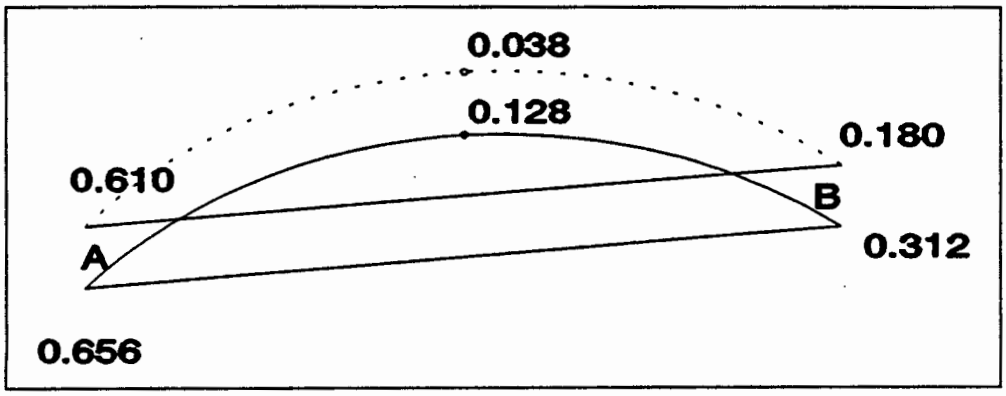

Value on line y = (-3.44e-4)x + 0.656 at x = 510 is 0.481 mm.
Value on line y = (-4.30e-4)x + 0.610 at x = 510 is 0.391 mm.
Therefore the error is 0.090 mm.
Thus value on new smoothed support frame curve AB is 0.038 mm.

Value on smoothed support frame curve CD at x = 510 is 0.503 mm.

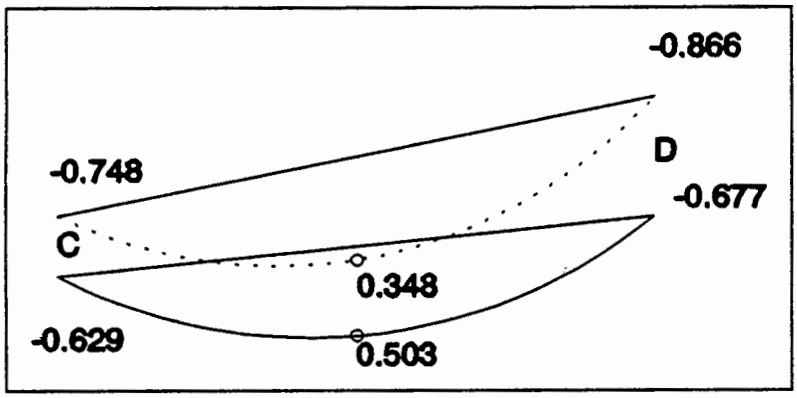

Value on line y = (-4.80e-5)x - 0.629 at x = 510 is -0.653 mm.
Value on line y = (-1.18e-4)x - 0.748 at x = 510 is -0.808 mm.
Therefore error is -0.155 mm.
Thus value on new smoothed support frame curve CD is 0.348 mm.

Value on line y = (3.1e-4)x + 0.038 at x = 500 is 0.193 mm. →

This is the value, at the position of maximum deflection of the slab, of a line running from the corresponding points on the two opposite sides AB and CD.

Value on smoothed support frame curve AC at y = 500 is 0.674 mm.

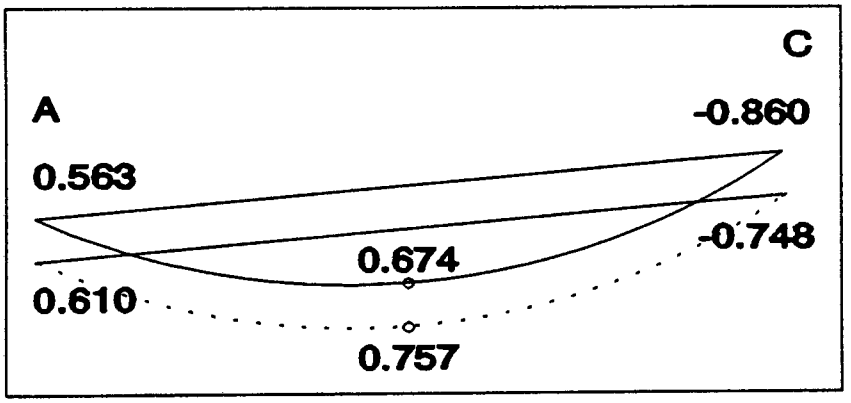

Value on line y = (-1.429e-3)x + 0.563 at x = 500 is -0.152 mm.
Value on line y = (-1.358e-3)x + 0.610 at x = 500 is -0.069 mm.
Therefore error is 0.083 mm.
Thus value on new smoothed support frame curve AC is 0.757 mm.

Value on smoothed support frame curve BD at y = 500 is 1.100 mm.

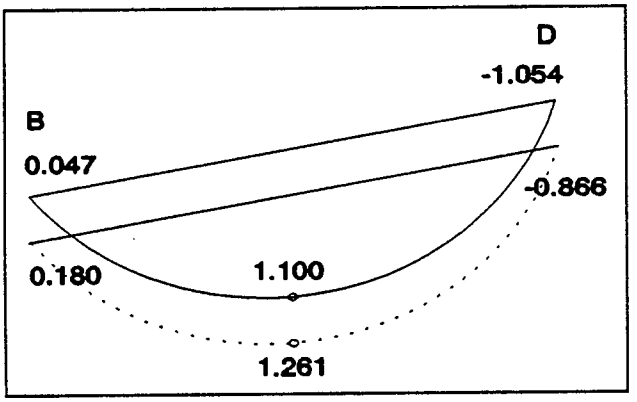

Value on line y = (-1.101e-3)x + 0.047 at x = 500 is -0.504 mm.
Value on line y = (-1.046e-3)x + 0.180 at x = 500 is -0.343 mm.
Therefore error is 0.161 mm.
Thus value on new smoothed curve BD actually is 1.261 mm.

Value on line y = (5.04e-4)x + 0.757 at x = 510 is <u>1.014 mm.</u> →

This is the value, at the position of maximum deflection of the slab, of a line running from the corresponding points on the two opposite sides AC and BD.

Average of the two calculated values is

$$(0.193 + 1.014)/2$$

$$= 0.604 \text{ mm.}$$

Therefore the maximum deflection relative to the zero datum is

$$3.589 - 0.604 \approx 3.0 \text{ mm.}$$